Preparation, Characterization and Performance Evaluation of Nanocomposite SoyProtein/Carbon Nanotubes (Soy/CNTs) from Soy Protein Isolate

by

OLAWUMI OLUWAFOLAKEMI SADARE

submitted in accordance with the requirements

for the degree of

MAGISTER TECHNOLOGIAE

in the subject

ENGINEERING: CHEMICAL

at the

UNIVERSITY OF SOUTH AFRICA

SUPERVISOR: PROF AS AFOLABI

CO-SUPERVISOR: DR MO DARAMOLA

APRIL 2015

Copyright

Publications

The following papers were submitted/published and presented from this study.

1. **Sadare, O.O.,** Okelana, TO and Afolabi, AS (2014) Characterization of process parameters of adhesive glue produced from leguminous seeds. *Manuscript accepted for publication at the 9th International Conference on Energy and Environment (EE 14) in Geneva Switzerland, December 29 – 31, 2014.*

2. **Sadare, O.O.,** Daramola, M.O. and Afolabi, A. S. (2015) Preparation and characterization of nanocomposite soy-carbon nanotubes (SPI/CNTs) adhesive from soy protein isolate. *Manuscript accepted for presentation at the World Congress on Engineering, United Kingdom, July 1 – 3, 2015.*

3. **Sadare, O.O.,** Daramola, M.O. and Afolabi, A.S. (2015) Synthesis and performance evaluation of nanocomposite soy protein/carbon nanotubes (Soy/CNTs) adhesive from soy protein isolate for wood applications. *Manuscript submitted for review and consideration for publication in International Journal of Adhesion and Adhesive.*

4. Daramola, M.O., **Sadare, O.O.** and Afolabi, A. S. (2015) Effect of functionalization of CNTs on the adhesive performance of nanocomposite soy protein/carbon nanotubes (Soy/CNTs) adhesive from soy protein isolate. *Manuscript submitted for review and consideration for publication in Journal of Adhesive Science Technology.*

5. Afolabi, A.S., **Sadare, O.O**. and Daramola, M.O. (2015) Effect of dispersion method of CNTs on the tensile shear strength of nanocomposite soy protein/CNTs adhesive for wood bonding. *Manuscript submitted for review and consideration for publication in Advances in Natural Sciences: Nanoscience and Nanotechnology.*

Declaration

I declare that this report is my own unaided work. It is being submitted for the award of M. Tech at the University of South Africa, Johannesburg. It has not been submitted before for any degree or examination in any other University.

23rd Of Dec., 2015

Olawumi Oluwafolakemi Sadare Date

Dedication

This dissertation is dedicated to my loving husband, Oluseye Folasayo Sadare, for his encouragement, moral and financial support, and my precious children Praise, Israel and Esther Sadare.

Acknowledgement

I give God all the glory for seeing me through this journey and for the successful completion of this degree. I thank him for his favour as promised. He is indeed too faithful to fail.

My sincere appreciation goes to my supervisor, Prof. Ayo Afolabi, for believing in me and giving me the platform to pursue this goal and dream. I thank him for his words of encouragement, supervisory guidance, advice and moral support. I will forever be grateful to him, because he will forever remain in my success book. My journey in this degree would not have been so smooth, if I had not met with my co-supervisor, Dr Michael Daramola. He is indeed God's answer to my prayers. He was always there to advice, counsel, supervise and help out in making sure I get materials and equipment that I needed on time, even when not convenient for him. May the good lord reward him abundantly. My appreciation also goes to Unisa for the financial assistance rendered during the course of this study. Thanks to Dr Nkasi for allowing me to use his laboratory. My gratitude goes to Dr Philips, Dr Enoch, Dr Gbenga, Dr Frank, Terrence Malama, Isuru Jinasena, Tsumi, Emmanuel, Karabo, Aliki, Julius, Ayotunde, Damilola, and Yemisi for their usual assistance. Thanks to Kwame Nwosu for taking time to listen and answer my calls, even when it was not convenient. Thanks to Zama, Brayner and Tumelo for taking time to analyze all my samples. To my partner, Miss Ajoke Hassan, I appreciate her for her words of encouragement since the beginning of this degree till the end which gave me strength to move on.

I want to use this medium to appreciate Toyin Agangan for standing by me at the beginning of this program. She took care of my daughter throughout the proposal stage while I would be away in the library from morning till late in the evening. My appreciation also goes to Mr Akeem Adenuga, for his career advice, when I was almost giving up.

This degree would not have been a success, if not for the assistance and help of my brother, Dr Olatayo Oladejo. I appreciate him for his guidance, financial and moral support, encouragement and pressure mounted on me to finish this programme on time. He has been a source of inspiration to me. His wife Lindiwe and children, Ife and Ladu, I thank them for hosting me and my daughter, even when it was not convenient for them. My appreciation also goes Rev Amos

and his family and the entire congregation of his church. My spiritual mother, Mrs Olakanmi Jumoke, thanks for your prayers. My cousins Gbenga and Michael and my friends, Ayeni, Falade, Funmi Oluboye, Funmi Adedapo, Funke, Kemi, Biodun, Bukola and Segun Ojoawo, thanks so much for your words of encouragement.

To my family; My in-laws, my mother, my brothers, Dr Olayinka Oladejo, Biodun, Dr Titilola Oladejo, Kehinde Omotoso and Sunday Ogunremi and my sisters Fola Ogunremi and Olaide Omotosho, thanks for your support and words of encouragement at all times.

Oluseye Folasayo, my dearest husband, he is my hero. I appreciate him so much for the trust he has in me, for allowing me to come this far. It means the whole world to me. He is indeed a blessing to me. May the lord reward him for this single act. My love and appreciation goes to my precious sons, Praise and Israel, I miss you endlessly. I will not forget how many times my daughter would have me get up from my laptop with many of her endless demands. She is my best and only companion in South Africa, my amiable daughter, Esther. Although she is just a child, but I so much appreciate her for comforting me most of the times when I was down and stressed up. She would hug me and pat me on my back and say "Mummy, what's wrong? Sowie, don't cry again. Hey?". Those words mean a lot to me. I love you.

I will like to appreciate the department of Chemical and Metallurgical Engineering, University of Witwatersrand, South Africa for permitting me to make use of their laboratory. Finally, I thank University of South Africa for the bursary awarded me during the course of this study.

Abstract

Formaldehyde-based adhesives have been reported to be detrimental to health. Petrochemical-based adhesives are non-renewable, limited and costly. Therefore, the improvement of environmental-friendly adhesive from natural agricultural products has awakened noteworthy attention. A novel adhesive for wood application was successfully prepared with enhanced shear strength and water resistance.

The Fourier transmform infrared spectra showed the surface functionalities of the functionalized carbon nanotubes (FCNTs) and soy protein isolate nanocomposite adhesive. The attachment of carboxylic functional group on the surface of the carbon nanotubes (CNTs) after purification contributed to the effective dispersion of the CNTs in the nanocomposite adhesive. Hence, enhanced properties of FCNTs were successfully transferred into the SPI/CNTs nanocomposite adhesive. These unique functionalities on FCNTs however, improved the mechanical properties of the adhesive. The shear strength and water resistance of SPI/FCNTs was higher than that of the SPI/CNTs.

SEM images showed the homogenous dispersion of CNTs in the SPI/CNTs nanocomposite adhesive. The carbon nanotubes were distributed uniformly in the soy protein adhesive with no noticeable clusters at relatively reduced fractions of CNTs as shown in the SEM images, which resulted into better adhesion on wood surface. Mechanical (shear) mixing and ultrasonication with 30 minutes of shear mixing both showed an improved dispersion of CNTs in the soy protein matrix. However, ultrasonication method of dispersion showed higher tensile shear strength and water resistance than in mechanical (shear) mixing method. Thermogravimetric analysis of the samples also showed that the CNTs incorporated increases the thermal stability of the nanocomposite adhesive at higher loading fraction.

Incorporation of CNTs into soy protein isolate adhesive improved both the shear strength and water resistance of the adhesive prepared at a relatively reduced concentration of 0.3%.The result showed that tensile shear strength of SPI/FCNTs adhesive was 0.8 MPa and 7.25MPa at dry and wet state respectively, while SPI/CNTs adhesive had 6.91 MPa and 5.48MPa at dry and wet state respectively. There was over 100% increase in shear strength both at dry and wet state compared

to the pure SPI adhesive. The 19% decrease in value of the new adhesive developed compared to the minimum value of ≥10MPa of European standard for interior wood application may be attributed to the presence of metallic particles remaining after purification of CNTs. The presence of metallic particles will prevent the proper penetration of the adhesive into the wood substrate. The type of wood used in this study as well as the processing parameters could also result into lower value compared to the value of European standard. Therefore, optimization of the processing parameter as well as the conversion of carboxylic acid group on the surface of the CNTs into acyl chloride group may be employed in future investigation.

However, the preparation of new nanocomposite adhesive from soy protein isolate will replace the formaldehyde and petrochemical adhesive in the market and be of useful application in the wood industry.

Key terms: Adhesive; Soy protein Isolate; Carbon nanotubes(CNTs); Shear strength; Nanocomposite; Scanning electron microscopy (SEM); Fourier transform infra-red; Thermo gravimetric analysis; Performance evaluation; Wood

Contents

Copyright ..... **i**

Publications ..... **iii**

Declaration ..... **iv**

Dedication ..... **v**

Acknowledgement ..... **vi**

Abstract ..... **viii**

Contents ..... **x**

List of Tables ..... **xiii**

List of Figures ..... **xiii**

List of Abbreviations ..... **xvii**

Chapter One **1**

1.0 Introduction 1

1.1 Background and motivation 1

1.2 Research questions 7

1.3 Aim and objectives of the study 8

1.4 Contribution to knowledge 8

1.5 Scope of study 9

1.6 Structure of the dissertation 9

References 10

Chapter Two **15**

2.0 Literature Review 15

2.1 Economic importance of adhesives 15

2.2 Mechanism of adhesion 16

2.3 Theories of adhesion 16

2.4 Characteristics of soy protein 17

2.4.1 Soy protein isolate 18

2.4.3 Functional properties of soy protein 21

2.4.4 Performance of soy protein adhesive 21

2.4.5 Modification of soy protein 23
2.5 The wood 26
2.5.1 Effect of polymer/composite adhesives on bond strength and water resistance 27
2.5.2 Effect of nanofillers on soy protein matrix 30
2.6 Carbon nanotubes 31
2.6.1 Types of carbon nanotubes 32
2.7 Synthesis of MWCNTs 36
2.7.1 Chemical vapour deposition (CVD) 36
2.8 Dispersion of CNTs in polymer matrix and CNTs/polymer composite materials 39
2.8.1 Methods of dispersion 41
2.9 Functionalization of CNTs 42
2.9.1 Physical functionalization 43
2.9.2 Chemical functionalization of CNTs 43
2.10 Properties of carbon nanotubes/polymer composite adhesive materials 45
2.10.1 Electrical properties 45
2.10.2 Thermal properties 46
2.10.3 Mechanical properties 46
References 47
Chapter Three 64
3.0 Materials and methods 64
3.1 Materials 64
3.2 Methods 64
3.2.1 Preparation of Iron –Cobalt Catalyst on calcium carbonate support (Fe- Co/$CaCO_3$) 64
3.2.2 Synthesis of carbon nanotubes (CNTs) 65
3.2.3 Functionalization of the synthesized catalysts 67
3.2.4 Preparation of SPI/CNTs nanocomposite adhesive from soy protein isolate (SPI) 67
3.2.5 Determination of percentage moisture and solid content of the alkaline –modified SPI and SPI/CNTs 68
3.2.6 Preparation of wood surface and application of SPI/CNTs nanocomposite adhesive samples 69
3.3 Characterization of samples 72
3.3.1 Scanning Electron Microscopy (SEM) 73

3.3.3 Fourier transform infrared (FTIR) analysis 74
Chapter Four **75**
4.0 Results and discussion 75
4.1 Effect of processing parameters on percentage moisture and solid content of the adhesive ... 75
4.1.1 Effect of concentration of CNTs on the percentage moisture and solid contents of SPI/CNTs nanocomposite adhesive 75
4.1.3 Effect of concentration of CNTs on adhesive nanocomposite 78
4.2 Morphological structures of CNTs, FCNTs SPI/CNTs and fractured surfaces of adhesive 79
4.2.1 Morphological structures of CNTs and FCNTs 79
4.2.2 Morphology structures of adhesive nanocomposites 82
4.2.3 Morphological structures of fractured surfaces 85
4.3.1 FTIR spectra of CNTs and FCNTs 86
4.3.3 FTIR spectra of pure SPI and SPI/CNTs nanocomposite adhesive samples 87
4.4 Thermal stability and thermal degradation of CNTs, FCNTs and SPI/CNTs nanocomposite adhesives 89
4.4.1 TGA profile of CNTs and FCNTs 89
4.4.2 TGA profile of pure SPI and SPI/CNTs nanocomposite adhesive samples 90
4.5 Performance evaluation of SPI/CNTs nanocomposite adhesive for wood application 91
4.5.1 Effect of concentration on the shear strength and water resistance of adhesive nanocomposite 91
4.5.2 Effect of dispersion method on the shear strength of adhesive nanocomposite 97
4.5.3 Comparison of effect of fillers on the shear strength of soy-based adhesives from literatures 99
References 100
Chapter Five 103
5.0 Conclusion and recommendation 104
5.1 Conclusion 104
5.1 Recommendation 105
References 106
Appendix A **107**

List of Tables

Table 2.1: Approximate distribution of the major components of soy proteins (Kinsella, 1979) 20
Table 2.2: Typical composition of soy protein preparation (Kinsella, 1979) 20
Table 3.1: European (EN-204) standard's conditioning sequence and minimum values of adhesive strength for thin bond line. 71
Table 4.1: Effect of concentration of CNTs and FCNTs on the percentage moisture and solid content of adhesive nanocomposite. 75
Table 4.2: Effect of temperature on pH of SPI adhesive 77
Table 4.3: Effect of CNTs and FCNTs on the pH of modified SPI adhesive 78
Table 4.4: Effect of concentration and method of dispersion on the shear strength and water resistance of adhesive nanocomposite 92
Table 4.5: Effect of concentration of CNTs on the shear strength of SPI nanocomposite adhesive at dry and wet state 93
Table 4.6: Effect of concentration of FCNTs on the SPI adhesive nanocomposite at dry and wet state. 94
Table 4.7: Effect of method of dispersion on the maximum force at breakage and shear strength of SPI nanocomposite adhesive 97
Table 4.8: Effect of dispersion method on the shear strength of SPI nanocomposite adhesive ... 97
Table 4.9: Comparison of effect of fillers on the shear strength of soy-based adhesives with literatures 100

List of Figures

Figure 1.1: (A) Amino and carboxyl functional group in protein (Russel, 2010) (B) Primary, secondary, tertiary and quaternary structure of protein molecules (Murzin el al., 1995)..... 4
Figure 2.1: Leading adhesive and sealant market end-use in 1995 15
Figure 2.2: Diagrammatic preparation of soy protein isolate 19
Figure 2.3: Scanning electron micrograph of surface microstructure of (A) walnut and (B) pine (Sun and Bian, 1999). 27
Figure 2.4: A hexagonal sheet of graphene rolled to form a CNT with different chiralities A = armchair; B = zigzag; C= chiral (Dresselhaus et al., 1995 and Thostenson et al., 2001). 33
Figure 2.5: shows SWNT of chiral vector of bond length 1.41 A0 and tube length 20 A0. Courtesy Nano tube modeller (Ma et al., 2010)..... 33
Figure 2.6: Computer generated image of DWCNT (www.nanotechweb.org) reproduced from Endo et al., 2005. 34
Figure 2.7: Multi walled carbon nano tube without cap Courtesy Nano tube modeller front View, Armchair (Ma et al., 2013) 35
Figure 2.8: Diagram of CVD to produce CNTs adopted from Mubarak et al., 2011. 37
Figure 2.9: Distribution of micro- and nano-scale fillers of the same 0.1 vol. % in a reference volume of 1 mm^3 (A: Al_2O_3 particle; B: carbon fiber; C: GNP; D: CNT) (Ma et al., 2010) 41
Figure 2.10: Electronic microscope images of different CNTs: (A) TEM image of SWCNT bundle (B) SEM image of entangled MWCNT agglomerates [Thess et al., 1996] 41
Figure 3.1: Salts of (A) calcium carbonate (B) cobalt nitrate (C) iron nitrate..... 65
Figure 3.2: Schematic of the synthesis process for CNTs by horizontal CVD reactor 66
Figure 3.3: Schematics of dispersion of SPI/CNTs by (A) mechanical stirring methods and (B) Sonication method 68
Figure 3.4: Assembly of maple wood composite to make a sample..... 70
Figure 3.5: (A) six adhesive nanocomposite bonded samples on a metal bar (B) bonded wood samples pressed by the hydraulic machine inside the furnace at a constant temperature and pressure. 70
Figure 3.6: Basic steps in adhesive bonding technique 70

Figure 3.7: (A) Set-up of tensile testing machine with a computer system showing the readings/data values (AG-IC 20/50 KN Shimadzu) (B) Bonded wood sample clamped to the tensile test machine. 72
Figure 3.8: (A) Field electronic scanning electron microscope (Model: Carl Zeiss sigma) 73
Figure 3.9: Thermogravimetry analyzer (Model: TA SDT Q600 (DRYCAL TA)) 74
Figure 4.1: Effect of Concentration of CNTs on the percentage solid and moisture content 77
Figure 4.2: Effect of temperature on the pH of SPI solution 78
Figure 4.3: Effect of CNTs and FCNTs on the pH of modified SPI adhesive 79
Figure 4.4: SEM images CNTs (A) bundles (B) diameter of as-synthesized 80
Figure 4.5: SEM images of FCNTs by shear mixing method of purification at 1 µm and 200 nm magnifications. 81
Figure 4.6: SEM images of FCNTs by sonication method of purification at 1 µm and 200 nm magnification 81
Figure 4.7: SEM images 0.1 wt% of SPI/CNTs nanocomposite adhesive dispersed by shear mixing method at (A) 1 µm and (B) 200 nm 83
Figure 4.8:SEM images of 0.1 wt% SPI/CNTs nanocomposite adhesive dispersed by 90 minutes sonication/ 30 minutes mixing method at (A) 1 µm and (B) 200 nm. 83
Figure 4.9: SEM images of dispersion of 0.1wt% FCNTs in SPI nano-composite adhesive by mechanical mixing 84
Figure 4.10:SEM images of dispersion of 0.1wt% FCNTs in SPI nanocomposite adhesive by 90 minutes sonication and 30min mechanical mixing. 84
Figure 4.11:SEM images of fractured surface of (A) 0.1wt% SPI/CNTs (B) 0.1wt% SPI/FCNTs (C) SPINaOH (D) 0.1wt% SPI/SFCNTs adhesive samples 85
Figure 4.12: FTIR spectra of CNTs and FCNTs. 86
Figure 4.13: FTIR spectra of SPIFCNTs 0.7wt % adhesive dispersed by mechanical and sonication/mixing methods 87
Figure 4.14: FTIR spectra of pure SPI/CNTs, SPI/FCNTs and SPI/SFCNTs at 0.7wt % concentration 88
Figure 4.15: TGA profiles of synthesized CNTs and FCNTs. 90
Figure 4.16: TGA profiles of adhesive nanocomposite with varying concentrations of FCNTs ranged from 0 wt% to 0.5 wt%. 91

Figure 4.17: Effect of concentration of CNTs on the tensile shear strength and water resistance of SPI adhesive nanocomposite at dry and wet state. 94
Figure 4. 18: Effect of concentration of FCNTs on the tensile shear strength of SPI adhesive nanocomposite at dry and wet state. 96
Figure 4.19: Effect of dispersion method on the tensile shear strength of SPI adhesive nanocomposite. 98

List of Abbreviations

CVD- Chemical vapour deposition

DWCNTs- Double walled carbon nanotubes

DSP- Defatted soy protein

EN- European standard

FCNTs- Functionalized carbon nanotubes

FTIR- Fourier transmission infrared

GNP- Gold nano particles

MWCNTs Multi walled carbon nanotubes

SEM- Scanning electron microscopy

SPC- Soy protein concentrate

SPI- Soy protein isolate

SWCNTs- Single walled carbon nanotubes

TGA- Thermogravimetry analysis

Chapter One

1.0 Introduction

1.1 Background and motivation

The traditional methods of joining have well known disadvantages and shortcomings. With mechanical technique such as riveting or bolting that allows stress concentration at the bonding point, damages and weakens the material (Glen, 1998). Thermal techniques such as welding and soldering change the specific properties of the material within the heat-affected area (Amancio-Filho and Dos – Santos, 2009). All these shortcomings have necessitated the developments of new methods of joining industrial materials. Advantages of adhesive bond, one of the alternative methods of joining over the aforementioned traditional methods include time saving, cost effectiveness, conservation of properties of the material and allocation of pressure at the bonding points. Additionally, the method repels moisture and rusts, provides attractive strength per weight ratio and does not need rivets and bolts for joining (Glen, 1998; Amancio-Filho and Dos–Santos, 2009). An adhesive is a substance that can be used to bind two similar or dissimilar surfaces together, thereby forming a bond that is difficult to pull apart unless a greater force is applied (Glen, 1998). Adhesives are used in the packaging industry, shoe making industry, paper board products, construction works, floor tiles, human bones and tissue, bridge sections, paper, plastic film label (Ebnesajjad, 2011) and wood composite, to mention a few. Examples of adhesives are acrylics, epoxies, silicones, animal glue, casein, protein based adhesives and natural rubber adhesives (Ebnesajjad, 2011).

There are two basic categories of adhesive bonding; structural adhesive bonding, in which the material being bonded experience large stress up to their yield point without losing its properties within specific limits. Non-structural adhesive bonding is used to hold in place weightless materials such as, pressure sensitive tapes and packaging adhesives. Adhesives can be classified into two groups; Synthetic adhesives, which comprise of epoxies, silicones, acrylics and pressure sensitive adhesive. Natural adhesives; these include animal glue, casein, protein based adhesive

and natural rubber adhesive (Ebnesajjad, 2011). The adhesives used in all the prehistoric civilization were naturally occurring materials such as gelatin from animal parts; hoof, horn and bones, gum arabic, starch, bitumen, protein from cheese or blood starch, paste and eggs (Hussey et al., 1996). These natural adhesives were constantly in use until the twentieth century, when they suffered environmental setbacks when bonding synthetic materials and metals, though providing adequate strength (Hussey et al., 1996). Adhesive bonding for wood has been the major factor in the effective application of raw material in the wood industry over the years. Therefore, its significance will give rise to the development of new adhesive system and wood product (Navi et al., 2012). The novel wood adhesives were made of collagen extracted from bones and hides, casein (milk), blood, fish, skins and soy beans (Rowell, 2012). Grains of some legumes are starting materials for obtaining casein, adhesives, and plastics (Yang et al., 2006). Examples of such grains are; soybeans, guinea pea, locust beans and guar oil seeds. Currently, attention is on soybean flour due to their low price, availability, and easy processing. Soybean has been used by many researchers as a source of adhesive (Li et al., 2011). New technologies and environmental issues have led to the discovery of proteins especially soy flour from soybeans as an important adhesive for interior plywood and wood flooring (Feng et al., 2005).

Soybean is an annual summer legume also known as soja bean (Shurtleff et al., 2014). A number of products are manufactured from soybeans, such as, beverages, sausage, binders, diabetes foods, paints and adhesive which is the aim of this proposed study. Soybean contains 40% protein, 18% fat, 32% carbohydrate, 4.5% ash and 5.5% crude fibre (Waggle and Kolar, 1979). The protein based adhesive from marine fauna which relates to the mechanism by which mussel clings to the substrate, suggests a remarkable research area because of their bond strength and high water resistance. However, they are too costly and not readily available for wood composites. A successful research has been carried out to imitate the bonding properties of marine fauna in other protein such as soy protein (Liu et al., 2004). Presently, most wood industries are interested in petrochemical-based and formaldehyde-based adhesives such as, phenol formaldehyde resin and urea-formaldehyde resins in the preparation of wood composites (Lin et al., 2012). Although, adhesives produced from them possess high glue strength and high water resistance, but formaldehyde released from wood composites was recently discovered to be poisonous and toxic to human. These endanger the lives of workers and users of the wood

composite. In addition to these, petrochemical-based adhesives are non-renewable, limited and costly (Lin et al., 2012). Therefore, the improvement of environmental-friendly adhesive from natural agricultural products has awakened noteworthy attention. Among many of the renewable resources, the soy protein has been discovered to be the best relevant starting material for wood adhesive (Feng et al., 2005). A soy protein based adhesives, when modified chemically is said to have the same good adhesive properties as petroleum-based and formaldehyde-based adhesives for interior wood products (Liu et al., 2010). Owing to poor water moisture of the presently available soy-based adhesives, the potential of soy bean has not been well utilized and has prevented many wood industries from using it as adhesive for wood composites. In view of this, many efforts have been made to enhance the water resistance of soy based adhesives, such as, bio enzyme alteration (Schmitz, 2009), improvement of cross linking (Lambuth, 1977) and nano modification (Qiaojia et al., 2012; Jin et al., 2006).

A protein comprises of 20 amino acids which differ from one another (Peng et al., 1984). Protein is a polymer of amino and carboxylic acids joined together by peptide bonds (Figure 1.1A). The unique features of proteins are the classification of side groups propagating from the peptide support. These side groups include hydrocarbons, amines, carboxylic acids, hydroxyl, thiol and phenolic groups (Berg et al., 2002). Each side group on the peptide bond is the reactive sites of protein. Proteins can be easily identified on the basis of sedimentation velocity using ultracentrifugation. Soy proteins can be grouped into four fractions; 2S, 7S, 11S, and 15S (letter S stands for Svedburg units). Each fraction is a complex mixture of protein (Aspinall, 1988; Wang, 2006). The structures of a protein are divided into: primary, secondary, tertiary and quaternary (Figure 1.1B). The primary structure is amino acid order, joined by peptide bonds (Wolf, 1970). The secondary structure is the relative location of amino acids within the polypeptide chain which determines the formation of helices and sheets. The tertiary structure relates to the location of a portion of the peptide chain with respect to other part of the same peptide chain while the quaternary structure is the arrangement in space of one peptide chain with another peptide chains (Pines et al., 1980). The types of bonds present in protein can be categorized into; covalent and non-covalent bonds. Covalent bonds are peptide link between amino acid residue and disulphide bonds. Non covalent bonds are the static interaction, hydrophobic interaction, Van der Waal interaction and hydrogen bonding (Feeney et al., 1977).

Chemical modification of protein is one of the most useful techniques in biochemical application since minor alterations in its structure can lead to great variations in their physical and biological properties (Wang, 2006).

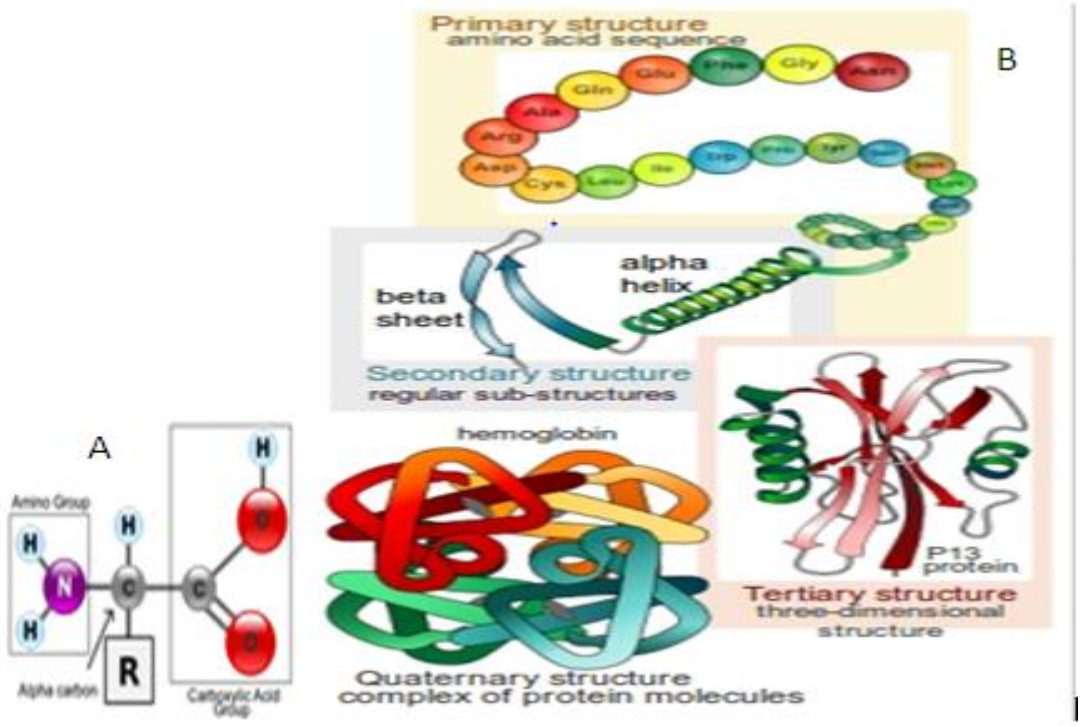

Figure 1.1: (A) Amino and carboxyl functional group in protein (Russel, 2010) (B) Primary, secondary, tertiary and quaternary structure of protein molecules (Murzin el al., 1995)

Soy protein is a plant protein with various potential applications due to its environmental friendliness, easy availability and relatively low cost (Wang et al., 2014). Soy proteins are mainly spherical and have hydrophilic behaviour. The major proteins are the globulins which are insoluble at iso electric point (IEP). The solubility of protein in water or salt solution is observed only at pH value above or below the IEP (Lambuth, 1977), that is 1.5 – 2.5 and $\geq$ 6.3. The iso electric point of proteins is at a pH of 4.5, which is responsible for the insolubility of protein between the pH of 3.75 and 5.25. Soy proteins have a well arranged structure with most hydrophilic group attached at the surface and most hydrophobic groups hidden inside (Horton et al., 1996). Protein – protein interaction and protein – substrate interaction is greatly affected by the structure and distribution of hydrophobic and hydrophilic groups on the protein glue (Mo et

al., 2004). Large variety of side groups present in soy protein results into many diverse functional properties, which can be varied through physical, chemical, and enzymatic modification at secondary, tertiary and quaternary levels without altering the primary level (Feeney et al., 1977). Modification of soy protein such as denaturation involves unfolding of the polar protein molecules by breaking hydrogen and disulfide bonds in the protein arrangement (Wu et al., 1974; Kinsella, 1979). Ordinarily the majority of polar and non-polar groups in protein are not available, because of the internal bonds resulting from Van der Waal's forces, hydrogen bonds and hydrophobic interaction. Therefore, a simple paste of soy flour is a poor adhesive and a chemical change is necessary to break the internal bonds and unfold or disperse the polar protein molecules (Lambuth, 1977; Kumar et al., 2008). Hydrolysis of protein enhances dispersion and unfolding of protein which result into increased amino and carboxylic groups (Lambuth, 1977; Thames, 1994). This will improve the adhesive strength and water resistance of soy protein adhesive but may as well reduces the service life (Lambuth, 1977).

Soy flour is a by-product from soybean and can be refined to produce defatted soy protein (DSP), soy protein concentrate (SPC) and soy protein isolate (SPI). In particular, soy protein isolate has higher percentage of proteins with 18 amino acids than other soy protein products (Wolf, 1970; Rhim, 2007). These make it a better alternative material for wood adhesive. The process of obtaining soy flour from soybean involves extraction of oil, using hexane as organic solvent, which is the most efficient method (Sun et al., 2003; Jim et al., 2004). Soy protein isolate is obtained with a precipitation method, including removal of some insoluble carbohydrate through precipitation in a milky alkaline water solution of protein at pH range of 8-9 (Sun, 2013). However the knowledge of chemistry, careful adjustment and functional properties of modified soy protein will help in the improvement of biodegradable industrial products such as different binders, plastics and adhesives from soy protein isolate (Feeney et al., 1977). SPI can be modified through physical, chemical, and enzymatic treatment (Sharma et al., 2011). These treatments enhance cross linking in SPI or adjust the side chain of SPI. Examples are, incorporation of filler, acetylation, blending with other polymers, esterification, and denaturation (Sharma et al., 2011). It has been shown that incorporation of proper nano filler can improve the mechanical properties of soy protein based adhesive (Wang et al., 2006).

Filler is incorporated into a polymer to improve its properties, regulate the viscosity, modify the surface properties or simply reduce cost (Callister, 1991). The commonly used fillers such as talc, calcium carbonate fibers, wood flour, which were introduced previously in the preparation of adhesive from soy protein often require large amounts of fillers in the polymer (Callister, 1991). However, nanofillers improve the properties of a polymer at reduced concentration. Presently, polymer composites with improved electrical, mechanical, thermal barrier and fire retardancy properties are broadly employed in numerous industrial applications (Cho et al., 2006 and Wetzel et al., 2003). Examples are actuators, non-electric chemical, manufacturing and scanning probes (Iijima, 1991). A composite is the combination of two or more dissimilar materials mixed in order to blend the unique properties of both (Twardowski, 2007). Nanocomposite is therefore, two or more dissimilar materials in which one of the components has at least one dimension at a nanoscale diameter around 10^{-9}m (Twardowski, 2007). Owing to the nano diameter of the nano fillers, they have a higher surface area, which makes polymer composites to exhibit exceptional mechanical properties than commonly used fillers (Jia et al., 1999). Examples of nanomaterials are carbon nanotubes, carbon nanofibers and nano particles such as gold, silver, diamond, copper, and silicon.

Carbon nanotubes (CNTs) are receiving great considerations owing to their matchless multifunctional and enhanced mechanical, thermal, electronic and magnetic properties (Rouff et al., 1995; Bernholc et al., 1997). Investigation has been carried out to mix carbon nanotubes with epoxy adhesive so as to improve their adhesion energy (Wang et al., 2006). The electrical conductivity properties of CNTs make adhesives suitable for electronic and display application (Baughman et al., 2002). CNT is a unique crystalline carbon form, having a rod-shaped sp^2 carbon structure alongside its length without any defects (Barba et al., 2002). One of the most significant uses of CNT is its role as filler in polymer nanocomposite. This has been found to enhance the mechanical properties such as, shear strength, tensile strength (Kanagaraj et al., 2007) and tensile modulus (Jim et al., 2007). In some cases, CNT adds to the instantaneous increase in strength, elongation, and thermal conductivity of polymer composites (Sankapal et al., 2007).

Owing to problems encountered in dispersion of nanofiller in a soy protein matrix and strengthening the interfacial adhesion between the soy protein matrix and the nanofiller, chemical modification of the nanofiller surface is necessary. This is to realize improvement in miscibility between the filler and the soy-protein matrix (Camponeschi et al., 2007). Various approaches have been taken to overcome these challenges, such as, high shear mixing, or sonication (Lau et al., 2006), surfactants (Gong et al., 2000) and lately attentions have been on chemical functionalization of the nanotubes (Gojny et al., 2004). Functionalization of CNTs can be successfully achieved, because multiwalled carbon nanotubes are layers of many pure carbons whose properties can be manipulated using the knowledge of chemistry. Consequently, the modification of the structure may improves solubility and dispersion of CNTs, thus allowing numerous applications of materials.

Although, recently there are research efforts towards incorporation of carbon nanotubes as filler in polymer adhesive such as, epoxy resin (Yu et al., 2010; Sydlik et al., 2013), plastics, such as polyamides (Meng et al., 2013) and polypropylene (Gandhi et al., 2013). This is because of their physical, mechanical, thermal conductivity and optical properties (Li et al., 2004). However, this study seeks to investigate the effect of methods of dispersion of carbon nanotubes on the mechanical properties of soy protein isolate adhesive. The study also aims at improving the tensile shear strength and water resistance of the soy protein adhesive by incorporating carbon nanotubes as the nanofiller.

1.2 Research questions

This study is set to answer the following questions:

(i) What will be the effect of carbon nanotubes on water resistance of soy protein adhesive?

(ii) What will be the effect of adding carbon nanotubes to soy protein adhesive on its mechanical properties?

(iii) What effect does functionalization of multiwalled carbon nanotubes has on improvement of dispersion of carbon nanotubes in the soy protein isolate adhesive?

(iv) Could dispersion of functionalized multiwalled carbon nanotubes in soy protein isolate improve the mechanical properties of the nanocomposite adhesive?

1.3 Aim and objectives of the study

The aim of this study is to prepare and characterize adhesive nanocomposite from soy protein isolate. Other specific objectives of the research are to;

- Synthesis of Fe-Co catalyst on $CaCO_3$ support and characterization of Fe-Co catalyst on $CaCO_3$ support using scanning electron microscopy (SEM).
- Synthesize carbon nanotubes by chemical vapour deposition method (CVD) using the catalyst and C_2H_2 carbon source and characterize the synthesized and functionalized CNTs using; SEM, thermogravimetric analysis (TGA) and Fourier transmission infrared (FTIR) spectroscopy.
- Prepare SPI/CNTs nanocomposite adhesive by dispersion of varying concentration of CNTs and FCNTs into the alkaline modified soy protein solution by mechanical (shear mixing) and sonication method. Characterize the SPI/CNTs nanocomposite adhesive oven-dried samples using; SEM, FTIR and TGA.
- Study the influence of functionalized multiwalled carbon nanotubes on the enhancement of mechanical properties of SPI/CNTs nanocomposite adhesive.
- Study and compare the moisture resistance and shear bond strength of ordinary alkaline modified SPI adhesive with SPI/CNTs nanocomposite adhesive on wood samples

1.4 Contribution to knowledge

This study is expected to provide specific information on how carbon nanotubes can enhance the mechanical properties of the soy protein isolate adhesive by;

- Investigate the effect of dispersion methods of functionalized multiwalled carbon nanotubes in the soy- protein isolate on the mechanical properties of the nanocomposite adhesive.
- Investigating the effect of dispersed carbon nanotubes on the mechanical properties of soy protein adhesive.
- Determining the effect of dispersed carbon nanotubes on water resistance of soy protein adhesive.

1.5 Scope of study

Wet impregnation method of synthesizing catalyst iron (III) nitrate and cobalt (II) nitrate catalyst supported on calcium carbonate (Fe-Co/$CaCO_3$) was employed in this study. The synthesized Fe-Co/$CaCO_3$ was used with acetylene as the carbon source and nitrogen as carrier gas in the production of carbon nanotubes in a horizontal chemical vapour deposition (CVD) reactor. The CNTs and FCNTs were limited to only characterizations by scanning electron microscope (SEM) analysis to determine their morphological structure, Fourier transmission infrared (FTIR) spectroscopy to determine the functionalities and the type of functional groups attached to the surface of the adhesive during functionalization and thermogravimetric analysis (TGA) for thermal stability and thermal degradation samples. There are different methods of dispersion of CNTs into a polymer matrix. However, only mechanical (shear mixing) and sonication methods were employed in this study and the homogeneous dispersion of the two methods were compared. The nanocomposite adhesives samples were characterized using SEM, FTIR and TGA only. The bond strength and water resistance of the ordinary SPI and SPI/CNTs composite adhesives were determined and compared according to European standard EN-200 standard of testing wood adhesive for interior purposes.

1.6 Structure of the dissertation

The structure of the dissertation is as follows:

Chapter one (Introduction)

This is the introductory part of the work which gives details of the background and motivation to the work, research questions, aim and objectives of the research and contribution of the research to knowledge.

Chapter two (Literature review)

This section of the write up gives the available information relating to the studies being carried out.

Chapter three (Materials and methods)

Materials: Under this section, the instrumentation used to carry out the analysis, characterization and tests on the samples are reported.

Methods: Here all the experimentations carried out during the course of the study are stated.

Chapter four (Results and discussion)

Results: This section presents the figures of experimental data which are represented by bar charts, tables, graphs, and images from micro- graphs.

Discussion: This is the interpretation of the data presented in the figures, tables and images.

Chapter five (Conclusion and recommendation)

Conclusion: This section of the dissertation gives the summary of the major findings or deductions obtained from the discussion of result in chapter four

Recommendation is for further studies that are not covered during the investigation of this study.

References

Amancio, F., Dos Santos, J.F. (2009) Joining of polymers and polymer – metal hybrid structures: Recent development and trends. Polymer Engineering and Science. Vol. 49, No 8, pp 1461 – 1464.

Barba, A.H., Chen, S.R., Kenig, S. and Wagner, H.D. (2004) Interfacial fracture energy measurements for multiwalled carbon nanotubes pulled from a polymer matrix. Composite Science and Technology. Vol. 64, pp 2283-2289.

Baughman, R.H. and Zarkhidov, A.A. (2002) Carbon nanotubes. The Route Towards Application Science. Vol. 297, pp 787-292.

Bernholc, J., Roland, C. and Yakobson, B.I. (1997) Nanotubes. Current Opinion in Solid State and Material Science. Vol. 2, pp 706-715.

Berg, J.M., Tymoczko, J.L., Stryer, L. (2002) Biochemistry 5th ed. W.H, Freeman and co. New York. NY.

Callister, W.D. (1991) Material Science and Engineering: An introduction. Material and Design. Vol. 12, No 1, pp 59.

Camponeschi, E.L. (2007) Dispersion and alignment of carbon nanotubes on polymer based composites. PhD thesis School of Material Science and Engineering, Georgia Institute of Technology, U.S. pp 1-3.

Cho, J., Joshi, M.S. and Sun, C.T. (2006) Effect of inclusion of size on the mechanical properties of polymeric composite with micro nanoparticles. Composite Science and Technology. Vol. 66, No. 13, pp 1941-1952.

Ebnesajjad, S. (2011) Handbook of adhesive and surface preparation: Preparation, Application, and Manufacturing. A Volume in Plastic Design Library, pp 3-13

Feeney, R.E., and Whitaker, J.R. (1977) Food protein: Improvement through chemical and enzymatic modification. Advanced Chemistry Symposium Series 160. Journal of American Chemistry Society. Washington DC, pp 3 - 31

Feeney, R.E., and Whitaker, J.R. (1985). Chemical modification of soy protein. Journal of American Chemical Society, vol. 5, pp 181 – 219.

Feng, F. and Ye, L. (2005) Food chemistry. Chemical Industrial Press. No 65.

Gandhi, R.A., Palanikumar, K., Ragunath, B.K. and Davim, J.P. (2013) Role of carbon nanotubes in improving wear properties of polypropylene (PP) in dry sliding condition. Material and Design. Vol. 48, pp 52-57

Glen, A.R. (1998) Adhesives. Journals of Adhesives and Adhesion. Vol. 71, pp 17-27.

Gojny, F.H., Wrehmann H.G., Kopke, U., Fudler, B. and Ye, M. (2004) Mechanical properties of multiwalled carbon nanotubes/epoxy composites, influence of network morphology. Composite Science and Technology. Vol. 64, pp 2363-2371.

Gong, X., Liu, J., Baskaran, S., Voise, R.D. and Young, J.S. (2000) Surfactant assisted processing of carbon nanotube/polymer composites. Chemistry Matter. Vol. 12, pp 1049-1052.

Horton, H.R., Moran, L.A., Ochs, R.S., Rawn, J.D. and Scimgeour, K.G. (2002) Protein: Three dimensional structure and function. In Principle of Biochemistry, pp 79 - 117

Hussey, R.J. and Josephine, W. (1996) Structural adhesive: Directory and Databook (1st ed.).Printed in Great Britain by Edmundsbury press, Bury St Edmunds, Suffolk. ISBN 0412714701.

Iijima, S. (1991) Helica microtube of graphitic carbon. Nature. Vol. 354, pp 56-59.

Jia, Z., Wang, Z., Xu, C., Liang J., Wei, B., Wu, D. and Zhu, S. (1999) Study on poly (methyl methacrylate) carbon nanotube composite. Material Science and Engineering. Vol. A 271, pp 395-400.

Jim, S.H., Park, Y.B. and Yoon, K.H. (2007) Rheological and mechanical properties of surface modified MWCNTs. Filled PET composite. Composite Science and Technology. Vol. 67, pp 3434-3440.

Kanagaraj, S., Varanda F.R., Zhiltsova, T.V. and Oliveira, M.S. (2007) Mechanical properties of high density polyethylene/CNTs composite. Composite Science and Technology. Vol. 67, pp 3071-3077.

Kinsella, J.E. (1979) Functional properties of soy protein. Journal of American Oil Chemistry. Vol. 56, pp 242 – 258.

Kumar, R., Liu, D. and Zhahg, L. (2008) Advances in proteinous biomaterials. Journals of Bio-based Matter. Vol. 2, pp 1-24.

Lau, K.T., Lu, M. and Liao, k. (2006) Improved mechanical properties of coiled CNTs reinforced epoxy nanocomposite. Composite A. Vol. 37, pp 1837-1840.

Li, N., Wang, Y., Telly, M., Bean, S.R., Wu, X., Sun, X.S. and Wang, D. (2011) Adhesive performance of sorghum protein extracted from sorghum DDSG and flour. Journal of Polymer Environment. Vol. 19, pp 755-765.

Li, C.S., Liang, T.X., Lu, W.Z., Tiang, C.H., Hu, X.Q., Cao, M.S. and Liang, T. (2004) Improving the antistatic ability of polypropylene fibers by inner antistatic agent filled with carbon nanotubes. Composite Science and Technology. Vol. 64, pp 2089-2096.

Lin, Q., Chen, N., Bian, L. and Fan, M. (2012) Development and mechanism characterization of high performance soy-based adhesive. International Journal of Adhesive. Vol. 34, pp 11-16.

Liu, Y., Li, K. (2004) Modification of soy protein for wood adhesive using mussel protein as a model: The influence of a mercapto group .Macromolecular Rapid Communication. Vol. 25, pp 1835 -1838.

Liu, L. and Wagner, H.D. (2005) Rubbery and glassy epoxy resins reinforced with carbon nanotubes. Composite Science and Technology. Vol. 65, pp 1861-1868.

Liu, D., Chen, H., Chang, P.R., Wu, Q., Li, K. and Guan, L. (2010) Biomimetic soy-Protein nanocomposite with calcium carbonate crystalline arrays for use as wood adhesive. Bio-resource Technology. Vol. 101, pp 6235-6241.

Mo, X., Sun, X., Wang, D. (2004) Thermal properties and adhesion strength of modified soy bean storage protein. Journal of American Oil Chemistry Society. Vol. 81, pp 395 – 400.

Murzin, A.G., Brenner, S., Hubbard, T. and Chothia, C. (1995) "SCOP; Astructural classification of protein database for the investigation of sequences and structures.Journal of Molecular Biology. 247(3), 536-540.

Peng, I.C., Quass, D.W., Dayton, W.R. and Allen, C.E. (1984) The physicochemical and functional properties of soybean 11s globulin- A review. Cereal Chemistry. Vol. 61, pp 480-490.

Pine, S.H., Hendrickson, J.D., Cram, D.J., Hambiond, G.S. (1980) Amino acids, peptides and proteins. Inorganic chemistry 4th ed. McGraw-Hill Kogakusha,Ltd, Tokyo.

Qiaojia, L., Chen, N., Bian L. and Fan, M. (2012) Development and mechanism Characterization of high performance soy-based bio adhesive. International Journal of Adhesion and Adhesive Vol. 34, pp 11-16.

Rouff, R.S. and Lorent, D.C. (1995) Mechanical and thermal properties of carbon nanotubes. Carbon. Vol. 33, pp 925-93.

Rowell, R.M. (2012) Handbook of wood chemistry and wood composite. CRS press, Boca Raton, U.S.

Russel, P.J. (2010) iGenetics: A Molecular Approach, 3rd ed.

Sankapal, B.R., Setyowati, K., Chen, J. and Liu, H. (2007) Electrical properties of air stable iodine-doped CNTs. Polymer Composite, Applied Physics. Vol. 91, pp 173105- 173110.

Schmits, J.F. (2009) Enzyme modified soy flour adhesive. PhD thesis. Food Science and Human Nutrition; Bio renewable Resources and Technology. Lowa State University, Ames, Lowa, pp 92 – 94.

Sharma, S.K., Clack, J.H., Mudhoo, A. (2011) Handbook of applied biopolymer technology: Synthesis, Degradation and Application. Royal Society of Chemistry. pp 110-112.

Shurtleff, W., Huang, H.T. and Aoyayi, A. (2014) History of soybean and soy food in China and Taiwan and in Chinese cookbooks, restaurants and Chinese work with soy foods outside China. ISBN 978-1-928914-68-6. pp 777.

Sun, X.S. (2005) Soy protein adhesives. Bio-based Polymer and Composite. pp 322 – 368.

Sun, X.S. (2013) Soy-protein as plywood adhesive: formulation and characterization. Journals of Adhesive Science and Technology. Vol. 27, No 18, pp 2014 – 2026.

Sydlik, S.A., Lee, J.Y., Walish, J.J., Thomas, E.L. and Swager, T.M. (2013) Epoxy functionalized multiwalled carbon nanotubes adhesives. Carbon. Vol. 59, pp 109 – 120.

Thames, S.F. (1994) Soy bean poly peptide polymers. In identifying new industrial use for soybean protein.C.P. Baumel, Johnson, L. and Greiner, C.A edss. Special Repo 95.Lowa State University. Ames, IA.

Twardowski, T.E. (2007) E-book on introduction to nanocomposite materials: Properties processing characterization. ISBN No. 978 – 1 – 932078 – 54 – 1

Twardowski, T.E. (2007) Introduction to nanocomposite materials: Properties, Processing and Characterization. ISBN 978-1-932078-54-1.Destech publication, Inc U.S.A.

Waggle, D.H. and Kolar, C.W. (1979) Types of soy-protein product. Soy protein and human nutrition. Academic Press, New York, pp 19-51.

Wang, Y. (2006) Adhesive performance of soy protein isolate enhanced by chemical modification and physical treatment. Journal of American Oil Chemistry Society. Vol. 81, pp

Wolf, W.J. (1970) Soy protein: Their functional, chemical and physical properties. Journals of Agricultural Food Chemistry. Vol. 18, pp 969 – 976.

Wang, L., Xiao, M., Dai, S., Sonf, J., Ni, X., Fang, Y., Corke, H. and Jiang, F. (2014) Interaction between carboxylmethyl konjac glucomannan and soy-protein isolate in blended films. Carbohydrate Polymers. Vol. 101, pp 136-145.

Wetzel, B., Haupert, F. and Zhang, M.Q. (2003) Epoxy nanocomposite with high Mechanical and tribological performances. Composite Science and Technology. Vol 66, issue 14, pp 2055-2067.

Wu, Y.V. and Inglet, G.E. (1974) Denaturation of plant protein related to functionality and food application. A Review. Journal of Food Science. Vol. 39, pp 218 – 225.

Yang, I., Kuo, M., Mayer, D.J. and Pu, A. (2006) Comparison of protein based adhesive resin for wood composite. Journals of Wood Science. Vol. 52, pp 503-508.

Yu, S., Tong, M.N. and Critchlow, G. (2010) Use of carbon nanotubes reinforced epoxy as adhesive to join aluminium plates. Material and Design. Vol. 31, pp 126 – 129.

Chapter Two

2.0 Literature Review

2.1 Economic importance of adhesives

The development of adhesives has gained a stable position in an increasing number of production processes over the years. There is almost no product in our surroundings that does not have at least one adhesive. Such as the protective coating on automobile, label on a beverage bottle and profiles on windows frames (Elias et al., 1990). Rising demand for adhesives will cause a dynamic economic development in developing countries like Brazil, India, China and Russia in the future (Elias et al., 1990). The prevalent markets for adhesives are packaging, industrial assembly and wood related products. Figure 2.1 shows the leading adhesive and sealant market end-use in 1995. Types of adhesive include non-reactive adhesives, drying adhesives, pressure sensitive adhesive, contact adhesive, multi part adhesive (polyester resin, polyurethane resins), one–part adhesive, natural adhesive, casein (animal glue, starch, dextrin) and synthetic adhesive (thermosetting, emulsion, thermoplastic, epoxy and polyurethane) (Takemura et al., 1985).

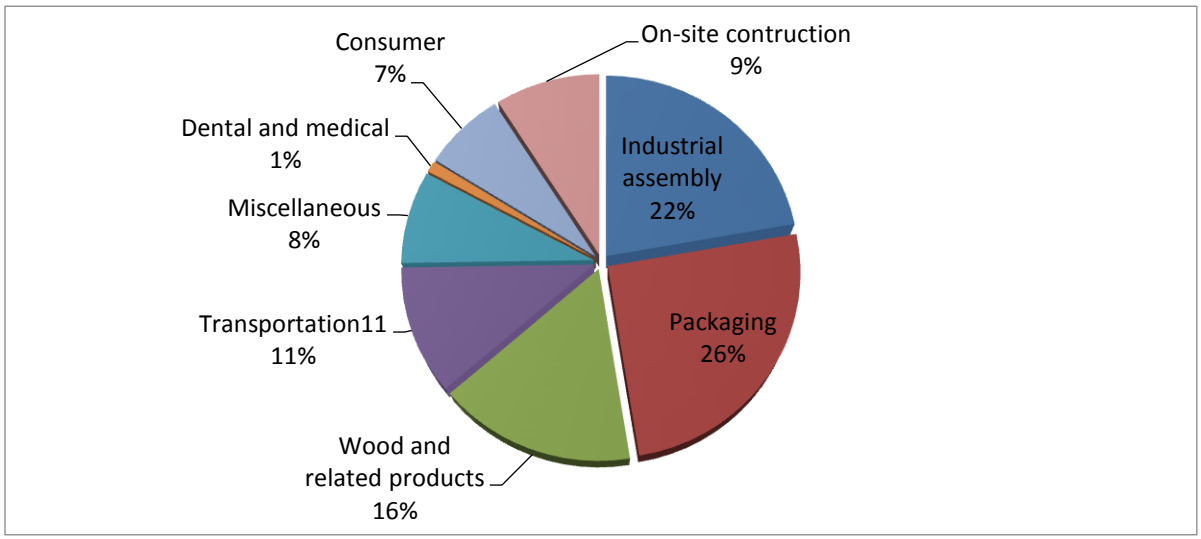

Figure 2.1: Leading adhesive and sealant market end-use in 1995

2.2 Mechanism of adhesion

When an adhesive is applied on the surface of a substrate, it works its way into small pores of the substrate. Adhesion may occur between adhesive and substrate either by mechanical means or by one of several chemical mechanisms (Ratna et al., 2001). The strength of adhesion is dependent on many factors including the means by which it takes place. In some circumstances, an actual chemical bond occurs between adhesive and substrate (Takemura et al., 1885). In other electrostatic forces, as in static electricity hold the substances together. Another mechanism involves the Vander Waal forces that develop between molecules and lastly the mechanism which involves the moisture-aided diffusion of the glue into the substrate, followed by hardening (Takemura et al., 1985 and Ratna et al., 2001).

2.3 Theories of adhesion

There are three main theories of adhesion which are adsorption, electrical and diffusion. Surface preparation of the substrate before applying adhesive is very important for these theories to hold (Petri, 2007). Adhesives are classified according to the way they react chemically after they have been applied to the surface to be joined. There are different kinds of adhesives, therefore the appropriate one must be chosen for the material to be joined. A material must meet four main requirements in order to perform as an adhesive (John, 1990 and Petri, 2007).

(i) It must displace all air and other contaminants present and wet the surfaces

(ii) It must adhere to the surfaces, stay in position and become tacky

(iii) It must develop strength.

(iv) It must remain stable i.e. unaffected by time, environmental conditions and other factors as long as the bond is required.

Adhesion between adhesives and substrates is complicated, and no single theory accurately describes the interactions that take place at the interface. Several adhesion mechanisms include mechanical interlocking, electron transfer, boundary layers and interfaces, adsorption, diffusion, and chemical bonding (Petri, 2007). Surface morphology and physicochemical surface properties of the substrate and adhesive influences the bonding strength for mechanical interlocking

mechanism. For electronic theory, an electron transfer may occur and different electronic bond structure exists between the substrate and the adhesive (Harshorn, 1986 and Petri, 2007). The theory of boundary layers is that even when the failure appears to be interfacial, the cohesive strength of a weak boundary layer can always be considered as the key factor in determining the level of adhesion (Petri, 2007). Adsorption theory is based on the postulate that provided that intimate contact is achieved, the adhesive will adhere to the substrate due to intramolecular and intermolecular forces developed at the interface through van der Waals and Lewis acid-base interactions (Koehn, 1954). Diffusion theory is based on the principle that a communal diffusion of macromolecules arises across the interface between the substrate and adhesives to form an interphase causing adhesion strength (Koehn, 1954 and Harshorn, 1986). For the chemical bonding theory, chemical bonds formed across the substrate-adhesive interface greatly improve the adhesion strength. Adhesion theory between protein polymers and wood substrates is mainly attributed to a combination mechanical bonding, physical adsorption, and chemical bonding, which are the three major mechanisms. The significance of each mechanism for a protein based adhesive should be determined by the nature of the adhesive and the substrate to be used (Harshorn, 1986).

2.4 Characteristics of soy protein

The protein content in soybean seed (Glycine max (L.)Merrill) is approximately 40% and the oil content is approximately 20%. This crop has the highest protein content and the highest gross output of vegetable oil among the cultivated crops in the world. In 2007, the total cultivated area of soybean in the world was 90.19 million ha and the total production was 220.5 million t (FAO, 2009). Soybean was originated from China, which was the world's largest producer of soybean and exporter during the first half of the 20th century (Qiu and Chang, 2010). Legumes such as soybeans, guinea pea, pigeon pea and guar oil have also been grown in various part of Africa of which the leading producers are Nigeria, South Africa and Tanzania (Abate et al., 2011). Soybean is a popularly grown crop in South Africa. However, people are unfamiliar with its economic importance, which affects demand and attitude towards its products. Recently, attitude towards soya products is dramatically changing because soybean is not only a good source of protein, it also has exceptional functional properties that make it useful for industrial applications (Penstone, 1996).

Soybean plants are legumes that originated in eastern Asia (Pearson, 1984). Soybeans are typically processed by cracking the seed, dehulling, drying, flaking, extracting oil, redrying, and milling the co-products into useful fractions (Bian et al., 1961). Soy-based products of the milling process include soy flours, from which soy protein concentrates and isolates can by produced, which are all defined by protein content (Bian et al., 1961). Defatted soy flours are the least refined soy-based products and are produced by simply grinding defatted soybeans. They are commonly comprised of 44-50% protein, 30% carbohydrates, and 20-25% fiber, ash, and water (Lusas and Rias, 1995). Soy protein concentrates are comprised of 65-72% protein, 20-22% carbohydrates, and 7.5-10% fibre and ash. Soy protein isolates are the most refined co-product and represent the highest overall protein concentration. Soy protein isolates contain at least 90% protein on a dry basis (Wolf, 1970). Soy protein products vary not only in protein concentration, but depending on the processing conditions, can vary based on particle size, solubility, water absorption, colour, nutritional quality, viscosity, and adhesive quality (De, 1979). Although carbohydrates play roles in water binding and viscosity, proteins are the primary functional component in soy-based materials coproducts (Kinsella, 1979). In general terms, protein is a polymer of α-amino carboxylic acids linked by peptide bonds.

2.4.1 Soy protein isolate

Soy protein isolate (SPI), the major component of soybean is readily available from renewable resources and agricultural processing by-products (Nielson, 1985; Zhong and Sun, 2001). The utilization of SPI in the preparation of biodegradable materials, such as adhesives, plastics, and various binders, has received more attention in recent years (Kumar et al., 2002). Plastics from SPI have very high strength and good biodegradability. However, they are also brittle and water sensitive, which limits their applications (Paetau et al., 1994; Lodha and Natravali, 2002). The SPI-polymer is highly hygroscopic/moisture sensitive in nature due to presence of amine, amide, carboxyl and hydroxyl groups (Creighton, 1993). Therefore, the properties of the SPI have commonly been modified by physical, chemical, or enzymatic treatments. Such treatments mainly promote cross-linking within SPI or modify the side chains of SPI, for example, acetylation and esterification, (Huang, 1994) denaturation (Rhim et al., 1998), incorporating fillers (Otaigbe and Adams 1997) and blending with other polymers (John and Bhattacharya, 1999).

Membrane technologies, ultrafiltration and electro-acidification have been considered for the production of SPI. Ultrafiltration has received considerable interest over the years as it represents a mild process for the concentration of soy proteins as the proteins are retained by the membrane while the oligosaccharides and minerals should be removed as they permeate through the membrane (Alibhai et al., 2006). One advantage of ultrafiltration is that products of ultrafiltration have improved properties over conventionally produced SPC and SPI probably because there are no excessive uses of chemicals (Liu et al., 1989).

SPI can also be obtained with a precipitation method, including removal of some insoluble carbohydrate through precipitation in a milky alkaline water solution of protein at pH range of 8-9 (Sun, 2013), as shown in Figure 2.1.

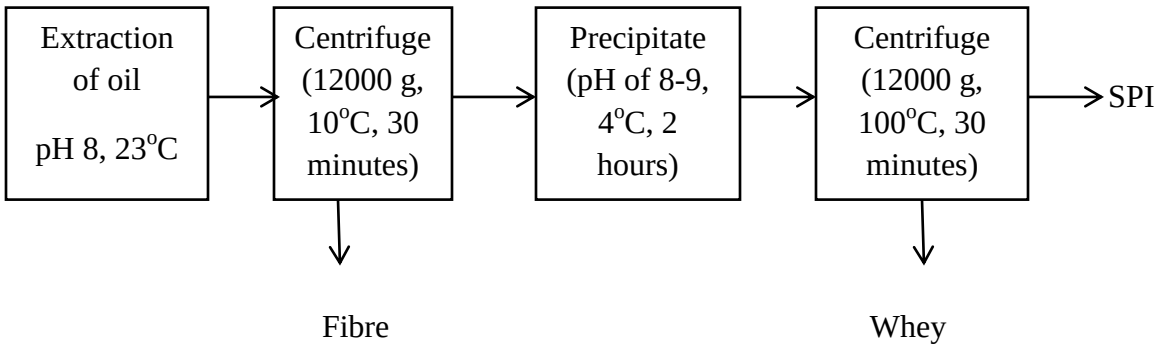

Figure 2.2: Diagrammatic preparation of soy protein isolate

2.4.2 Fractional properties of soy protein

Table 2.1: Approximate distribution of the major components of soy proteins (Kinsella, 1979)

Fraction	Content	Principal components
2S	8	Trypsin inhibitor, Cytochrome
7S	35	Lipoxygenase, Amylase, Globulins
11S	52	Globulins
15S	5	Polymers

Table 2.2: Typical composition of soy protein preparation (Kinsella, 1979)

Component	Soy flours (%)	Concentrates (%)	Isolates (%)
Protein	56.0	72.0	96.0
Fat	1.0	1.0	0.1
Ash	3.5	4.5	0.1
Fibre	6.0	5.0	0.1
Carbohydrates	33.5	17.5	0.3

2.4.3 Functional properties of soy protein

A protein comprises of 20 amino acids which differ from one another (Peng et al. 1984). The amino ($-NH_2$) and carboxyl (-COOH) groups form peptide bonds and the amino acid. Soy proteins are mainly spherical and have hydrophilic behaviour. They have their isoelectric point (IEP) at approx. pH of 4.5. Soy protein can be divided into 2 groups, globulin which is the major fraction and albumin. Globulins are soluble in salt solution while albumins are soluble in water. Globulin can be further categorized into glycinin and conglycinin. Glycinin have a molecular weight between 200000- 4000000 g/mol and conglycinin have a molecular weight of between 100000-200000 g/mol. Soy proteins have great potential as bio-based adhesives. Soy protein can be fractionated into 4 main groups on the basis of sedimentation velocity as 2S, 7S, 11S, and 15S (Rhee, 1994). The most abundant soy protein (approx. 70%) are the globulins which are largely glycinin (11S) and conglycinin (globulin portion of 7S).The functional properties of soy protein include structure formation (emulsification, foam and film formation) and texture modification (gelation and thickening). More often the functional properties of soy protein are limited by their relative poor solubility particularly close to the iso-eletric point (Kinsella, 1979).

2.4.4 Performance of soy protein adhesive

The adhesive performance of soy protein is dependent upon the particle size, nature of surface, structure of protein, its viscosity and pH. Other factors which can affect their performance are the processing parameters, such as press temperature, pressure and time.

Particle size: This has a significant effect on its suitability and performance. Finess of the grind is often expressed in terms of specific surface area (cm^3/g according to standard test) than mesh size. A specific surface area of 3000-6000cm^2/g is considered to be satisfactory for adhesive grade or in other words at least 97% should pass through 325 mesh screen.

Nature of surface and substrate: Adhesive properties are also dependent on the nature of the surface to be bonded. If the surface is too rough, it will cause a cohesive failure and if the surface structure is too smooth, it will cause an adhesive failure (Schmitz, 2009). The bonding between adhesive polymers and wood polymers is mostly caused by a combination of mechanical

adhesion (interlocking by adhesive penetration through porous wood surfaces) and molecular attractive forces (Van der Waal's forces, hydrogen bonds). Rough surface structure produces a random micro "finger joint" under pressure whereas, too smooth a surface might have less micro random 'finger joint" effect which may be responsible for the low gluing strength (Kalapathy et al., 1995). Moisture content of the substrate can also affect the adhesive strength. Adhesive strength is dependent upon the type of substrate, wood, paper, metals, etc.

Viscosity: Is an important property which largely governs the adhesive behaviour and performance (Lambuth, 1977).The operating viscosity limit of soy bean glue are very large ranging from 500- 75,000 cp depending upon the application and nature of the materials to be glued. A viscosity of 500-5000 cps is needed for gluing materials which are highly absorbing, such as paper, soft board and dried wood. Aggregate 5000- 25,000 cp for most laminating purposes (both cold and hot press) and over 50000 cp for mastic consistency wood laminating operations (Schmitz, 2009). A viscosity range of about 8000- 20,000 cp has been specified for no damp press, cold press adhesive techniques (Barth, 1977). Viscosity of protein can be varied by treating with salt or by using reducing agent without affecting the adhesive strength or water resistance (Kalapathy et al., 1996). Enzymatic or alkaline hydrolysis also reduces viscosity (Hittiarachchy et al., 1995). The higher the pH, the higher will be the rate of hydrolysis, better strength and water resistance, but short storage life (Hittiarachchy et al., 1995).

pH: At higher pH, viscosity decreased with storage time and adversely affect the adhesive properties. Optimum treatment conditions for alkali-modified soy protein (AMSP) that resulted in the highest bond strengths were 9.0/70°C (pH/temperature), 10.0/50°C, 11.0/50°C and 12.0/40°C(Schmitz, 2009).

Structure of protein: The adhesive strength of protein glue depends on its ability to disperse in water and on the interaction of polar and apolar groups of the protein with wood material. In a native protein, the majority of polar and apolar groups are unavailable due to the internal bond resulting from Vander Waal's forces, hydrogen bond and hydrophobic interaction. For this reason, a simple paste of soy flour is a poor adhesive and a chemical change is required to break the internal bonds and uncoil or disperse the polar protein molecule. Dispersion and unfolding of protein are enhanced by hydrolysis or by increasing the pH to about 11 or higher (Lambuth,

1977). Treatment with sodium hydroxide unfolds the protein molecule exposing the polar and apolar groups which in turn can interact with wood thereby leading to an improvement in the adhesive strength and improved water resistance, but at the same time shorten the useful life (Lambuth, 1977).

Processing parameter: Adhesive strength increases with increasing concentration to an optimum limit. Too high concentration of adhesive gives high viscosity which has poor flow and was not easy to spread whereas, too low concentration can easily penetrate the porous structure and is not available on the surface of the gluing (Lambuth, 1977). The shear strength of SPI adhesive on fibre card board was affected significantly by the ratio of SPI/ water and reached a maximum value at 12:100 (w/w). For making an adhesive for wood or paper, soy flour is first dampened with water. Its then solubilized or dispersed by reacting with strong alkali such as sodium hydroxide or trisodium phosphate. During initial wetting, alkali is avoided otherwise it leads to the formation of permanent lumps. Treatment with alkali also helps to unfold the protein structure thus exposing all functional sites for interaction with wood and enhances the hydrolysis reaction which in turn affects the viscosity as well as the adhesive efficiency. The working life is only 6-8 hour, depending on the pH and concentration of alkali. Mixed alkalis (mixture of NaOH and $Ca(OH)_2$ or magnesium salt) have been used to improve water resistance and assembly time tolerance of the soybean adhesive by reacting with protein constituents to yield insoluble protemates and altered glue consistency (Kalapathy et al., 1995).

2.4.5 Modification of soy protein

Alkali modification: Viscosity is effectively reduced by alkaline hydrolysis. Alkali helps to unfold the protein structure therefore exposing all functional sites for interaction with wood and improve the hydrolysis reaction. This in turn affects viscosity as well as adhesive efficiency (Kalapathy et al., 1995). Higher pH increases the rate of hydrolysis and improves bond strength and water resistance, but affects the storage life negatively. At higher pH, viscosity decreases with storage time, which adversely affects adhesive properties. The highest bond strengths at optimum treatment condition for alkali modified soy protein (AMSP) were at pH/temperature of 9.0/70°C 10.0/50°C, 11.0/50°C and 12.0/40°C. AMSP adhesive made at pH >11 causes

discolouration of wood products, because alkali salts react with wood resulting in a brown colour and therefore limits the potential use of adhesives (lambuth, 1977). Mild alkaline treatments such as ammonium hydroxide, disodium phosphate, and calcium hydroxide were tested, but are not suitable for wood product applications due to poor bond strength (Lambuth, 1977). Soy protein ingredients used in adhesives have typically been modified using high sodium hydroxide concentrations and pressure which was stronger with improved water resistance compared to adhesives containing unmodified soy protein (Kalapathy et al., 1995).

Enzymatic modification*:* Proteases, such as trypsin, pepsin, papain and alcalase, have also been studied as modifiers (Kalapathy et al., 1995; Sun and Bian, 1999; Shera et al., 2007). The advantages of enzymatic modification include high rates of reaction and mild conditions using low cost processing equipment to produce improved performance properties. Proteases hydrolyze peptide bonds modify proteins but leave carbohydrates untouched. Hydrophobicity is affected by modification of SPI. It also affects the solubility and emulsifying properties of the SPI adhesive. Papain-modified SPI has significantly higher solubility and better emulsifying properties. Trypsin-modified SPI (TMSP) has lower viscosity than unmodified SPI enabling adhesives with greater solids contents to be formulated (Shera et al., 2007). TMSP and trypsin-modified soybean flour have much higher bond strengths with soft maple compared to unmodified SPI. The bond strength increases with increased heating time at 120°C initially, but decreases in strength with treatments over 1 hour (Kalapathy et al., 1995). The highest shear strength is reached when 30% UF adhesive is replaced by trypsin-modified soy components, however, urea formaldehyde (UF) can be partially substituted for TMSP adhesive (Kalapthy et al., 1995). Cellulases and protease treatments are also useful in preparing soy flour for adhesives, depending on adhesive application requirements.

Chemical modification*:* Reagents such as, guanidine hydrochloride (GH), urea, sodium dodecyl sulphate (SDS) and sodium dodecyl benzene sulfonate (SDBS) are used to denature or unfold the structure of protein and improve bond strength and water resistance (Bian and Sun, 1998; Huang and Sun, 2000). Chemical modifications with these reagents at low concentrations (<3 M) all increase the adhesive functionality of SPI (Sun and Bian, 1999; Huang and Sun, 2000; Huang and Sun, 2000). Urea and GH concentrations significantly affect the extent of protein unfolding and adhesive properties, but SDS- and SDBS-modified SPI give enhanced water resistance as

well as improved bond strength (Huang and Sun, 2000). Wet and dry heating, grinding, pressure, freezing, irradiating and exposing to high frequency sound waves can also be used to unfold proteins structure, however adhesive functionality is diminished when soy protein is subjected to these modifications (Kalapathy et al., 1995). The effects of ionic strength on the functional properties of soy proteins have been well documented by Kinsella, (1979), Kella et al., (1989) and Klemazewski and Kinsella, (1991). They all stated in their researches carried out that ionic surroundings weaken electrostatic interaction between protein molecules. Soy protein adhesives have also been modified to reduce viscosity by using ionic solutions. In addition to these, Kalapathy et al., (1996) in his study concluded that concentrations of 0.1 M sodium chloride, sodium sulphate or sodium sulphite reduce viscosity of soy protein without significant negative effects on bond strength and water resistance. Viscosity was reduced from 30,000 to 6000 cps with 0.1 M NaCl and 1050 cps with 0.1 M Na_2SO_4. Similaly, Na_2SO_3 treatment results in modified SPI with 110 cps viscosity and 28% decrease in disufide linkages. Result also showed that treatment with >0.1 M of any ionic solution decreases viscosity further, along with the bond strength (Kalapathy et al., 1996). Chemical modification with dopamine has also been used to enhance bond strength as well as water resistance for SPI adhesives (Liu and Li, 2002). Dopamine is an amino acid with two adjacent phenolic hydroxyl groups, and is the primary component responsible for marine adhesive properties. Bond strength depends on the phenolic functionality in the synthesized compounds and improved water resistance compared to other non-modified SPI adhesives has been achieved.

Blended adhesives*:* Adhesives with enhanced performance properties can be obtained by blending soy protein based adhesives with other protein or synthetic adhesives. Blends of soy flour with casein, blood, phenol formaldehyde (PF), and phenol-resorcinol formaldehyde (PRF) have been used to produce wood glues with exceptional properties (Lambuth, 2001). Blended adhesives for biodegradable plant containers have been obtained by blending SPI with varying amounts of poly-(vinyl alcohol) or poly- (vinyl acetate) (Brown, 1987; Zhao et al., 2000). Blends of soy protein and PRF resins are useful in finger-jointing green lumber with the Honeymoon System (Steele et al., 1998; Clay et al., 1999). Soy protein and PRF blends cure rapidly at room temperature and have excellent water resistance and reduced formaldehyde emissions.. Anhydride groups were found effective by John and Bhattacharya, (1999) in compatibilizing immiscible blends of soy protein and polyester. It was evident that improved mechanical

strength, moisture sensitivity, and processing conditions can be achieved using a small amount of compatibilizer.

2.5 The wood

Wood has an inherent potential to satisfy the criteria for being a viable and justifiable industrial material i.e. a renewable resource available in vast quantities and formed as a natural composite with an extraordinary high strength-to-weight ratio. However, for outdoor usage, it is essential to improve the performance and enduring strength of wood-based materials and the products associated with their assembly, like coatings and adhesive (Peruzzo et al 2014). Wood composites are broadly used in furniture, cabinets, houses and several other applications. There are two basic steps in the assembly of wood composites. The conversion of concrete wood into chips or fibres, veneer and strands that are afterward bonded together with a wood adhesive to form huge composite sheets (Liu and Li, 2004) and the surface structure, surface roughness, degree of cross-link and entanglements between protein molecules. The molecular weight and distribution contribute significantly to the bonding strength. For example, the gluing strength with pine is much lower than that for walnut, cherry, maple, and poplar samples (Sun and Bian, 1999).

The surface microstructure of the pine sample is smoother, with a fibre oriented structure, than walnut wood samples, as shown in Figure 2.3 If the surface of the wood sample is too rough, it causes cohesive wood failure and if too smooth, it causes adhesion failure (machay, 1998). Protein molecules penetrate into the pores from the wood surface, forming a complex matrix upon curing. The rough surface under pressure can form random micro "finger joint" effects, enhancing gluing strength (Machay, 1998).

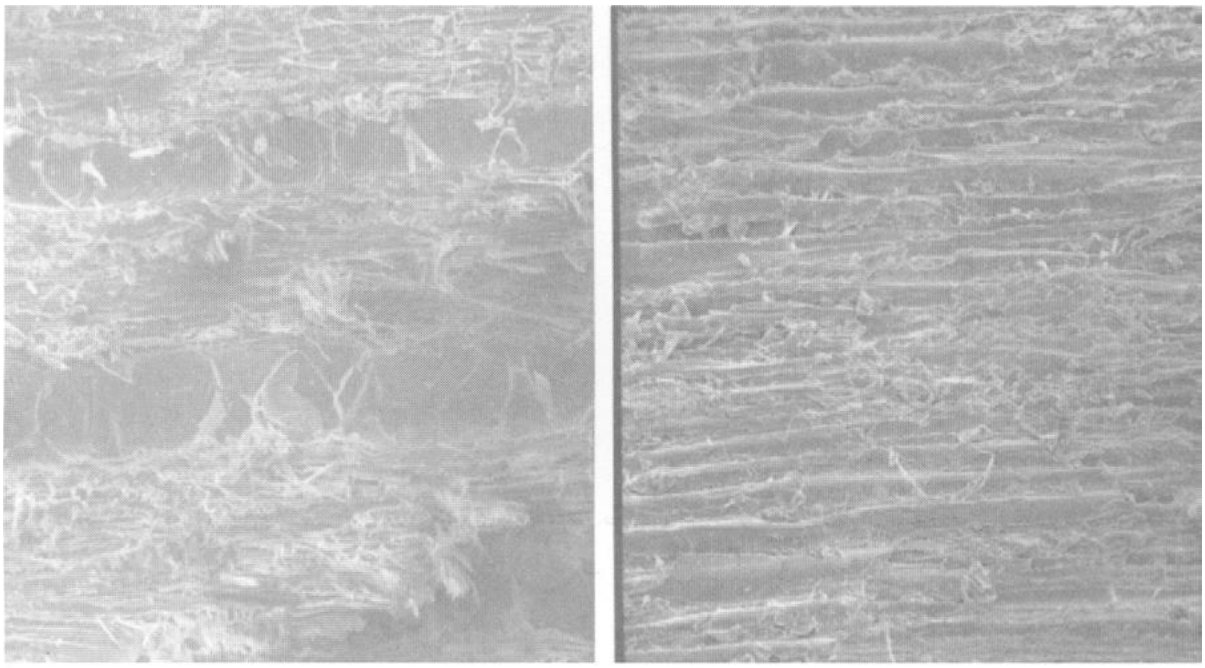

Figure 2.3: Scanning electron micrograph of surface microstructure of (A) walnut and (B) pine (Sun and Bian, 1999).

2.5.1 Effect of polymer/composite adhesives on bond strength and water resistance

In an attempt made to improve the adhesion strength of hybrid wood glue, Liu et al. (2010), devised a biomimetic soy protein/$CaCO_3$ composite adhesive. In this investigation, the fracture bonding interface, the morphology, structure and the bond strength of the adhesive were studied. Results revealed that the joining links and ion crosslinking of calcium carbonate and hydroxyl ions in the adhesive significantly improved the water resistance and bonding strength of soy protein adhesives (Liu et al., 2010). In the current work of Schmitz, (2009), enzyme hydrolysates of soy flour (SF) and soy protein isolate (SPI) were evaluated in phenol formaldehyde (PF) and polyamide-epichlorohydrin (PAE) adhesive formulations. However, in soy/PF blends the degree of hydrolysis (DH) was an integral factor in both strength and durability. Peruzzo et al. (2014) added nanoclay as filler into polyvinyl adhesive to produced adhesives with higher water and heat resistance. They reported that this was judged by the water swelling performance and thermal degradation properties of the adhesive which was mirrored also in their improved

adhesive performance under wet state (D3 tests according to EN204) and high temperatures (WATT 91) of the samples containing clay with respect to the pristine dispersions.

Soy protein isolate (SPI) was first modified with maleic anhydride (MA) to form MA-grafted SPI (MSPI) by Li et al. (2007). The result showed that wood composites bonded with MSPI alone had low dry shear strength and delaminated when subjected to a boiling water test. The result of the investigation in conclusion stated that, a combination of MSPI and polyethylenimine (PEI) vividly increased the strength and water resistance of the subsequent wood composites. A study was conducted by Huang and Sun (2000) on adhesive strength and water resistance properties of soy protein isolates improved by sodium dodecyl sulphate (SDS) (0.5, 1, and 3%) and sodium dodecyl benzene sulfonate (SDBS) (0.5, 1, and 3%).The modified adhesives were applied on walnut, cherry, and pine plywood. The results indicated that soy proteins modified with SDS and SDBS have improved water resistance in addition to adhesive strength. Sun and Bian (1999) carried out a research on alkali and urea modified soy protein adhesive. They discovered that plywood made with adhesive containing urea-modified proteins adhesive had improved water resistance than those joined with adhesives containing alkali-modified and heat-treated proteins adhesives. They also reported that modified soy proteins had stronger bond strength than those containing unmodified soy proteins.

The effects of proteolytic enzyme modification of soy protein isolate (SPI) on its functional and molecular properties were evaluated by Kim et al. (1990). They treated a viable SPI, Ardex F, with trypsin, rennet, achymotrypsin, Liquozyme, and alcalase. The molecular size of SPI was effectively decreased by trypsin followed by Alcalase and a-chymotrypsin. They further reported that hydrolytic breakdown arose more comprehensively in the α^{I}, α, and β subunits of 7s globulins than in the acidic and basic polypeptides of 11s globulins. Improvement of solubility at pH 7.0 and 4.5, emulsifying capability and ability to endure thermal aggregation is associated with partial hydrolysis of the SPI (Kim et al., 1990).

Wood adhesives show a large variability of mechanical properties in the cured state. The modulus of elasticity determined by different methods covers a wide range from 0.1 GPa up to 15GPa. Results are highly influenced by adhesive formulation and ambient conditions but also by sample preparation and by the testing method used (Stoeckel et al., 2013). Tensile shear

strength measurements were performed on beech wood substrates bonded with either dispersions of soy protein isolate or wheat gluten to investigate bond strength and water resistance. The results reveal a significant difference in bond strength between the plant proteins. Soy protein isolate is superior to wheat gluten, especially regarding water resistance, both under acidic and alkaline conditions (Nordqvista et al., 2013). Possibilities of using soy protein isolate (SPI) and wheat gluten (WG) as binders for particleboards was studied by Khosravi et al., 2010. It appeared that SPI is superior to WG when it comes to the water resistance as well as the mechanical properties of the boards. However, it is not possible to compare these two proteins explicitly, since SPI contains a higher percentage of protein. Additionally, WG contains more starch, which is known to give poorer water resistance properties (Khosravi et al., 2010).

An investigation was conducted on the adhesive and water-resistance properties of soy protein isolates that were modified by varying solutions of urea between 1 and 8 M or guanidine hydrochloride (GH) between 0.5 and 3 M and applied on walnut, cherry and pine plywoods. These results indicated that soy proteins modified with urea and GH enhances water resistance as well as adhesive strength. Secondary structures of globule proteins may enhance adhesion strength and the exposure of hydrophobic amino acids may enhance water resistance (Huang and Sun, 2000). Proteolytic enzymes commonly used are pepsin, papain, ficin, trypsin, bacterial and fungal proteases. Differences in the modification behavior of different proteases would depend on their specific hydrolytic action on the substrate. (Bernardi Don et al., 1991) Solubility, foaming capacity and foam stability of denatured soy protein concentrate obtained from toasted flour were improved by proteolysis with fungal or bacterial proteases. By limited hydrolysis up to degree of hydrolysis 10% most functional properties were improved without greatly reducing emulsion stability and water absorption (Bernardi Don et al., 1991). Adhesive and hydrophobic properties of alkali modified soy protein (AMSP) and trypsin-modified soy protein (TMSP) on wood were investigated. Modified soy protein adhesives with higher hydrophobicities (AMSP and TMSP) had enhanced water-resistance properties (Hettiarachchy et al., 1995).

2.5.2 Effect of nanofillers on soy protein matrix

Additives and modifieirs such as, rheology modifiers, plasticizers, extenders, tackifiers and fillers are required in the preparation of adhesives for specific applications (Brinson, 1990). Among the functions of fillers added to the adhesive is the reduction of cost since they replace resin solids without decreasing the aggregate solid content. They can also increase viscosity, and hinder penetration of the adhesive into porous substrates (Qiao et al., 1999). The elastoplastic behaviour of the filler treated Poly vinyl acetate emulsion wood adhesive was studied by Qiao et al. (1999). The results showed that the viscosity of the adhesive and their performance on wood were greatly affected by fillers. There was no significant change in the glass transition temperature (Tg) of the polymer by the addition of the fillers, while the tensile modulus, hardness and stiffness were changed altogether. They concluded that the acidity of the fillers effects the setting time for bonding of the emulsions to wood and the water resistance, since some chemical reactions can take place during curing (Qiao et al 1999). Xiang et al. (2009) have successfully prepared bionanocomposites of soy protein isolate (SPI)/montmorillonite (MMT) via simple melt mixing. In this research, MMT was used as nanofiller and glycerol as plasticizer. A noteworthy improvement of the thermal stability and mechanical strength of SPI/MMT nanocomposites was said to have been achieved. Santoni et al., (2013) evaluated the effect of the addition of denaturing agents such us urea and guanidine hydrochloride on Zain, soy and pea protein. Standard bonding tests on wood-to-wood joints were carried out according to EN 205, both in dry and in wet conditions, this latter after 4 days of immersion in water. The result showed that shear strength values were above the minimum threshold limit of 10 MPa required by the standard for both the 2 soy and the pea proteins. In contrast, all proteins were not suitable for wet conditions. They however concluded that, improvement of water resistance of soy protein with an additive is essential. Other factors, such as chemical affinity, specific surface area and dispersibility in the adhesives also greatly affect the performance of the adhesives (Kovacevic et al., 1994).

2.6 Carbon nanotubes

A CNT can be viewed as a hollow cylinder formed by rolling graphite sheets. Bonding in nanotubes is essentially sp^2.However, the circular curvature will cause quantum confinement and rehybridization in which three bonds are slightly out of plane; for compensation the orbital is more delocalized outside the tube. This makes nanotubes more mechanically stronger, electrically and thermally more conductive and chemically and biologically more reactive than graphite (Meyyappan, 2005). Since their discovery in 1991, carbon nanotubes have generated huge activity in most areas of science and engineering due to their unprecedented physical and chemical properties. No previous material has displayed the combination of superlative mechanical, thermal and electronic properties attributed to them. These properties make nanotubes ideal, not only for a wide range of applications but as a test bed for fundamental science ((Baughman et al., 2002 and Cao et al., 2004). Particularly, this combination of properties makes them ideal candidates as advanced filler materials in composites. Researchers have envisaged taking advantage of their conductivity and high aspect ratio to produce conductive plastics with exceedingly low percolation thresholds (Kilbride et al., 2002). In another area, it is thought that their massive thermal conductivity can be exploited to make thermally conductive composites (Biercuk et al., 2002). However, probably the most promising area of composites research involves the mechanical enhancement of plastics using carbon nanotubes as reinforcing filler.

The idea of using pseudo one-dimensional fillers as an enforcing agent is nothing new: straw has been used to reinforce mud bricks since about 4000 BC. In more recent times, fibres made from materials such as alumina, glass, boron, silicon carbide and especially carbon have been used as fillers in composites. However, these conventional fibres have dimensions on the meso-scale with diameters of tens of microns and lengths of order of millimetres. Their mechanical properties are impressive with carbon fibres typically displaying stiffness and strength in the ranges 230–725 GPa and 1.5–4.8 GPa, respectively (Callister, 2003). In recent years carbon nanofibres have been grown from the vapour phase with diameters of order of 100 nm and lengths between 20 and 100 lm. These small dimensions mean they have much higher surface area per unit mass than conventional carbon fibres allowing much greater interaction with composite matrices. They also tend to have impressive mechanical properties with Young's

modulus in the range 100–1000 GPa and strengths between 2.5 and 3.5 GPa (Tibbetts and Beets, 1987). However the ultimate mechanical filler material must be carbon nanotubes. Nanotubes can have diameters ranging from 1 to 100 nm and lengths of up to millimetres (Hata et al., 2004). Their densities can be as low as 1.3 g/cm3 and their Young's moduli are superior to all carbon fibres with values greater than 1 TPa (Wong et al., 1997). However, their strength is what really sets them apart. The highest measured strength for a carbon nanotube was 63 GPa (Lourie et al., 2000). This is an order of magnitude stronger than high strength carbon fibres. Even the weakest types of carbon nanotubes have strengths of several GPa (Xie et al., 2000). Carbon nanotubes have been regarded as materials (Ebbesen, 1998) and most naturally related to the other intractable carbon allotropes graphite and diamond. Their application as structural reinforcement, however, (specifically in polymer composites) is going to depend on the ability to transfer load from the matrix to the nanotubes (Calvert, 1999).

2.6.1 Types of carbon nanotubes

There are two main types of nanotubes available today. Single walled nanotubes (SWNT) (Bethune et al., 1993; Iijima and Ichihashi, 1993) consist of a single sheet of graphene rolled seamlessly to form a cylinder with diameter of order of 1 nm and length of up to centimetres. Multi-walled nanotubes (MWNT) consist of an array of such cylinders formed concentrically and separated by 0.35 nm similar to the basal plane separation in graphite (Iijima, 1991) MWNTs can have diameters from 2 to 100 nm and lengths of tens of microns. There are three forms of nanotubes, armchair, zigzag, and chiral (Figure 2.4). Carbon nanotubes can be either a metal or a semi-conductor. They differ symmetrically and can vary in function due to the way they "roll up." The diameter of a carbon nanotube can be 50,000 times thinner than a human hair yet a nanotube is stronger than steel per unit weight (Ganesh, 2013).

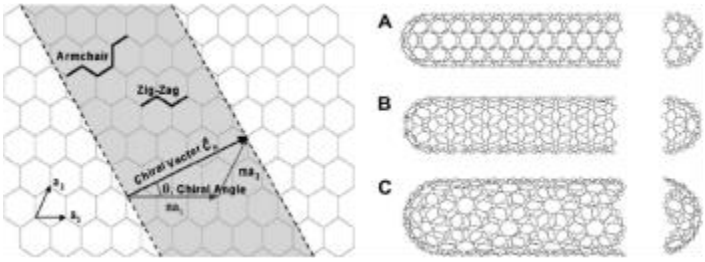

Figure 2.4: A hexagonal sheet of graphene rolled to form a CNT with different chiralities A = armchair; B = zigzag; C= chiral (Dresselhaus et al., 1995 and Thostenson et al., 2001).

Single walled nanotubes

Single-walled nanotubes (SWNTs) have structures that can be visualized mentally as wrapping a one-atom thick layer of graphite into an unbroken cylindrical wall (Solvetat et al. 2004) (Figure 2.5). The methods currently applied to synthesize SWNTs in high yields are: the electric arc discharge method (Journet et al., 1997), pyrolysis (Rao et al., 1997; Cheng et al., 1998) and the laser-ablation technique (Tess et al., 1996). A simple laser-ablation set-up consisting of a continuous-operating CO_2-laser in combination with a vertical evaporation chamber has been successfully employed to produce high-quality SWNT material (Maser et al., 1998).

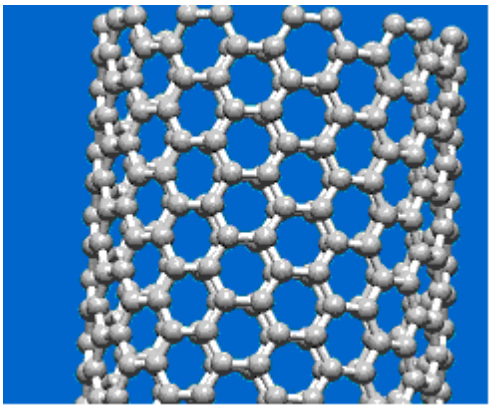

Figure 2.5: shows SWNT of chiral vector of bond length 1.41 A0 and tube length 20 A0. Courtesy Nano tube modeller (Ma et al., 2010)

Doublewalled nanotubes

Double-walled nanotubes (DWNTs) are composed of exactly two single walled nanotubes with one seated in another (Shen et al., 2011) (see Figure 2.6).

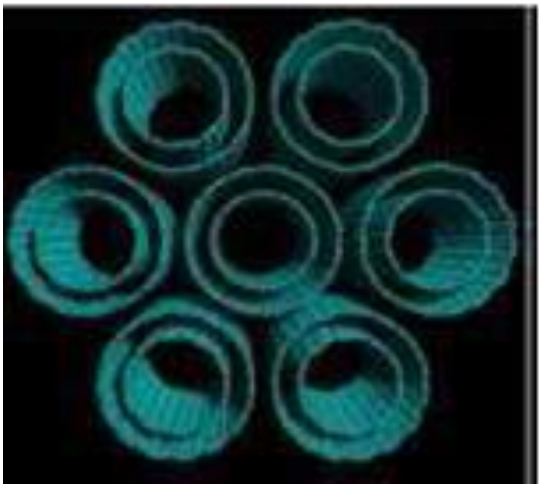

Figure 2.6: Computer generated image of DWCNT (www.nanotechweb.org) reproduced from Endo et al., 2005.

Muiltiwalled carbon nanotubes

Multiwalled carbon nanotubes (MWNTs) consist of severally rolled layers of graphene (Solvetat et al., 2011). The methods for producing carbon nanotubes are mainly electric-arc and catalytic-pyrolysis of hydrocarbon (CVD) (see Figure 2.8). Compared to the electric-arc, CVD has a high yield and a high proportion of carbon nanotubes in raw products, so it can be used in large-scale production. However, the carbon nanotubes made by CVD are not only curved, but are also entangled into big masses. Jia et al., 1999 produced multi-walled carbon nanotubes made by catalytic-pyrolysis of ethylene which have curved bodies and exhibit entangled masses (Jia et al., 1999).

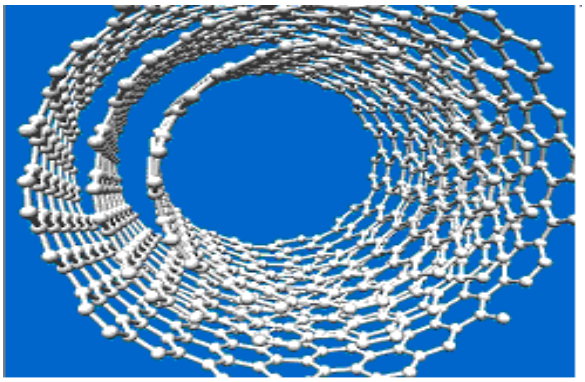

Figure 2.7: Multi walled carbon nano tube without cap Courtesy Nano tube modeller front View, Armchair (Ma et al., 2013)

High purity, aligned multi-wall carbon nanotube films were grown on quartz substrates by Singh et al., (2003) by injecting a solution of ferrocene in toluene into a suitable reaction furnace. The injection CVD method allows excellent control of the catalyst to carbon ratio. Primary growth was found to occur via a base growth mechanism, although overgrowths of single wall carbon nanotubes were obtained under certain conditions. They concluded that such a method also allows nanotubes of various packing densities to be produced which may be useful for specific applications such as electrodes. Couteau et al., (2003) reported that Multiwalled carbon nanotubes (MWCNTs) were synthesized in a catalytic reaction using $CaCO_3$ as catalyst support. Impregnated with conventional catalysts $CaCO_3$ enabled the production of MWCNTs in a fixed-bed flow reactor at relatively low reaction temperature. The purification was performed in one step: both metallic particles and catalyst support were dissolved in a diluted acid. Hence, disadvantages, namely multi-step processes and hazardous chemicals, were avoided. A further advantage of $CaCO_3$ support is efficient and stable growth of MWCNTs. First results obtained in our new rotary-tube oven indicated high quality and pure MWCNTs with a yield of 100 g/day by this method.

An experimental study was conducted to examine the role of hydrogen in the chemical vapor deposition (CVD) synthesis of multiwalled carbon nanotubes (MWCNTs) in a flow tube reactor using xylene as a carbon source and ferrocene as a catalyst (Wasel et al., 2007). The role of hydrogen is suggested to reduce the rate of carbon production by dehydrogenation so that the more ordered and thermodynamically stable MWCNTs can be produced rather than less ordered

and thermodynamically stable soot and carbon fibers (Wasel et al., 2007). The role of different gases in CNT or nano-fibers formation, such as nitrogen (Lin et al., 2003) and hydrogen (Wasel et al., 2007), has also been investigated. Inert argon is often used as a carrier gas in many CVD reactors; while hydrogen is added to it especially when a liquid hydrocarbon like xylene, toluene or benzene is used as the carbon source. What the role of hydrogen is in MWCNTs formation is an open question. Some previous work has attempted to explain the effect of hydrogen in carbon fiber formation (Kim et al., 1991), it suggests the role of hydrogen is to limit or alleviate the poisoning of the metal catalysts by elemental carbon. More recently, it has been proposed that an intermediate, known as precursor soot or free radical condensates, is involved in the formation of MWCNTs and that hydrogen acts to reduce the rate of spontaneous dehydrogenation of the intermediate to form soot (Reilly and Whitten, 2006).

2.7 Synthesis of MWCNTs

Generally, there are few techniques employed to produce CNTs such as electric- arc discharge, laser ablation and CVD. By using any of these techniques, different type of CNTs, can be produced such as vapor grown, carbon fiber and types of carbon nanostructure materials. Thess et al. (1996) synthesized bundles of aligned SWNTs by the laser- ablation technique. For the first time, catalytic growth of MWNTs by CVD was proposed by Yacaman et al. (1993). The arc-discharge technique produces high quality.MWNTs and SWNTs. MWNTs do not need a catalyst for growth, while SWNTs can only be grown in the presence of a catalyst in this method. In this reaserch emphasis was laid on the synthesis of CNTs using CVD method.

2.7.1 Chemical vapour deposition (CVD)

Controlled growth of CNTs can be obtained through manipulation of the size of the nanoparticles that are used as catalysts in the CNT synthesis. The most widely used metals are Fe, Co and Ni as well as the alloys of these nanoparticles. The metals are usually supported on materials that are stable at high temperatures such as SiO_2, Al_2O_3, TiO_2 and zeolites (Hernadi et al., 1996 and Balch et al., 1998). Mhlanga et al., (2009) prepared a Fe-Co bimetallic catalysts supported on $CaCO_3$ by a wet impregnation, a deposition-precipitation and a reverse micelle method. It was reported that a Clean' multi-walled carbon nanotubes (MWCNTs) were obtained from all three Fe-Co synthesis procedures under optimal reaction conditions. The CNTs produced gave yields

ranging from 623 % to 1215 % in 1 h under the optimal conditions, with similar outer diameters (o.d.) of 20–30nm and inner diameters (i.d.) ~10 nm. The Fe/Co catalyst formed in the wet impregnation method revealed that the yield, diameter and purity of the CNTs were influenced by the C_2H_2/N_2 ratio, time and temperature. At 700 °C, $CaCO_3$ changes to CaO (lime), which is an environmentally friendly material that can readily be dissolved in dilute acids such as HNO_3 and HCl. As a result, this support can be removed from the produced CNTs with ease, resulting in clean materials that are relatively free of contaminants. (Couteau et al., 2002).

The CVD is essentially a thermal dehydrogenation reaction whereby a transition metal catalyst e.g. iron, nickel, or cobalt is used to lower the temperature required in order to 'crack' a gaseous hydrocarbon feed into carbon and hydrogen. The CVD is a versatile process suitable for the manufacturing of coatings, powders, fibers, and monolithic components. With the CVD, it is possible to produce most metals, many nonmetallic elements such as carbon and silicon as well as a large number of compounds including carbides, nitrides, oxides, intermetallics, and many others. This technology is now an essential factor in the manufacturing of semiconductors and other electronic components in the coating of tools, bearings, and other wear-resistant parts and in many optical, optoelectronic and corrosion applications (Mubarack et al., 2013).

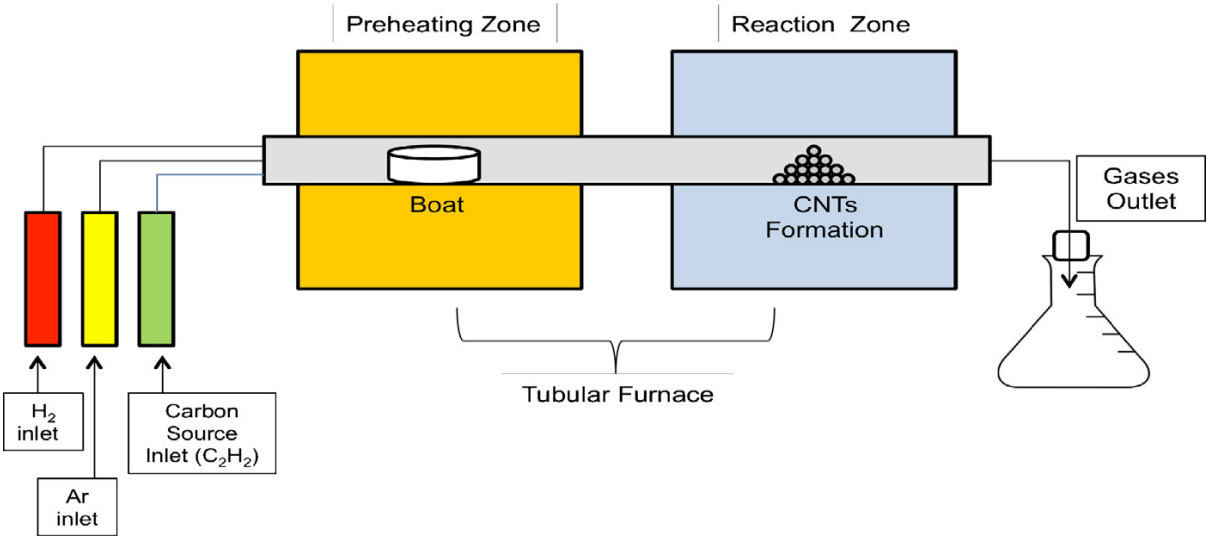

Figure 2.8: Diagram of CVD to produce CNTs adopted from Mubarak et al., 2011.

Advantages of CVD method over other methods

Recently, the CVD used in the synthesis of CNTs has attracted much attention because it has many advantages compared to arc discharge and laser ablation. These can be summarized as follows (Hugh, 1999):

i. Easily available raw material abundant in the form of gases.
ii. With the CVD, it is possible to coat almost any shape of almost any size.
iii. Unlike other thin film, techniques such as sputtering CVD can also be used to produce,
iv. vertically aligned nanotubes, fibers, monoliths, foams and powders.
v. The CVD is economically competitive

The CVD is a relatively uncomplicated and flexible technology, which can accommodate many variations, and the reaction process and reactor design is simple as the reaction is easy to control and manipulate.

In a research carried out by Louis et al., (2005), ethane was successfully used as an active and efficient carbon source in a large scale synthesis of high quality carbon nanotubes by chemical vapour deposition (CVD) over Fe/Al_2O_3 catalyst with an iron loading of 20 wt.%. The result showed that the reaction products only contained multi-walled carbon nanotubes with very homogeneous diameters of around 30 nm and lengths up to several hundred nanometers without any trace of other impurities such as nanoparticles or amorphous soot. According to the observed results ethane is an active carbon source for growing multiwalled carbon nanotubes with high yield and selectivity.

Factors influencing the growth mechanism of carbon nanotubes

Among the parameters that influence the growth mechanism of CNTs are the catalyst, carrier gas, substrate, temperature of synthesis, reaction time and the flow rate of carrier gas. Most effective and widely used catalysts are Fe/Co/Ni (Mubarak et al., 2013). Catalysts play an important role in controlling the structure of SWCNTs. The growth rate of CNT is a function of catalyst particle size and the diffusion rate of carbon through the catalyst. As the catalyst particle size increases, the growth rate will decrease. Meanwhile, the growth rate of CNTs is directly proportional to the diffusion rate of carbon through the catalyst (Kim et al., 2003). Synthesized

CNT (Mukhopadhyay et al., 1999) precursors are methane, (Kong et al., 1998) ethylene (Satishkumar et al., 1998), acetylene (Sen et al., 1997) benzene, (Wei et al., 2002) xylene, (Endo et al., 1991) and carbon monoxide (Nikolaev et al., 1999). Endo et al., (1992) reported the CNT growth from pyrolysis of benzene at 1100^0C, whereas Jose-Yacaman et al. got clear helical MWCNTs at 700^0C from acetylene. The carrier gas also affects the growth of CNTs. Carrier gas such as H_2 and Ar effects the growth of CNTs. Hydrogen is the most effective carrier gas as it provides a reducing atmosphere and scavenges oxygen. However, excess hydrogen will push the reaction in the opposite direction which is not desirable. Nitrogen has been found to be effective for the growth of bamboo type CNTs by delaying the surface of passivation of the catalyst particle and enhance carbon diffusion through the catalyst (Mubarack et al., 2013). Hana et al. studied the influence of flow rate of precursor and carrier gas, and it is found that if the flow rate of carrier gas is increased, with the precursor flow rate remain constant, the mean diameter of CNTs will decrease. If the flow rates of both carrier and precursor gas are increased, the diameter essentially remains constant, but then growth rate will increase. The growth of CNTs is observed to be strongly substrate dependent. The amount of substrate crystallinity also affects the ability for CNTs growth and nucleation (Mubarack et al., 2013). On crystalline surface of substrate, the growth of SWCNTs seems to be favoured, while on amorphous and polycrystalline surface, the MWCNTs growth is preferred. The rate of reactions is a strong function of temperature, thus it is expected that the concentration of each species will vary with temperature. At a low temperature, a decrease in the formation of CNTs formation has been observed possibly due to the partial deactivation of catalyst (Perez Cabero et al., 2004). It is reported that lower synthesis temperatures than optimum synthesis temperature resulted in lower CNTs yield in the product (Sinha et al., 2000). It is also reported that reaction temperature plays an important role in the alignment properties and diameter of the synthesized nanotubes (Singh et al., 2003). Generally, the CNT growth temperature used is between 550^0C and 1000^0C, and reaction temperature may vary according to the catalyst support material pair (Mubarak et al., 2013). It is also noted that the yield is proportional to the time of reaction..

2.8 Dispersion of CNTs in polymer matrix and CNTs/polymer composite materials

Many research efforts have been directed towards producing CNT/polymer composites for functional and structural applications (Coleman et al., 2006 and Ajayan et al., 2008) However,

even after a decade of research, the full potential of employing CNTs as reinforcements has been severely limited because of the difficulties associated with dispersion of entangled CNT during processing and poor interfacial interaction between CNTs and polymer matrix. The nature of dispersion problem for CNTs is rather different from other conventional fillers, such as spherical particles and carbon fibers, because CNTs are characteristic of small diameter in nanometer scale with high aspect ratio (>1000) and thus extremely large surface area. In addition, the commercialized CNTs are supplied in the form of heavily entangled bundles, resulting in inherent difficulties in dispersion. Examples of commonly used fillers, include Al_2O_3 particles, carbon fibers, graphite nanoplatelets (GNPs) and CNTs (Peng-Cheng et al., 2007). A large surface area of fillers means a large interface or interphase area present between the filler and matrix. A classic definition of the ‘‘interface” in composites is a surface formed by a common boundary of reinforcing fillers and matrix that is in contact and maintains the bond in between for load transfer (Kim and Mai, 1998). In contrast, the ‘‘interphase” is defined as the region with altered chemistry, altered polymer chain mobility, altered degree of cure and altered crystallinity that are unique from those of the filler or the matrix (Ma et at., 2010). Meanwhile, the interphase size of CNT/polymer–matrix composites has been reported to be as large as about 500 nm according to the size and dimension of fillers (Thostenson et al., 2001). The three-D distribution of these micro- and nanoscale fillers in a polymer matrix is schematically presented in Figure 2.9, that gives a clear impression on the different dispersion behaviour of particles in the matrix due to the size and geometry effects. The dispersion of micro-scale fillers (A and B in Figure 2.9) is uniform throughout the matrix, and the differentiation of individual particles in a matrix can be done easily. However, when gold nano particles (GNPs) and CNTs (C and D in Figure 2.9) are filled into the same volume of matrix, it is hard to disperse individual particles homogeneously (Ma et al., 2010). Even if the interfacial region is only a few nanometers thick, the CNTs would poise tremendous problems in uniform dispersion. In addition to the size effect of fillers, the physical nature of particles also plays an important role in dispersing them into polymer matrix. As-produced CNTs are held together in bundles or entanglements consisting of 50 to a few hundred individual CNTs by van der Waals force. It has been proved that these bundles and agglomerates result in diminished mechanical and electrical properties of composites as compared with theoretical predictions related to individual CNTs (Thostenson et al., 2001; Coleman et al., 2006). Therefore the challenge is how to incorporate individual CNTs

(from CNT bundles or CNT agglomerates) into a polymer matrix or at least relatively thin CNT bundles or disentangled CNTs, inside a polymer matrix. Figure 2.10 shows the electronic microscope images of CNT bundles and entanglements. In other words, dispersion of CNTs is not only a geometrical problem, dealing with the length and size of the CNTs, but also relates to a method on how to separate individual CNTs from CNT agglomerates and stabilize them in polymer matrix to avoid secondary agglomeration. There are different methods of dispersion of carbon nanotubes. They include ultrasonication, calendaring processes, ball milling, stir and extrusion.

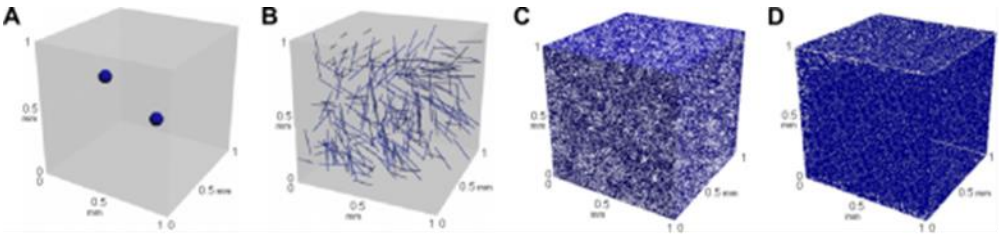

Figure 2.9: Distribution of micro- and nano-scale fillers of the same 0.1 vol. % in a reference volume of 1 mm^3 (A: Al_2O_3 particle; B: carbon fiber; C: GNP; D: CNT) (Ma et al., 2010)

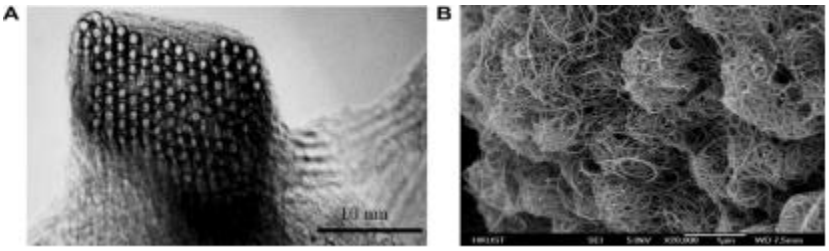

Figure 2.10: Electronic microscope images of different CNTs: (A) TEM image of SWCNT bundle (B) SEM image of entangled MWCNT agglomerates [Thess et al., 1996]

2.8.1 Methods of dispersion

There different effective methods of dispersion of CNTs in a polymer matrix. These include: Ultrasonication, calendaring, ball mixing, shear mixing, and functionalization. In this research, emphasis was laid on two major effective methods of dispersion; ultrasonication and shear mixing.

Ultrasonication

Ultrasonication is the act of applying ultrasound energy to agitate particles in a solution for various purposes. In the laboratory, it is usually achieved using an ultrasonic bath or an ultrasonic probe/ horn (A and B in Figure 6), also known as a sonicator (Ma et al., 2010). Ultrasonication is an effective method to disperse CNTs in liquids having a low viscosity, such as water, acetone and ethanol. However, most polymers are either in a solid or viscous liquid state, which requires the polymer to be dissolved or diluted using a solvent to reduce the viscosity before dispersion of CNTs. An example of solution based composite formation is described by Jim et al. (2007). In this work, MWNT produced by arc discharged were dispersed in chloroform by sonication for 1 hr. The chosen polymer polyhydroxyl amino ether was dissolved in the MWNT-chloroform dispersion. Mixing was achieved by applying another hour of sonication. High loading level of up to 50 wt % and reasonably good dispersion was achieved.

Shear stirring

Stir is a common technique to disperse particles in liquid systems and can be used as well to disperse CNTs in a polymer matrix. After intensive stirring of CNTs in polymer matrix, a relatively fine dispersion can be achieved (Sander et al., 1999). MWCNTs can be dispersed more easily than SWCNTs by employing this technique, although the MWCNTs tend to re-agglomerate. Many factors, such as physical (solid or liquid) and chemical (thermoplastic or thermoset) states of polymer matrix, dimensions and content of CNTs to be added, availability of techniques and fabrication processes, should be taken into account when selecting a proper technique for CNT dispersion(Ma et al., 2010). Sandler et al., (1999) dispersed CNTs in epoxy under high speed stirring 2000 rpm for 1 hour and proved that in intense stirring was an effective process to achieve dispersed CNTs uniformity in epoxy. Besides, adding a proper compatibilizer to polymer/CNTs is another efficient method.

2.9 Functionalization of CNTs

This is another method for effective dispersion of CNTs in SPI matrix.There are several comprehensive review papers that describe the chemistry of functionalized CNTs and the reaction mechanisms between the CNTs and functional groups (Hirsch and Vostrowsky, 2005;

Tasis et al., 2006). These methods can be conveniently divided into chemical functionalization and physical methods based on the interactions between the active molecules and carbon atoms on the CNTs.

2.9.1 Physical functionalization

Functionalization of CNTs using covalent method can provide useful functional groups onto the CNT surface (Hirsch, 2002). However, these methods have two major drawbacks: firstly, during the functionalization reaction, especially along with damaging ultrasonication process, a large number of defects are inevitably created on the CNT sidewalls, and in some extreme cases, CNTs are fragmented into smaller pieces. These damaging effects result in severe degradation in mechanical properties of CNTs as well as disruption of p electron system in nanotubes (Ma et al., 2010). The disruption of p electrons is detrimental to transport properties of CNTs because defect sites scatter electrons and photons that are responsible for the electrical and thermal conductions of CNTs, respectively (Ma et al., 2010). Secondly, concentrated acids or strong oxidants are often used for CNT functionalization, which are environmentally unfriendly. Therefore, many efforts have been put forward to developing methods that are convenient to use, of low cost and less damage to CNT structure.

Non-covalent functionalization is an alternative method for tuning the interfacial properties of nanotubes. The suspension of CNTs in the presence of polymers, such as poly (phenylene vinylene) (McCarthy et al., 2001) or polystyrene (Hill et al., 2002), lead to the wrapping of polymer around the CNTs to form supermolecular complexes of CNTs. This is a typical example of non-covalent functionalization of CNTs.

2.9.2 Chemical functionalization of CNTs

In recent times, significant efforts have been made towards developing techniques to modify the surface properties of CNTs. CNTs fillers are inert and can interact with the surrounding matrix primarily through van der Waals interactions, because the carbon atoms on their walls are chemically stable due to aromatic nature of the bond (Hirsch, 2002). This disallows them from providing an efficient load transfer across the CNT/matrix interface. There are quite a lot of comprehensive review papers that describe the chemistry of functionalized CNTs and the

reaction path-way between the CNTs and functional groups (Hirsch, 2002 and Hirsch, 2005). These can be performed at the termini of the tubes or the sidewalls of the CNTs (Ma et al., 2010). Indirect covalent functionalization takes advantage of chemical alterations of carboxylic groups at the open ends and holes in the sidewalls. These carboxylic groups might have existed on the as-grown CNTs and also be further generated during oxidative purification. Hiura et al. (1995) treated CNTs by a mixture of concentrated sulfuric acid and potassium permanganate, although this might not be a good method for large-scale separation. Purification method suggested by Tohji et al. (1997) includes hydrothermal treatment along with extraction of fullerenes, thermal oxidation and dissolution in 6 M hydrochloric acid. Bandow et al. (1997) and Bonard et al. (1997) in order to prevent CNTs from being destroyed during purification, dispersed the CNTs in polar solvents assisted by surfactants, such as sodium dodecyl sulfate, followed by micro-filtration and size exclusion chromatography. There is a possibility of separating CNTs into selected sizes without destruction by this technique. Disentangling process is necessary for CNTs to open the tubes and provide active sites for functionalization. Liu et al., (1998) "cut'' CNTs into 150 nm length by a 3:1 mixture of concentrated sulfuric acid and nitric acid. The short and open-ended CNTs were then treated by a 4:1 mixture of concentrated sulfuric acid and 30% aqueous hydrogen peroxide. As a result of these treatments, more functional groups such as carboxylic acid and hydroxyl groups were created on the CNT surface. Later, Shaffer et al., (1998) and Shaffer and Windle. (1999) used a 3:1 mixture of concentrated sulfuric acid and nitric acid to ''cut'' CNTs and an electrostatic stabilized dispersion of CNTs in water with an average length of 1.1 mm was achieved. The carboxylic acid groups are usually needed to be converted into acyl chloride group by reaction with thionyl chloride at room temperature, in order to increase the reactivity of CNTs (Liu et al., 1998). Hydroxyl groups on the surface of CNTs were converted into hydroxymethyl groups ($–CH_2OH$) by Wu et al., (1995) by the formalization reaction with formaldehyde.

Concerning the oxidation reaction of sulphuric acid/hydrogen peroxide mixture (piranha) with CNTs, Ziegler et al. (2005) have shown that the one-dimensional nanostructures can be cut in a controlled manner under specific conditions. At high temperatures, piranha was found to attack existing damage sites, generating vacancies in the graphene sidewall, and consume the oxidized vacancies to yield shorter nanotubes. Different types of MWNTs/epoxy composites were prepared with diglycidyl ether of bisphenol F (DGEBF) and bisphenol A (DGEBA) used as

epoxy resins. MWNTs were functionalized to enhance the properties of epoxy composites by treatment with strong acids (acid-treated MWNTs, a-MWNTs) followed by m-phenylenediamine grafting (amine grafted MWNTs, m-MWNTs). Raw, a-, and m-MWNTs were dispersed in DGEBF or DGEBA to a concentration of 1 wt. %. X-ray photoelectron spectroscopy and thermogravimetric analysis verified the effectiveness of acid treatment and confirmed the amine-functionalization of the MWNTs (Kwon et al., 2011). He finally concluded that, further, the thermal conductivity of MWNTs/epoxy composites was higher than that of pure epoxy resins. In particular, the m-MWNT/epoxy composite has the best heat dissipation properties, due to the formation of an effective network for heat flow. Paiva et at., (2004) reported that carbon nanotubes were functionalized with poly (vinyl alcohol) (PVA). It was found that the mechanical properties of these nanocomposite films were significantly improved compared to the neat polymer film. They finally concluded that functionalization allowed good distribution of the nanotubes in the matrix, leading to higher film strength.

Concerning the use of CNTs as reinforcements in composite materials, the incorporation of oxygen-containing functionalities onto the graphitic surface is a very crucial step for the enhancement of interfacial adhesion. As a result, the unique mechanical and electrical properties of CNTs can be transferred to the properties of CNT-based composites. (Datsyuka et al., 2008).

2.10 Properties of carbon nanotubes/polymer composite adhesive materials

2.10.1 Electrical properties

Brown et al. (2005) measured the A.C. conductivity for SWCNT/epoxy matrix and their results showed that the composite conductivity was very low at 0.01 wt% of CNTs, almost the same as that of pure epoxy polymer. However, as the amount of CNT was increased to 0.1 wt%, the conductivity of the composite also increased. A rise in conductivity value was observed between the percolation threshold of 0.01 and 0.05 wt% of CNTs. Choi et al. 2003 prepared epoxy/MWCNT nanocomposites with MWCNTs aligned under a 25 T magnetic field leading to a 35% increase in electric conductivity compared to those related composites with no magnetic aligned CNTs.

2.10.2 Thermal properties

The thermal conductivity For CNT/polymer nanocomposites, depends on several factors, such as the aspect ratio, content, dispersion of CNTs and their interfacial interactions with polymer matrix. The incorporation of CNTs could increase the melting, glass transition and thermal decomposition temperatures of the polymer matrix due to their limitation effect on the polymer segments and chains. It is important to increase the thermal endurance of polymer composites. Therefore, with a surfactant, addition of 1 wt. % CNTs to epoxy increased the glass transition temperature from 63 to 88^0C (Gong et al., 2000). Also, due to the excellent thermal conductivity of CNTs, the incorporation of CNTs could enhance the thermal transport properties of polymer composites. This offers an opportunity for polymer/ CNT composites for applications as connectors, lids and housings, printed circuit boards, heat sinks, thermal interface materials, and high-performance thermal management from satellite structures down to electronic device packaging.

2.10.3 Mechanical properties

Incorporation of CNTs into a polymer matrix can potentially provide structural materials with dramatically increased modulus and strength. Biercuk et al. (2002) have observed a monotonic increase of resistance to indentation (Vickers hardness) by up to 3.5 times on adding 2 wt. % SWCNTs in epoxy resin. Yu et al., (2010) studied the bonding strength and durability for the aluminum plates bonded with epoxy adhesives in terms of Boeing Wedge test. The result revealed that both properties increased greatly with the incorporation of CNTs. The joint with 1 wt. % of CNT in particular, showed highest initial and final fracture toughness among all the joints tested. Samal, [2009] synthesized an epoxy based MWCNTs reinforced composites by method of sonication. The variation in the nature of reinforcement (aligned & randomly oriented MWNTS) has given rise to enhancement of mechanical properties like hardness, flexural modulus and tensile strength. The result indicated that a small change in chemical treatment of the nanotubes has a great effect in the mechanical and morphological properties of nanocomposites due to effective load transfer mechanism and state of dispersion.

Various investigations have been carried out on the incorporation of nanoparticles such as montmorillonites (nanoclay) or silica oxides (SiO_2) into soy-protein adhesive (Neng et al. 2011).

In this study an attempt will be made to investigate the mechanical properties of adhesive nanocomposite by incorporating carbon nanotubes into soy protein isolate adhesive. SPI and CNTs were considered together as raw materials for preparing adhesive nanocomposite with enhanced mechanical properties. This environmental friendly SPI adhesive shall replace the non-renewable and costly petroleum and formaldehyde adhesive which is dangerous to health. Considering its industrial applications and significance such as, biogradability, ready availability and easy processability at low cost, in addition to the potential applications of carbon nanotubes.

References

Abate, T., Alene, A.D., Berguinson, D., Shiferaw, B., Silim, S., Orr, A. and Astaw, S. (2011) Tropical grain legumes in Africa and South Asia: Knowledge and Opportunity. Research Report. International Crop Research Institute for the Semi- Arid Tropics, Nairobi, Kenya

Afolabi, A.S., Abdulkareem, A.S., Mhlanga S.D. and S.E. Iyuke (2011) Synthesis and purification of bimetallic catalysed carbon nanotubes in a horizontal CVD reactor. Journal of Experimental Nanoscience. Vol. 6:3, pp 248-262.

Ajayan P.M., Schadler L.S. and Braun P.V. (2003). Nanocomposite science and technology. Weinheim: Wiley-VCH, pp. 77–80.

Ajayan, P.M., Schadler, L.S., Giannaris, C. and Rubio, A. (2000) Single-walled carbon nanotube– polymer composites: strength and weakness. Adv Mater. Vol. 12 pp 750–753.

Alibhai, Z., Mondor, M., Moresoli, C., Ippersiel, D. and Lamarche, F. (2006) Production of soy protein concentrates/isolates: traditional and membrane technologies. Desalination. Vol. 191, pp 351–358

Ávila-Orta, C.A., Cruz-Delgado, V.J., Neira-Velázquez, M.G. and et al. (2009) Surface modification of carbon nanotubes with ethylene glycol plasma. Carbon. Vol. 47, pp 1916–21.

Bain, W., Circle, S., Olson, R., 1961. Synthetic and Protein Adhesives for Paper Coating. TAPPI Monograph Ser. No. 22. Technical Assoc. Pulp and Paper Inc. New York, NY.

Bandow, S., Rao, A., Williams, K.A., Thess, A., Smalley, R.E. and. Eklund, P.C. (1997) Purification of single-wall carbon nanotubes by microfiltration. J Phys Chem B.Vol. 101, pp 8839–42.

Barth, B.P., 1977. Phenolic Resin Adhesives. In: Skeist, I. ed, Handbook of Adhesives, 2nd ed. New York, NY.

Baughman, R.H., Zakhidov, A.A. and de Heer, W.A. (2002) Carbon nanotubes—the route toward applications. Science; Vol. 297, No. 5582, pp. 787–92.

Bemardi Don, L.S., Pilosofl, A.M.R. and G.B. Barlholomail, G.B. (1991) Enzymatic Modification of Soy Protein Concentrates by Fungal and Bacterial Proteases. Journal of American Oil Chemist Society. Vol. 68, No. 2, Pp 102-105.

Berber S., Kwon Y.K. and Tománek D. (2000) Unusually high thermal conductivity of carbon nanotubes. Phys Rev Lett. Vol. 84, pp 4613–4616.

Bethune, D.S., Kiang, C.H., Devries, M.S., Gorman, G., Savoy, R. and Vazquez, J. (1993) Cobalt-catalyzed growth of carbon nanotubes with single atomic- layerwalls. Nature. Vol. 363, No 6430, pp 605–7.

Bian, K., Sun, X.S., 1998. Adhesive performance of modified soy proteins polymers. Polym Prepr (Am Chem Soc, Div Polym Chem). Vol. 39, No. 53, pp. 72-73.

Biercuk M.J., Llaguno M.C., Radosavljevic M., Hyun J.K., Johnson A.T. and Fischer J.E. (2002) Carbon nanotube composites for thermal management. Appl Phys Lett. Vol. 80, pp 2767–2769.

Bonard, J.M., Stora, T., Salvetat, J.P., Maier, F., Stockli, T., Duschl, C., Forro, L., deHeer, W.A. and Chatelain, A. (1997) Adv. Mater. Vol. 9, pp 827.

Brinson, H.F. (1990), Engineered Materials Handbook, Vol. 3, ASM International, Materials Park.

Brown, O.E., 1987. Labeling adhesives. U.S. Patent 4,675,351.

Brown, J.M., Anderson, D.P., Justice, R.S., Lafdi, K., Belfor, M., Strong, K.L. and Schaefer, D.W. (2005) Hierarchical morphology of carbon single–walled nanotubes during sonication in an aliphatic diamine. Polymer. Vol. 46, pp 10854–10865.

Cabero, M.P., Monzon, A., Ramos, I.R. and Ruiz, A.G. (2004) Catal. Today 93-95 pp 681–687.

Callister, W.D. (2003) Materials Science and Engineering. An Introduction. New York: Wiley.

Calvert, P. (1999) Nanotubes composites: A recipe for strength. Nature. Vol. 399, pp 21.

Cao, J., Wang. Q., Rolandi, M., Dai, H. and Aharonov–Bohm(2004) Interference and beating in single-walled carbon-nanotube interferometers. Phys Rev Lett. Vol. 93, No 21, pp 1–4.

Chen, M., Chen, C.M., Koo, H.S. and Chen, C.F. (2003) Diamond Relat. Mater. Vol. 12, pp 1829– 1838.

Choi, E.S., Brooks, J.S., Eaton, D.L.,. Al-Haik, M.S., Hussaini, M.Y., Garmestani, H., Li, D. and Dahmen, K (2003) J. Appl. Phys. . Vol. 94 pp 6034.

Cheng, H.M., Li, F., Sun, X., Brown, S.D.M., Pimenta, M.A., Marucci, A., Dresselhaus, G. and Dresselhaus, M.S. (1998) Bulk morphology and diameter distribution of single-walled carbon nanotubes synthesized by catalytic decomposition of hydrocarbonsChem. Physics Letters. Vol. 289, No. 5-6, pp 602-610.

Clay, J.D., Vijayendran, B., Moon, J., 1999. Rheological study of soy-proteinbased PRF wood adhesives. Annu. Tech. Conf. Soc. Plast. Eng. 57th.

Coleman, J.N., Khan, U. and Gunko, Y.K. (2006). Mechanical reinforcement of polymers using carbon nanotubes. Adv Mater. Vol. 18:689–706.

Creighton, T.E. (1993) “Proteins: Structure and Molecular Properties,” 2nd ed. (Freeman, New York, pp 1.

Cui, S., Canet, R., Derre, A. and et al. (2003) Characterization of multiwall carbon nanotubes and influence of surfactant in the nanocomposite processing. Carbon. Vol.41, pp 797–809.

Datsyuk, V., Kalyva, M., Papagelis, K., Parthenios, J., Tasis, D., Siokou, A., Kallitsis, I. and Galiotis, C. (2008) Chemical oxidation of multiwalled carbon nanotubes. Carbon. Vol. 46, No. 6, pp 833–840.

De, S.S., 1979. Technology of production from soybeans. FAO Agricultural Service Bulletin. Rome, Italy.

Dresselhaus, M.S., Dresselhaus, G. and Saito, R. (1995) Physics of carbon nanotubes. Carbon. Vol. 33, pp 883–891.

Ebbesen, T.W., Hiura, H., Fujita, J., Ochiai, Y., Matsui, S. and Tanigaki, I.L. (1993) Patterns in the bulk growth of carbon nanotubes. Chemical Physics Letters. Vol. 209, pp I-2.

Ebbesen, T. W. (1998) Cones and Tubes: Geometry in the Chemistry of Carbon. Acc. Chem. Res., Vol. 31, pp 558-566.

Elias, M. G., et. al., (1990) ‘‘Sealants Markets and Applications’’Adhesives and Sealants. Vol. 3 of Engineered Materials Handbook, ASM International, 1990.

Endo, M., Fijiwara, H. and Fukunaga, E. (1991) 18th Meeting Japanese Carbon Society, Japanese Carbon Society, Saitama. Pp. 34–35.

Endo, M., Takeuchi, K., Igarashi, S., Kobori, K., Shiraishi, M. and Kroto, H. W. (1992), 19th Meeting Japanese Carbon Society, Japanese Carbon Society, Kyoto, December pp. 192.

Endo M, Muramatsu H, Hayashi T, Kim Y.A., Terrones M. and Dresselhaus M.S. (2005) Nanotechnology:'buckypaper' from coaxial nanotubes. Nature. Vol. 433, pp 476-477

Esumi, K., Ishigami, M., Nakajima, A. and et al. (1996) Chemical treatment of carbon nanotubes. Carbon. Vol. 34, pp 279–281.

Ganesh, E.N. (2013) Single walled and multi walled carbon nanotube structure, synthesis and applications. International Journal of Innovative Technology and Exploring Engineering. Vol. 2, No. 4, pp 311-320.

Gao, B., Bower, C., Lorentzen, J.D. and et al. (2000) Enhanced saturation lithium composition in ball-milled single-walled carbon nanotubes. Chem Phys Lett. Vol. 327, pp 69–75.

Geng, Y., Liu, M.Y., Li, J., Shi, X.M. and Kim, J.K. (2008) Effects of surfactant treatment on mechanical and electrical properties of CNT/epoxy nanocomposites. Composites Part A. Vol. 39, pp 1876–83.

Gong, X., Liu, J., Baskaran, S., Voise, R.D. and Young, J.S. (2000) Surfactant-assisted processing of carbon nanotube/polymer composites. Chem Mater. Vol. 12, pp 1049–1052.

Gojny, F.H., Wichmann, M.H.G., Köpke, U., Fiedler, B. and Schulte, K. (2004) Carbon nanotube reinforced epoxy-composites: enhanced stiffness and fracture toughness at low nanotube content. Compos Sci Technol. Vol. 64, pp 2363–71.

Hamon, M.A., Hui, H. and Bhowmik, P. (2002) Ester-functionalized soluble single-walled carbon nanotubes. Appl Phys A. Vol. 74, pp 333–338.

Harshorn, S. R., ‘‘Introduction’’, Chapter 1, Structural Adhesives: Chemistry and Technology (New York: Plenum Press, 1986).

Hata, K., Futaba, D.N., Mizuno, K., Namai, T., Yumura, M. and Iijima, S. (2004) Water-assisted highly efficient synthesis of impurity-free singlewalled carbon nanotubes. Science. Vol. 306, No 5700, pp 1362–4.

Hernadi, K., Fonseca, A., Nagy, J.B., Bernaerts, D., Riga, J. and Lucas, A. (1996) Catalytic synthesis and purification of carbon nanotubes. Synthetic Metals. Vol. 177, pp 31–34.

Hettiarachchy, N.S., Kalapathy, U. and Myers, D.J. (1995) Alkali-Modified Soy Protein with Improved Adhesive and Hydrophobic Properties. Journals of American Oil Chemist Society. Vol. 72, pp 1461-1464.

Hill, D.E., Lin, Y., Rao, A.M., Allard, L.F. and Sun, Y.P. (2002) Functionalization of carbon nanotubes with polystyrene. Macromolecules. Vol. 35, pp 9466–9671.

Hirsch, A. (2002) Functionalization of single-walled carbon nanotubes. Angew Chem Int Ed. Vol. 41, pp 1853–1859.

Hirsch, A.and Vostrowsky, O. (2005) Functionalization of carbon nanotubes. Top Curr Chem. Vol. 245, pp 93–237.

Hu, H., Zhao, B., Hamon, M.A. and et al. (2003) Sidewall functionalization of single-walled carbon nanotubes by addition of dichlorocarbene. J Am Chem Soc. Vol. 125, pp 14893–900.

Huang, H. M. S. (1994) PhD Dissertation, Iowa State University, Ames, IA.

Huang, W. and Sun, X.S. (2000) Adhesive properties of soy proteins modified by sodium dodecyl sulphate and sodium dodecylbenzene sulfonate. Journal of American Oil Chemist Society. Vol. 77, pp 705–708.

Huang, W. and Xiuzhi Sun, X. (2000) Adhesive Properties of Soy Proteins Modified by Urea and Guanidine Hydrochloride. Journal of American Oil Chemist. Vol. 77, pp 101–104.

Hugh, O.P. (1999) Handbook of chemical vapours deposition (CVD) principles, Technology, and Applications, in: Second Edition, William Andrew publishing, llc Norwich, New York, USA.

Iijima, S. and Ichihashi, T. (1993) Single-shell carbon nanotubes of 1-nm diameter. Nature. Vol. 363, No 6430, pp 603–605.

Iijima S. (1991) Helical microtubules of graphitic carbon. Nature. Vol. 354, No 6348, pp 56–8.

Jia, Z., Wang, Z., Liang, J., Wei, B. and Wu, D. (1999) Production of short multi-walled carbon nanotubes. Carbon. Vol. 37, No. 6, pp 903–906.

John, P. (1990) A symposium on “Adhesive Technology” by polymer group of the NZIC

John, J. and Bhattacharya, M. (1999) Properties of reactively blended soy protein and modified polyesters. Polymer International. Vol. 48, No. 11, pp 1165–1172.

Johnson, L.A., Myers, D.J. and Burden, D.J. (1984) Early Uses of Soy Protein in Far East, Inform. Vol. 3, pp 282–284.

Journet, C., Maser, W.K., Bernier, P., Loiseau, A., de la Chapelle, M.L., Lefrant, S., Deniard, P., Lee, R. and Fischer, J.E. (1997) Large-scale production of single-walled carbon nanotubes by the electric-arc technique. Nature. Vol. 388, pp 756.

Kalapathy, U., Hettiarachchy, N.S., D. Myers, D. and Hanna, M.A. (1995) Modification of Soy Proteins and Their Adhesive Properties on Woods. Journal of American Oil Chemist Society. Vol. 72, pp 507-510.

Kalapathy, U. Hittiarachchy, N.S., Myers, D.J. and Rhee, K.C. (1996) Alkali- modified soy protein: Effect of salts and disulphide bond cleavage on adhesion and viscosity. Journal of American Oil Chemist Society. Vol. 73, pp. 1063- 1066.

Kilbride, B.E., Coleman, J.N., Fraysse, J., Fournet, P., Cadek, M. and Drury, A. (2002) Experimental observation of scaling laws for alternating current and direct current conductivity in polymer–carbon nanotube composite thin films. J Appl Phys; Vol. 92, pp 4024–4030.

Kim, K.S., Bae, D.J., Kim, J.R. and et al. (2002) Modification of electronic structures of a carbon nanotube by hydrogen functionalization. Adv Mater. Vol. 14, pp 1818–21.

Kim, M.S., Rodriguez, N.M. and Baker, R.T.K. (1991) The interaction of hydrocarbons with copper nickel and nickel in the formation of carbon filaments. Journal of Catalysis. Vol. 131, pp 60–73.

Kim J.K. and Mai, Y.W. (1998) Engineered interfaces in fiber reinforced composites. Oxford: Elsevier, pp. 1–100.

Kim, J.K., Sham, M.L. and Wu, J.S. (2001) Nanoscale characterisation of interphase in silane treated glass fibre composites. Composites Part A. Vol. 32, pp 607–18.

Kim, N.S., Lee, Y.T., Park, J., Han, J.B., Choi, Y.S., Choi, S.Y.C., Choo, J.C. and Lee, G.H. 0(2003) J. Phys. Chem. B. Vol. 107, No. 35, pp 9249–9255.

Kinsella, J.E. (1979) Functional Properties of Soy Proteins. Journal of the American Oil Chemist Society. Vol. 56, pp 242-258.

Klemazewski, J.L., Kinsella, J.E., 1991. Sulfitolysis of whey proteins: Effect on emulsion properties. J. Agr. Food Chem. Vol. 39, pp. 1033-1035.6.

Koehn, G. W. (1954) ‘‘Design Manual on Adhesives’’ Machine Design, pp 14-16

Kong, J., Cassell, A.M. and Dai, H. (1998) Chemical vapor deposition of methane for single-walled carbon nanotubes. Chemical Physics Letters. Vol. 292, pp 567–574.

Kovacevic, V., Lucic, S., Hace, D., Glasnovic, A., Smit, I. and Bravar, M. (1994) Investigation of the influence of fillers on the properties of poly (vinyl acetate) adhesives, J. Adhesion, Vol. 47, pp. 201-215.

Kumar, R., Choudhary, V., Mishra, S., Varma, I.K. and Mattiason, B.O. (2002) Adhesives and plastics based on soy protein products. Industrial Crops and Products. Vol. 16, No. 3, pp 155–172.

Kwon, Y., Yim, B., Kim, J.M. and Kim, J. (2011) Dispersion, hybrid interconnection and heat dissipation properties of functionalized carbon nanotubes in epoxy composites for electrically conductive adhesives (ECAs) Microelectronics Reliability. Vol. 51 pp 812–818.

Lambuth, A.L. (1977) Soybean Glues, in Handbook of Adhesion, 2nd edn., edited by I.S. Skiest, Van Nostrand Reinhold, New York, pp. 72-180.

Lambuth, A.L., 2001. Blood and casein glues. In: Satas, D., Tracton, A.A. ed, Coatings Technology Handbook. Marcel Dekker Inc, New York,NY.

Lambuth, A.L. (1994) Protein Adhesives for Wood, in Advanced Wood Adhesive Technology, edited by A. Pizzi and K.L. Mittal, Marcel Dekker, Inc., New York, pp. 259–281.

Lee, S.Y., Yamada, M. and Miyake, M. (2005) Synthesis of carbon nanotubes over gold nanoparticle supported catalysts. Carbon. Vol. 43, No. 13, pp 2654–2663.

Li, Y.B., Wei, B.Q., Liang, J. and et al. (1999) Transformation of carbon nanotubes to nanoparticles by ball milling process. Carbon. Vol. 37, pp 493–497.

Li, Z., Chen, J., Zhang, X., Li, Y. and Fung, K.K. (2002) Catalytic synthesized carbon nanostructures from methane using nanocrystalline Ni. Carbon. Vol. 40, pp 409–415.

Li, Y., Zhang, X.B., Tao, X.Y., Xu, J.M., Huang, W.Z., Luo, J.H., Luo, Z.Q., Li, T., Liu, F., Bao, Y. and Geise, H.J. (2005) Mass production of high-quality multi-walled carbon nanotube bundles on a Ni/Mo/MgO catalyst. Carbon. Vol. 43, No. 2, pp 295–301.

Lin Q., Chen, N., Bian, L. and Fan, M. (2012) Development and mechanism characterization of high performance soy-based bio-adhesives .International Journal of Adhesion & Adhesives Vol. 34, pp 11–16

Lin, C.H., Chang, H.L., Hsu, C.M., Lo, A.Y. and Kuo, C.T. (2003) Diam Relat Mat. Vol. 12, pp 1851–1857.

Liu, J., Rinzler, A.G., Dai, H., Hafner, J.H., Bradley, R.K., Boul, P.J. and et al. (1998) Fullerene pipes. Science. Vol. 280, pp 1253–1256.

Liu, J., Rinzler, A.G., Dai, H.J., Hafner, J.H., Bradley, R.K., Boul, P.J., Lu, A., Iverson, T., Shelimov, K., Huffman, C.B., Rodriguez-Macias, F., Shon, Y.S., Lee, R., Colbert, D.T., Smalley, R.E. (1998) Fullerene pipes. Science. Vol. 280, pp 1253–1256.

Liu P. (2005) Modifications of carbon nanotubes with polymers. Eur Polym J. Vol. 41, pp 2693–2703. Liu, Y. and Li, K. (2007) Development and characterization of adhesives from soy protein for bonding wood. International Journal of Adhesion and Adhesives. Vol. 27, pp 59–67.

Liu, D., Chen, H., Chang, P.R., Wu, Q., Li, K. and Guan, l. (2010) Biomimetic soy protein nanocomposites with calcium carbonate crystalline arrays for use as wood adhesive. Bioresource Technology. Vol. 101, pp 6235–6241.

Liu, F.K., Nie, Y.H. and Shen, B.Y. (1988) Manufacturing soy protein isolate by ultrafiltration, Proc. World Congress on Vegetable Protein Utilization in Human Foods and Animal Feedstuffs, Singapore, pp 84–90.

Lusas, E.W., Riaz, M.N., 1995. Soy protein products: processing and use. J. Nutri. Vol. 125, pp. 573-580.

Meyyappan, M. (2005) Carbon nanotubes: Science and Application. CRC press LLC, 2000 NW, Corporate Blvd, Boca Raton, Florida 33431. pp 3.

Mhlanga, S.D., Mondal, K.C., Carter, R., Witcomb, M.J. and Coville, N.J. (2009) The effect of synthesis parameters on the catalytic synthesis of multiwalled carbon nanotubes using Fe-Co/$CaCO_3$ catalysts, S. Afr. J. Chem. Vol. 62, pp. 67–76.

Mubarak, N.M. and Y. Faridah, Y. (2011) Chem. Eng. J. Vol. 168, pp 461–469

Ma, P.C., Kim, J.K. and Tang, B.Z. (2006) Functionalization of carbon nanotubes using a silane coupling agent. Carbon. Vol. 44, pp 3232–3238.

Machay, C. D. (1998) Good Adhesive Bonding Starts with Surface Preparation, Adhesive Age. Vol. 41, pp 30-32.

McCarthy, B., Coleman, J.N., Czerw, R., Dalton, A.B., Carroll, D.L. and Blau, W.J. (2001) Microscopy studies of nanotube-conjugated polymer interactions. Synth Met. Vol. 121, pp 1225–1226.

Montazeri, A., Javadpour, J., Khavandi, A., Tcharkhtchi, A. and Mohajeri, A. (2010) Mechanical properties of multi-walled carbon nanotube/epoxy composites. Materials and Design. Vol. 31, pp 4202–4208.

Mukhopadhyay, K., Koshio, A., Sugai, T., Tanaka, N., Shinohara, H., Konya, Z. and Nagy, J.B. (1999) Bulk production of quasi-aligned carbon nanotubes bundles by the catalytic chemical vapour deposition (CCVD) method. Chemical Physics Letters. Vol. 303 pp 117–124.

Mukul, K. and Yoshinori, A. (2010) Nanotechnology. Journal of Nanoscience. Vol. 10, pp 3739–3758.

Neng, X.U., Shufeng, M., Wenping L.V. and Zhouping, W. (2011). Soy-protein adhesives improved by SiO2 nanoparticles for plywoods. Pigment and Resin Technology, vol 40(3)

Nielsen, N.C. (1985) The structure and complexity of the 11S polypeptides in soybeans. Journal of the American Oil Chemists' Society. Vol. 62, No. 12, pp 1680-1686.

Nikolaev, P., Bronikowski, M.J., Bradley, R.K., Rohmund, F., Colbert, D.T., Smith, K.A. and Smalley, R.E. (1999) Gas-phase catalytic growth of single-walled carbon nanotubes from carbon monoxide. Chemical Physics Letters. Vol. 313, pp 91–97.

Nordqvista, P., Nordgrena, N., Khabbazc, F. and Malmströma, E. (2013) Plant proteins as wood adhesives: Bonding performance at the macro- and nanoscale Industrial Crops and Products. Vol. 44, pp.246– 252.

Paetau, I., Chen, C. L. and Jane, J.L. (1994) Biodegradable plastic made from soybean products. Effect of Preparation and Processing on Mechanical Properties and Water Absorption. Ind. Eng. Chem. Res., Vol. 33 No. 7, pp 1821–1827.

Paiva, M.C., Zhou, B., Fernando, K.A.S., Lin, Y., Kennedy, J.M., Sun, Y.P. (2004) Mechanical and morphological characterization of polymer–carbon nanocomposites from functionalized carbon nanotubes. Carbon. Vol. 42, pp 2849–2854.

Pearson, A.M., 1984. Soy Proteins, In "Development in Food Proteins-II." B.J.F Hudson ed. Elseveir Applied Science Publisher. New York, NY.

Petri, E.M. (2007) Handbook of adhesive and sealants. "An Introduction to Adhesive and Sealants". McGraw-Hill Company Inc. Second Edition, chapter 1, pp 14 18.

Peruzzo, P., Bonnefond, A., Reyes, Y., Fernández, M., Fare, J., Ronne, E., Paulis, M. and Leiza, J. J. (2014) Beneficial in-situ incorporation of nanoclay to water borne PVAc/PVOH dispersion adhesives for wood applications. International Journal of Adhesion and Adhesives Vol. 48, pp 295–302.

Peng-Cheng Ma, Siddiqui, N.A., Marom, G. and Kim, J. (2010) Dispersion and functionalization of carbon nanotubes for polymer-based nanocomposites: A review. Composites. Vol. 41, pp 1345–1367.

Qiao, L., Easteal, A.J., Bolt, C.J., Coveny, P.K., and Franich, R.A. (1999) The effects of filler materials on poly (vinyl acetate) emulsion wood adhesives. Pigment and Resin Technology. Vol. 28, No. 6, pp 326-330.

Qian, W., Liu, T., Wang, Z., Yu, H., Li, Z., Wei F. and G. Luo, (2003) Effect of adding nickel to iron–alumina catalysts on the morphology of as-grown carbon nanotubes. Carbon. Vol. 41, 2487–2493.

Qiu, L.J. and Chang, R. (2010)The national key facility for crop gene resources and genetic improvement/ key lab of germplasm utilization (MOA),Institute of Crop Science, Chinese Academy of Agricultural Sciences, Beijing, PR Chin

Reilly, P.T.A. and Whitten, W.B. (2006) The role of free radical condensates in the production of carbon nanotubes during the hydrocarbon CVD process. Carbon. Vol. 44, pp 1653-1660.

Rao, R., Govindaraj, A. and Rao, C.N.R. (1997) Nanotubes and Nanowires. Chemistry Matter. Vol.9, No. 10, pp 2078.

Ratna D, Banthia A K, Deb P C. (2001) Acrylate based liquid rubber as impact modifier for epoxy resin; Journal of Applied Polymer Science. Vol. 80, No.10, pp 1792 - 1801

Rhim, J.W., Gennadios, A., Weller, C.L., Cezeirat, C. and Hanna, M.A. (1998) Soy protein isolate–dialdehyde starch films1. Industrial Crops and Products. Vol. 8, No. 3, pp 195–203

Samal, S.S. (2009) Role of temperature and carbon nanotube reinforcement on epoxy based nanocomposites. Journal of Minerals, Materials Characterization and Engineering, Vol. 8, No.1, pp 25-36.

Sandler, J.K.W., Shaffer, M.S.P., Prasse, T., Bauhofer, W., Schulte, K. and Windle, A.H. (1999) Development of a dispersion process for carbon nanotubes in an epoxy matrix and the resulting electrical properties. Polymer. Vol. 40, pp 5967–5671.

Santoni, I. and Pizzo, B. (2013) Evaluation of alternative vegetable proteins as wood adhesives. Industrial Crops and Products. Vol. 45, pp 148– 154.

Satishkumar, B.C., Govindaraj, A., Sen, R., Rao, C.N.R. (1998) Single- walled nanotubes by the pyrolysis of acetylene- organometallic mixtures. Chemical Physics Letters. Vol. 293, pp 47–52.

Schmitt, T.C., Biris, A.S., Miller, D.W., Biris, A.R., Lupu, D., Trigwell, S. and Rahman, Z.U. (2006) Analysis of effluent gases during the CCVD growth of multi-wall carbon nanotubes from acetylene. Carbon. Vol. 44, pp. 2032–2038.

Sen, R., Govindaraj, A., Rao, C.N.R. (1997) Carbon nanotubes by the metallocene route. Chemical Physics Letters. Vol. 267, pp 276–280.

Shen, C., Brozena, A. and Wang, Y. (2011).Double walled nanotubes, challenges and opportunities. Nanoscale. Vol. 3, pp. 503-518.

Sinha, A.K., Hwang, D.W. and Hwang, L.P. (2000) A novel approach to bulk synthesis of carbon nanotubes filled with metals by a catalytic chemical vapour deposition method. Chemical Physics Letters. Vol. 332, pp 455–460.

Schmitz, J.F. Jr. (2009) Enzyme modified soy flour adhesives. PhD dissertation submitted to Iowa State University. Ames, Iowa.

Schultz, J. and Nardin, M. (1994) Theories and Mechanisms of Adhesion. Handbook of Adhesive Technology, Pizzi, A.; Mittal, K. L., Eds., Marcel Dekker, New York.

Shaffer, M.S.P., Fan, X. and Windle, A.H. (1998) Dispersion and packing of carbon nanotubes. Carbon. Vol. 36, pp 1603-1612.

Shaffer, M.S.P. and Windle, A.H. (1999) Fabrication and characterization of carbon nanotube/poly (vinyl alcohol) composites. Adv. Mater. Vol. 11, pp 937-941.

Sham, M.L. and Kim, J.K. (2006) Surface functionalities of multi-wall carbon nanotubes after UV/ozone and TETA treatments. Carbon. Vol. 44, pp 768–77.

Shera, J.N., Rawlins, J.W., Thames, S.F., 2007. Characterization of enzymemodified soy protein isolate. Abstracts of Papers, 233rd ACS National Meeting. Chicago, IL.

Singh, C., Shaffer, M.S.P. and Windle, A.H (2003) Production of controlled architectures of aligned carbon nanotubes by an injection chemical vapour deposition method. Carbon. Vol. 41, No. 2, pp 359–368.

Song Y.S. and Youn J.R. (2005) Influence of dispersion states of carbon nanotubes on physical properties of epoxy nanocomposites. Carbon. Vol. 43, pp 1378–1385.

Solvetat, S., Breton Y., Desarmot, G., Berguin, F. and Bonnamy, S. (2004). Mechanical properties of multiwalled CNTs/epoxy composite. Influence of Network Morphology of Carbon, vol.42, pp. 1027-30.

Sook, Y., Kim, L., Peter, S., Park, W. and Rhee, K.C. (1990) Functional Properties of Proteolytic Enzyme Modified Soy Protein Isolate. J. Agric. Food Chem., Vol. 38, pp 651-656.

Stoeckel, F., Konnerth, J. and Gindl-Altmutter, W. (2013) Mechanical properties of adhesives for bonding wood—A review. International Journal of Adhesion & Adhesives. pp 4532–41.

Steele, P.H., Kreibich, R.E., Steynberg, P.J., Hemingway, R.W., 1998. Finger jointing green southern yellow pine with a soy based adhesives. Adhes. Age. Vol. 41, pp. 49–56.

Stephenson, J.J., Sadana, A.K., Higginbotham, A.L. and Tour, J.M. (2006) Highly functionalized and soluble multiwalled carbon nanotubes by reductive alkylation and arylation: the billups reaction. Chem Mater. Vol.18, pp 4658–4661.

Sun, X. and Bian, K (1999). Shear Strength and Water Resistance of Modified Soy Protein Adhesives. Journal of American Oil Chemist Society Vol. 76, pp 977–980.

Thess, A., Lee, R., Nikolaev, P., Dai, H., Petit, P., Robert, J., Xu, C., Lee, Y.H., Kim, S.G., Rinzler, A.G., Colbert, D.T., Scuseria, G.E., Tománek, D., Fischer, J.E. and Smalley, R.E. (1996). Science, Vol. 273, pp 483.

Tasis, D., Tagmatarchis, N., Bianco, A. and Prato, M. (2006) Chemistry of carbon nanotubes. Chem Rev. Vol. 106, pp 1105–36.

Takemura A, Tomita,B I, Mizumachi H. (1985) Dynamic mechanical properties and adhesive strengths of epoxy resins modified with liquid rubber I: Modification with ATBN; Journal of Applied Polymer Science.Vol. 30, No. 10, pp 4031- 4043.

Tibbetts, G.G. and Beetz, C.P. (1987) Mechanical-properties of vapor-grown carbon-fibers. J Phys D—Appl Phys. Vol. 20, No. 3, pp. 292–7.

Thostenson, E.T., Ren, Z.F. and Chou, T.W. (2001) Advances in the science and technology of CNTs and their composites: A review. Composite Science Technology. Vol. 61, pp 1899–1912.

Tohji, K., Takahashi, H., Shinoda, Y., Shimizu, N., Jeyadevan, B., Matsuoda, I., Saito, Y., Kasuya, A., Ito, S. and Nishina, Y. J. (1997) Phys. Chem. B 101, pp. 1974.

Vaisman, L., Wagner, H.D. and Marom, G. (2006) The role of surfactants in dispersion of carbon nanotubes. Adv Colloid Interface Sci. Vol. 128–130, pp 37–46.

Wang, S.C., Chang, K.S. and Yuan, C.J. (2009) Enhancement of electrochemical properties of screen-printed carbon electrodes by oxygen plasma treatment. Electrochim Acta. Vol. 54, pp 4937–4943.

Wei, B.Q., Vajtai, R., Jung, Y., Ward, J., Zhang, R., Ramanath, G. and Ajayan, P.M. (2002) Microfabrication technology: Organized assembly of carbon nanotubes. Nature 416 495–496.

Wernik, J.M. and Meguid, S.A. (2014) On the mechanical characterization of carbon nanotube reinforced epoxy adhesives. Materials and Design. Vol. 59, pp. 19–32.

Whitsitt, E.A. and Barron, A.R. (2003) Silica coated single walled carbon nanotubes. Nano Lett. Vol. 3, pp 775–778.

Wolf, W.J. (1970) Soybean Proteins: Their Functional, Chemical, and Physical Properties, J. Agric. Food Chem. Vol. 18, pp 969–976.

Wong, E.W., Sheehan, P.E. and Lieber, C.M. (1997) Nanobeam mechanics: elasticity, strength, and toughness of nanorods and nanotubes. Science. Vol. 277, pp 1971–5.

Wong, S.S., Woolley, A.T., Joselevich, E. and Lieber, C.M (1999) Functionalization of carbon nanotube AFM probes using tip-activated gases Chemical Physics Letters. Vol. 306, No. 5–6, pp 219–225.

Wu, Y.V. and Inglet, G.E. (1974) Denaturation of Plant Proteins Related to Functionality and Food Applications. A Review, J. Food Sci. Vol. 39, pp. 218–225.

Wu, B.Y., Liu, A.H., Zhou, X.P., Jiang, Z.D. (1995) Chem. J. Chinese Univ. Vol. 16, pp 1641.

Xiang, L.X., Tang, C.Y., Cao, J., Wang, C.Y., Wang, K., Zhang, Q. and Fu, Q. (2009) Preparation and characterization of soy protein isolate (SPI)/montmorillonite (MMT) bionanocomposites. Chinese Journal of Polymer Science Vol. 27, No. 6, pp 843−849.

Xie, S., Li, W., Pan, Z., Chang, B and Sun, L. (2000) Mechanical and physical properties on carbon nanotube. J Phys Chem Solids, Vol. 61, No 7, pp 1153–1158..

Yu, J., Grossiord, N., Koning, C.E. and Loos, J. (2007) Controlling the dispersion of multi-wall carbon nanotubes, in aqueous surfactant solution. Carbon. Vol. 45, pp 618–623.

Yu, R., Chen, L., Liu, Q., Lin, J., Tan, K.L., Ng, S.C. and et al. (1998) Platinum deposition on carbon nanotubes via chemical modification. Chem Mater. Vol. 10, pp 718–722.

Yu, M., Lourie, O., Dyer, M.J., Kelly, T.F. and Ruoff, R.S. (2000) Strength and breaking mechanism of multiwalled carbon nanotubes under tensile load. Science. Vol. 287, pp 637–40.

Yu, S., Tong, M.N. and Critchlow, G. (2010) .Use of carbon nanotubes reinforced epoxy as adhesives to join aluminum plates. Materials and Design. Vol. 31, pp 126–129.

Zhang, Q.H. and Chen, D.J. (2004) Percolation threshold and morphology of composites of conducting carbon black/polypropylene/EVA. J Mater Sci. Vol. 39:1751–1757.

Zhao, K., Hao, X.F., Liu, D.J., 2000. Soy protein isolate composite adhesive. Zhengzhou Gongye Daxue Xuebao. Vol. 21, pp. 15-18.

Zeng, X., Sun, X., Cheng, G., Yan, X. and Xu, X. (2002) Production of multi-walled carbon nanotubes on a large scale. Physica B. Vol. 323, pp 330–332.

Ziegler, K.J., Gu, Z., Peng, H., Flor, E.L., Hauge, R.H. and Smalley, R.E. (2005) Controlled oxidative cutting of single-walled carbon nanotubes. J Am Chem Soc, Vol. 127, pp. 1541–1547.

Zhu, Y., Bakis, C.E., James H. Adair, J.H. (2012) Effects of carbon nanofiller functionalization and distribution on interlaminar fracture toughness of multi-scale reinforced polymer composites. Carbon. Vol. 50, pp 1316 –1331.

Chapter Three

3.0 Materials and methods

3.1 Materials

Analytically graded calcium carbonate was purchased from Rochelle chemicals, South Africa. Sodium hydroxide (≥ 98 %), Acetone (≥ 98 %), 55 % Nitric acid with ≥ 99.9 % purity, ferrous nitrate and cobalt nitrate with ≥ 98 % purity were of analytical grade and were purchased from Sigma-Aldrich St Luis MO, USA. Nitrogen and acetylene gasses with purities of ≥ 99.9 % and ≥ 99.0 % respectively were purchased from Afrox, South Africa. Commercial soy-protein isolate (SPI) was purchased from Solae, LLC, North America 4300 Duncan Avenue St. Louis, MO 63110, USA. The original moisture and protein content of SPI were 5.5% and 90.0% respectively. Maple wood specimens were purchased from H & S timber company, Benoni, South Africa.

Equipment: Electronic weigh balance (AND EK-610i, max 600g, d= 0.01g, A & D Co., LTD Japan),

electric stirrer (FMH instrument, STR-MO), , chemical vapour deposition (CVD) reactor, quartz tube (27 mm i.d × 30 mm o.d × 980 mm length), quartz boat (120 mm ×15 mm), thermocouple, oven dryer, sonicator (UMC 20), pH meter, beaker, retort stand, burette and funnel and Suction pump, 80 grit sand paper, metal bar, furnace (thermopower furnace (PTY) LTD), Enerpac hydraulic machine 39 and tensile testing machine (AG-IC 20/50KN Shimadzu, 346-54411-51).

3.2 Methods

3.2.1 Preparation of Iron –Cobalt Catalyst on calcium carbonate support (Fe- Co/$CaCO_3$)

Wet impregnation method was used to prepare Fe-Co catalyst on calcium carbonate support. 3.62 g of iron nitrate and 2.47 g of cobalt nitrate were weighed on an electronic weigh balance and were mixed together in a beaker. The two mixtures were dissolved in 30 mL of distilled water. The solution was stirred with a stirring rod until it was completely dissolved. 10 g of

calcium carbonate was measured into another beaker. Burette clamped on a retort stand was set up, and 30 mL of the solution of Fe-Co nitrate was poured into the burette. This solution was drop wisely added to 10 g of calcium carbonate support in the beaker and at the same time allowed to stir on an electric stirrer for 45 minutes so as to allow homogenous mixture of solution of calcium carbonate and Fe-Co nitrate. The total mass metal loading of Fe-Co was 5 wt % in the ratio 1:1 (50:50). The homogenous solution was then dried in a vacuum oven at 110^0C for 12 hours. The catalyst supported on calcium carbonate support was removed from the oven and allowed to cool down to room temperature and weighed (24.34 g).

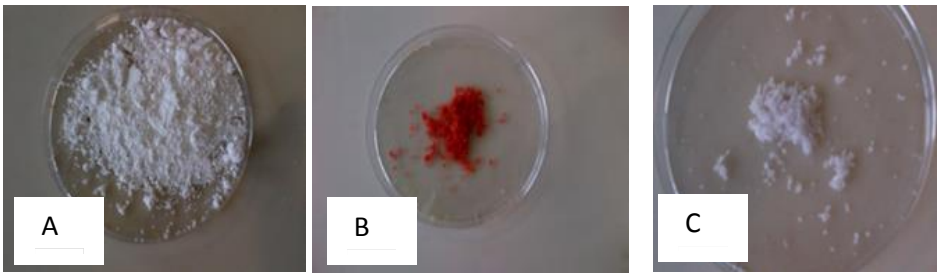

Figure 3.1: Salts of (A) calcium carbonate (B) cobalt nitrate (C) iron nitrate

3.2.2 Synthesis of carbon nanotubes (CNTs)

Temperature and time set up for CVD reactor

PV 1 = 700^0C for 1 hour 20 minutes, while Nitrogen gas flows to purge the system off oxygen

PV 2 = 700^0C for 1 hour for the acetylene

PV3 = 25^0C for 1 hour 20 minutes for the set up to cool off after turning off acetylene and nitrogen gasses.

The reaction time, reaction temperature and gas flow rate were electronically (PID) controlled to favour the yield of Carbon nanotubes. About 1 g of Fe-Co/$CaCO_3$ supported catalyst was put inside the quartz boat and was centered in a quartz tube inside the CVD reactor. The furnace

temperature was set at reaction temperature of 700^{o}, at 10^{0}C/min for 1 hour 20 minutes. This temperature was accurately monitored by a high sensitivity thermocouple. Nitrogen was allowed to flow at 180 mL/ min to remove any traces of air. When the temperature reached 700^{0}C, the acetylene gas was allowed to flow continuously at 90 mL/min for a reaction time of 1 hour. The flow of acetylene was then stopped after 1 hour of reaction time, and the furnace was allowed to cool down to room temperature under continuous flow of nitrogen, after which the flow of nitrogen was stopped. The quartz tube was removed from the CVD reactor and the quartz boat was gently taken out. The carbon deposit formed inside the quartz boat was weighed and recorded. The schematic of the set-up for synthesis of CNTs is shown in Figure 3.2

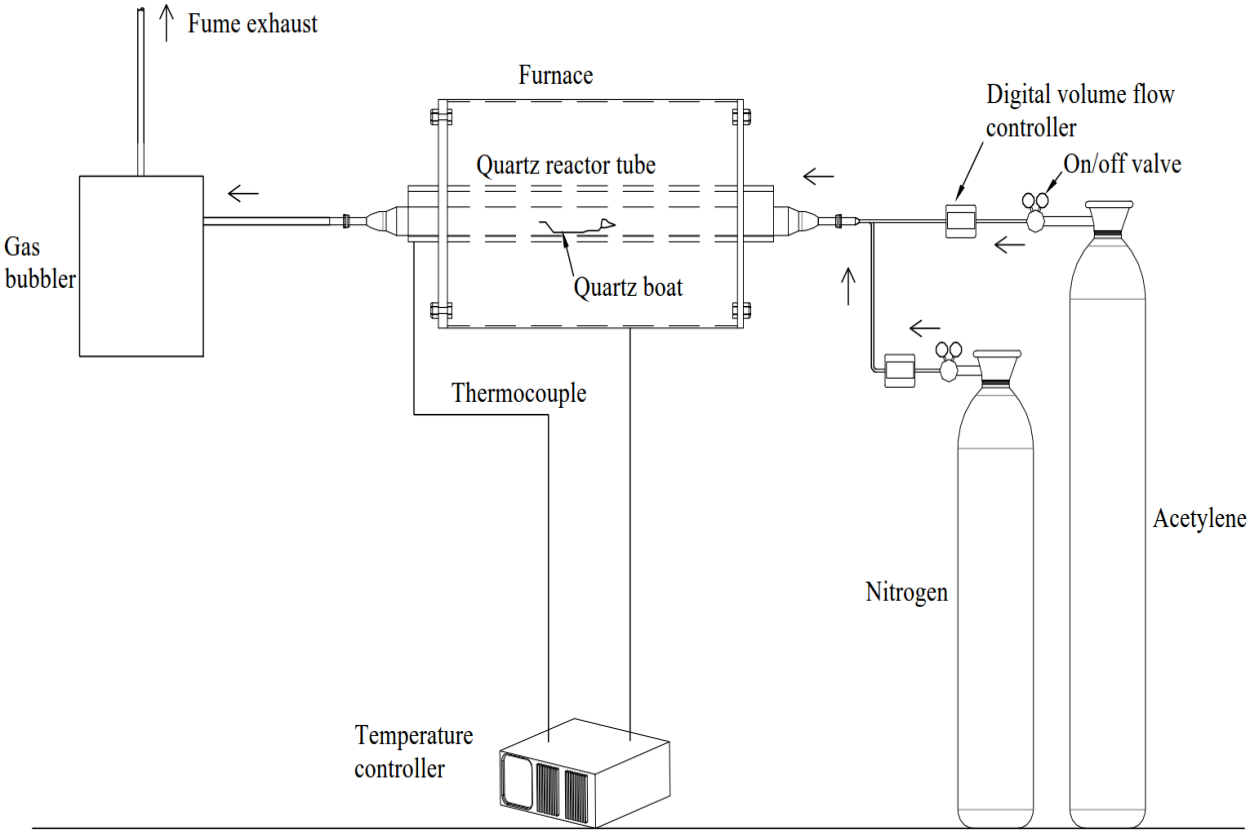

Figure 3.2: Schematic of the synthesis process for CNTs by horizontal CVD reactor

3.2.3 Functionalization of the synthesized catalysts

A liquid-phase oxidation purification technique was employed to get rid of the catalyst support, metallic and the amorphous particles in the synthesized CNTs. 0.5 g of CNTs was measured into a beaker and 100 mL of 55 % nitric acid was poured into the beaker containing CNTs. The solution in the beaker was put inside a sonicator for 4 hours, and the solution was stirred through an ultrasound vibration. The homogenous solution was removed from the sonicator and soaked in 800 mL of distilled water over night. Another CNT-nitric solution was stirred on a magnetic stirrer for the same number of hours as for the sonicator. The mixture of CNTs and nitric acid was filtered with a filtration set-upby a filter paper placed inside a funnel. The CNTs were washed severally with distilled water until the residue was neutral to litmus paper (pH of 7). The functionalized CNTs were dried inside an oven for 12 hours at 120^0C. The CNTs were removed from the oven and allowed to cool down and were weighed. The functionalized CNTs samples were characterized using, scanning electron microscopy (SEM), Fourier transform infra-red (FTIR) spectroscopy and thermogravimetry analysis (TGA) for morphology, surface chemistry, and thermal stability respectively.

3.2.4 Preparation of SPI/CNTs nanocomposite adhesive from soy protein isolate (SPI)

In order to dissolve SPI flour, 10 g of SPI flour was measured into 90 mL of distilled water in a beaker and stirred on a magnetic stirrer for 1 hour 30 minutes at room temperature to ensure homogeneous mixture. The pH meter was first calibrated using buffer 4 and 7 solutions, to ensure accurate reading. The pH probe was dipped into the SPI solution and the reading on the pH meter was noted and recorded. 1 M solution of sodium hydroxide (NaOH) was prepared by dissolving 40 g of NaOH pellets in 500 mL of distilled water inside a beaker. The homogeneous solution was poured into a volumetric flask and made up 1 dm^3. The pH of the SPI solution of each sample was adjusted to 10 drop-wisely adding NaOH solution through an adjustable pipette until the pH read 10.0 ± 0.1. The mixture was then stirred at 50^oC for 1 hour and the pH of the

solution was read and recorded again. CNTs/FCNTs of varied concentrations from 0.1 - 1.0 wt % were weighed into different portions of the SPI solution prepared. The samples were labeled as; SPICNTs 0.1, SPICNTs 0.3, SPICNTs 0.5, SPICNTs 0.7 and SPICNTs 1.0. The samples for FCNTs were labeled as; SPI/FCNTs 0.1, SPI/FCNTs 0.3, SPI/FCNTs 0.5, SPI/FCNTs 0.7 and SPI/FCNTs 1.0. Two methods of dispersion of CNTs into SPI were employed here; 90 minutes sonication/30 minutes stirring and mechanical (shear) stirring for 2 hour (Figure 3.3 A and 3.3 B). The samples were labeled as SPI/SCNTs and SPI/SFCNTs for samples dispersed by sonication method. The SPI/CNTs and SPI/FCNTs solutions at varied CNTs and FCNTs concentrations were stirred at room temperature for 2 hours, after which the pH values were taken and recorded. These samples were divided into two portions; one for preparation and characterization and the other portion for application on wood specimens

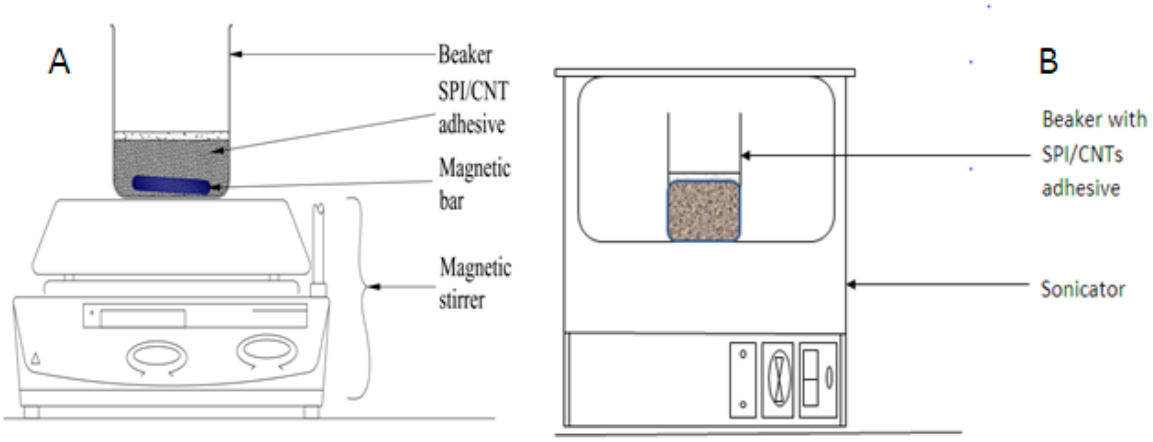

Figure 3.3: Schematics of dispersion of SPI/CNTs by (A) mechanical stirring methods and (B) Sonication method

3.2.5 Determination of percentage moisture and solid content of the alkaline –modified SPI and SPI/CNTs

About 25 g of SPI/CNTs nanocomposite adhesive solutions samples was weighed into a beaker and dried in an over dryer at 120^{O}C for 2 hours. The weight of the samples was recorded after drying and the percentage solid and moisture content of the samples were calculated using equation 3.1 and equation 3.2 respectively. The dried samples were then characterized for scanning electron microscopy (SEM), Fourier transmission infrared (FTIR) spectroscopy, and thermogravimetric analysis (TGA).

$$\%\ Solid\ content = \frac{\text{Final wt}}{\text{Initial wt}} \times 100 \tag{3.1}$$

$$\%\ Moisture\ content = \frac{\text{Initial wt} - \text{Final wt}}{\text{Initial wt}} \times 100 \tag{3.2}$$

3.2.6 Preparation of wood surface and application of SPI/CNTs nanocomposite adhesive samples

The surface of the wood specimens was prepared with 80 grit sand paper, to prevent adhesive and cohesive failure. The surfaces were also cleaned with a solvent (acetone) moistened cloth to wipe out any form of dirt or grease from the surface of the wood. Three pieces (50 mm by 20 mm by 3 mm each) of maple wood specimens made a sample for bond strength test (Figure 3.4). SPI nanocomposite adhesive was applied on the surface of the wood specimen area of (20 ×15) mm^2 and two other specimens were bonded to it as shown in Figure 3.5 A. The samples were placed on a metal bar and another metal bar was placed on it. These metal bar with 6 samples was placed inside a furnace (thermopower furnace (PTY) LTD) and pressed with Enerpac hydraulic machine 39 (Figure 3.5 B) at a pressure of 1.4 MPa (513.76 kg), calculated using equation 3.3 and 120^{o}C for 10 minutes. It was allowed to cool down and dry at ambient temperature for 7 days. The steps in adhesive bonding technique is as shown in Figure 3.6

$$Pressure = \frac{Force}{\text{Area}} \tag{3.3}$$

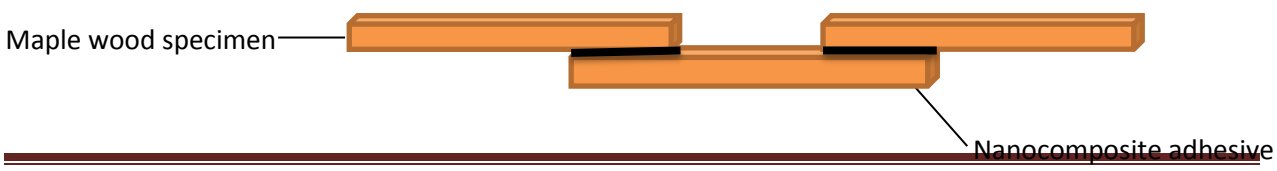

Figure 3.4: Assembly of maple wood composite to make a sample

Figure 3.5: (A) six adhesive nanocomposite bonded samples on a metal bar (B) bonded wood samples pressed by the hydraulic machine inside the furnace at a constant temperature and pressure.

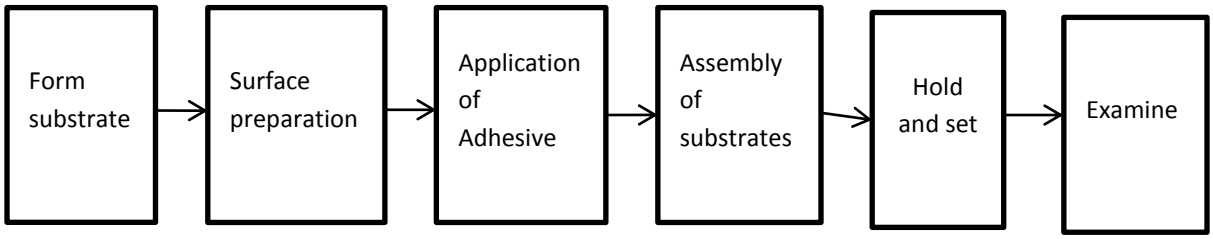

Figure 3.6: Basic steps in adhesive bonding technique

3.2.7 Evaluation of bond strength of SPI/CNTs adhesive nanocomposite on wood

Dry bond test: The composite wood samples were allowed to dry for seven days after bonding with nanocomposite adhesive samples according to European standard, EN-204 (durability class D1 for interior use) and the bond strength test was determined on them (Table 3.1).

Water soaking and drying (WSAD): EN-204 durability class D2 (for interior use and occasional short-term exposure to water or moisture) standard was used to determine the water resistance of the nanocomposite adhesive. The bonded wood samples were immersed in water (23^{o}C) for 3 hours and dried for 7 days under standard atmosphere, after which the bond strength test was carried out on them (Table 3.1).

Table 3.1: European (EN-204) standard's conditioning sequence and minimum values of adhesive strength for thin bond line.

Conditioning sequence, duration and condition	Adhesive strength (Mpa)	Durability classes
7days in standard atmosphere	≥10	D1
7 days in standard atmosphere, 3hrs in water at (20±5) ^{o}C, 7 days in standard atmosphere.	≥8	D2

Evaluation of bond strength of the nanocomposite adhesives on the wood samples was done by a tensile testing machine (AG-IC 20/50 KN Shimadzu, 346-54411-51). Load cell of 20 KN was used with cross head speed of 1.0 mm/min. The highest force values at breakage of the maple wood samples were taken and recorded for each sample. Three samples of wood were tested for each nanocomposite adhesive sample and the average bond strength was calculated and recorded. The bond strength (MPa) was calculated using Equation 3.4 and 3.5. The diagram of the set-up is as shown in Figure 3.7.

$$Pressure = \frac{\text{Force (KN)}}{\text{Area}(m^2)} \quad (3.4)$$

$$\text{Pressure (Mpa)} = \frac{\text{Force} \times 1000\text{(N)}}{\text{Area} \times 10^{-6}(m^2)} \quad (3.5)$$

Figure 3.7: (A) Set-up of tensile testing machine with a computer system showing the readings/data values (AG-IC 20/50 KN Shimadzu) (B) Bonded wood sample clamped to the tensile test machine.

3.3 Characterization of samples

The characterization of the catalyst, CNTs, FCNTs and SPI/CNTs nanocomposite adhesive samples were achieved by a number of analytical techniques that include SEM, TGA and FTIR.

3.3.1 Scanning Electron Microscopy (SEM)

The samples were coated with 60 % palladium and 40 % gold (Pd/Au) prior to SEM analysis to prevent charge up. Carl Zeiss sigma field electronic scanning electron microscope (FESEM) as shown in Figure 3.8 was used to observe the surface morphology of the catalyst, CNTs, FCNTs and SPI/CNTs nanocomposite adhesive samples at different magnifications.

Figure 3.8: (A) Field electronic scanning electron microscope (Model: Carl Zeiss sigma)

3.3.2 Thermogravimetry analysis (TGA)

The thermal stability and weight degradation of the samples were determined by TA SDT Q600 thermogravimetric analyzer (DRYCAL TA) as shown in Figure 3.9. Nitrogen gas was set at 10mL/min. Temperature commenced at room temperature to 800^{o}C at 10^{o}C/min. 5.0 ± 0.2 g of CNTs and FCNTs samples and 11.0 ± 0.2 g of SPI/CNTs adhesive nanocomposite samples were

weighed into a small container and placed on the alumina pan. The furnace was closed and the TG analysis was run on the samples. The data were automatically recorded and plotted.

Figure 3.9: Thermogravimetry analyzer (Model: TA SDT Q600 (DRYCAL TA))

3.3.3 Fourier transform infrared (FTIR) analysis

Infrared analyzer, Bruker Tensor 27 was used to determine the attachment of functionalities and the type of functional groups on the surfaces of samples prepared for CNTs, FCNTs and SPI/CNTs nanocomposite adhesive samples. The oven dried powdered samples (2mg) were mixed with 200 mg of potassium bromide (KBr), and pressed for 3 minutes at 20 Mpa prior to the commencement of the scanning. The spectra ranged from 500 cm^{-1} to 5000 cm^{-1}.

Chapter Four

4.0 Results and discussion

4.1 Effect of processing parameters on percentage moisture and solid content of the adhesive

4.1.1 Effect of concentration of CNTs on the percentage moisture and solid contents of SPI/CNTs nanocomposite adhesive

Table 4.1 shows the effect of concentration on the percentage Solid and moisture content of SPI/CNTs nanocomposite wood adhesive. From this table, it can be observed that the percentage solid content of the SPI adhesive increased by 10.6% when the pH was adjusted from 7.37 to 10.00. This indicated that increase in pH of SPI adhesive increases the percentage solid content and reduces the moisture content, because the higher the pH the higher the hydrolysis. As the concentration of the CNTs and FCNTs increased, the percentage solid content also increased which may be attributed to the absorption of water in the system by CNTs (Figure 4.1) (Zhang et al., 2014).

Table 4.1: Effect of concentration of CNTs and FCNTs on the percentage moisture and solid content of adhesive nanocomposite.

Adhesive nanocomposite samples	**Initial wt of samples (g)**	**Final wt of samples (g)**	**Weight loss Initial wt- Final wt**	**% Solid content**	**%Moisture content**
SPINaOH	25	1.99	23.01	7.96	92.04
SPISNaOH	25	2.10	22.90	8.40	91.60
SPIH_2O	25	1.80	23.20	7.20	92.80
SPI0.1	25	2.37	22.63	9.48	90.52
SPI/FCNTs0.1	25	2.36	22.64	9.44	90.56
SPI/CNTs0.3	25	2.47	22.53	9.88	90.12
SPI/FCNTs0.3	25	2.46	22.54	9.84	90.16
SPI/CNTs0.5	25	2.55	22.45	10.20	89.80
SPI/FCNTs0.5	25	2.54	22.46	10.16	89.84

SPI/CNTs0.7	25	2.67	22.33	10.68	89.32
SPI/FCNTs0.7	25	2.66	22.34	10.64	89.36
SPICNTs1.0	25	2.78	22.22	11.12	88.88
SSPI/FCNTs1.0	25	2.75	22.25	11.00	89.00
SPISCNTS0.1	25	2.40	22.60	9.60	90.40
SPI/SFCNTs0.1	25	2.39	22.61	9.56	90.44
SPISCNTs0.7	25	2.69	22.31	10.76	89.24

Table 4.1 shows SPIH_2O- SPI mixed with water in ratio 1: 9. SPINaOH- SPI adjusted to pH 10 with NaOH solution stirred by high speed magnetic stirrer, SPISNaOH – stirred by sonication method, SPI0.1-1.0- SPI/CNTs with varying concentration from 0.1-1.0% by high speed magnetic stirring,SPIFCNTs0.1-1.0- SPI with varying concentration(0.1-1.0%) of FCNTs by high speed magnetic stirring, SPISCNTs0.1- CNTs (0.1%) dispersed in SPI by sonication method/mixing and SPISFCNTs0.1- FCNTS (0.1%) dispersed in SPI by sonication method/mixing.

From figure 4.2 and table 4.2, it could be observed that the pH of the SPI adhesive dropped by 3.2% when the alkaline modified SPI was stirred for 1 hour at 50^{o}C. This reduced the percentage solid content and increased the moisture content. The decrease in solid content is attributed to the drop in pH values and the result indicates that temperature reduces the pH value and hence reduces the solid content of the adhesive. An appropriate solid content can improve the shear strength of the adhesive by preventing the penetration of adhesive into the veneer. Thus, allowing the adhesive to stay on the surface of the wood for effective bonding (Gao et al., 2012).

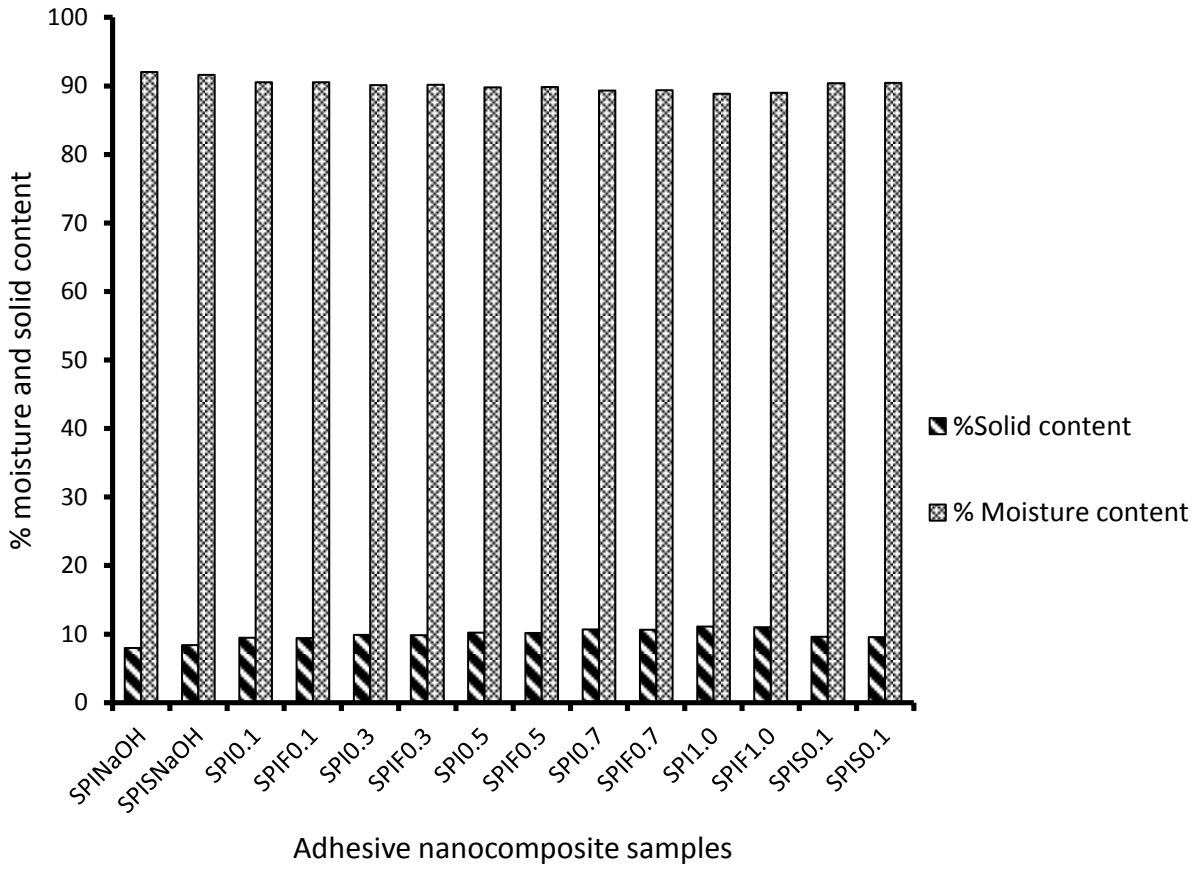

Figure 4.1: Effect of Concentration of CNTs on the percentage solid and moisture content

4.1.2 Effect of temperature on adhesive nanocomposite

Table 4.2 shows the effect of temperature on the adhesive nanocomposite.

Table 4.2: Effect of temperature on pH of SPI adhesive

Samples	pH of SPI in H_2O	pH of SPI NaOH before stirring	pH of SPINaOH after stirring at 50^oC
A	7.48	10.00	9.68
B	7.46	10.12	9.85
C	7.44	10.02	9.74
D	7.48	10.10	9.80

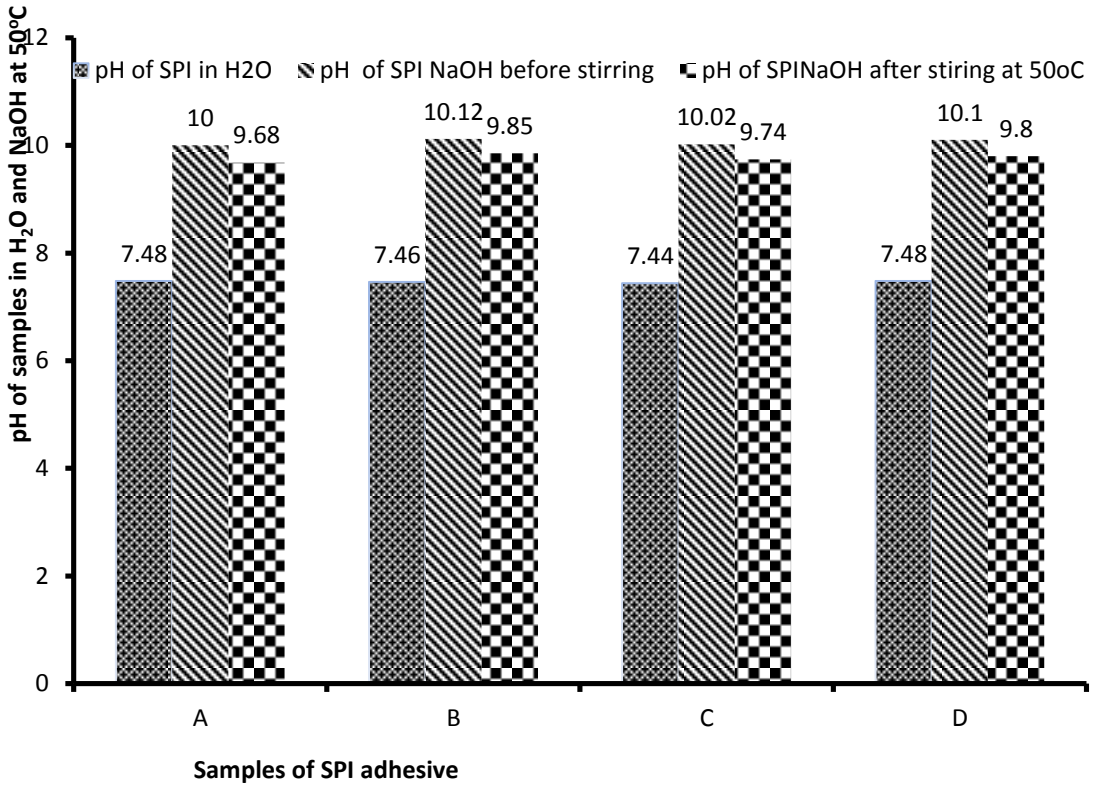

Figure 4.2: Effect of temperature on the pH of SPI solution

4.1.3 Effect of concentration of CNTs on adhesive nanocomposite

Table 4.3 shows the effect of CNTs concentration on the adhesive nanocomposite. From this table, it can be seen that is a slight change in the pH of SPI/FCNTs and the pH of SPI/CNTs. Figure 4.3 shows that the pH of the SPI/FCNTs nanocomposite adhesive are higher than the pH of SPI/CNTs. The lower pH values in SPI/CNTs may be attributed to the presence of metal oxide (CaO) on the CNTs. This shows that the amount of CaO on the FCNTs has been reduced after purification

Table 4.3: Effect of CNTs and FCNTs on the pH of modified SPI adhesive

Samples	pH of SPI/CNTs	pH of SPI/FCNTs
A	9.69	9.82
B	9.66	9.72
C	9.59	9.60
D	9.56	9.58
E	9.40	9.44

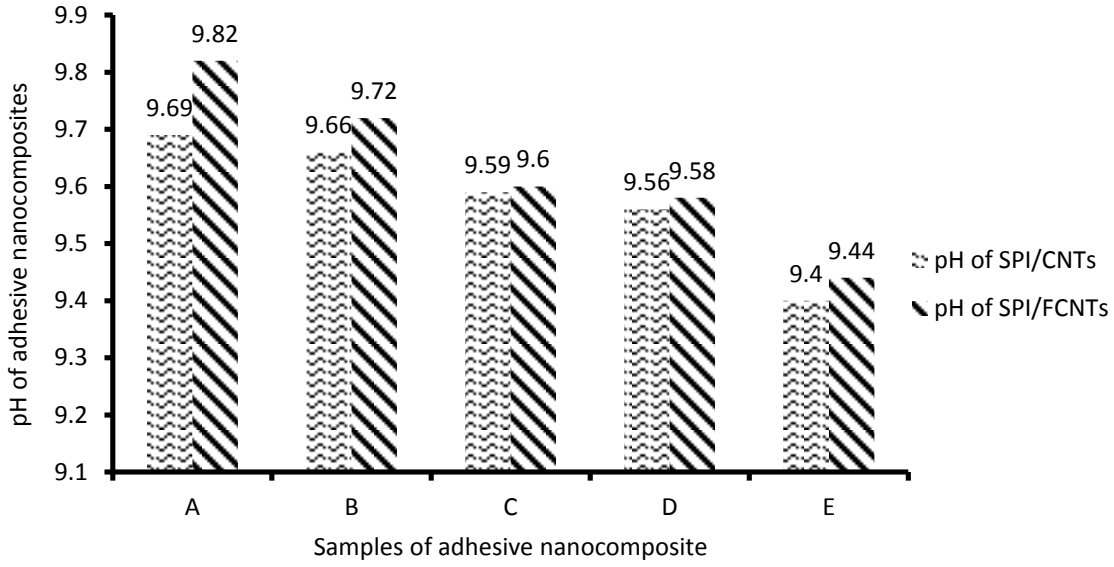

Figure 4.3: Effect of CNTs and FCNTs on the pH of modified SPI adhesive

4.2 Morphological structures of CNTs, FCNTs SPI/CNTs and fractured surfaces of adhesive

4.2.1 Morphological structures of CNTs and FCNTs

Figures 4.4 (A and B) describe the morphological structures of as-synthesized CNTs. These SEM images indicate the structure of as-synthesized CNTs in bundles (Figure 4.4 A) and outer diameter of 34.28 nm (Figure 4.4 B) (Stobinski et al., 2010). The result indicated that the as-synthesized CNTs were aggregated and not well dispersed.

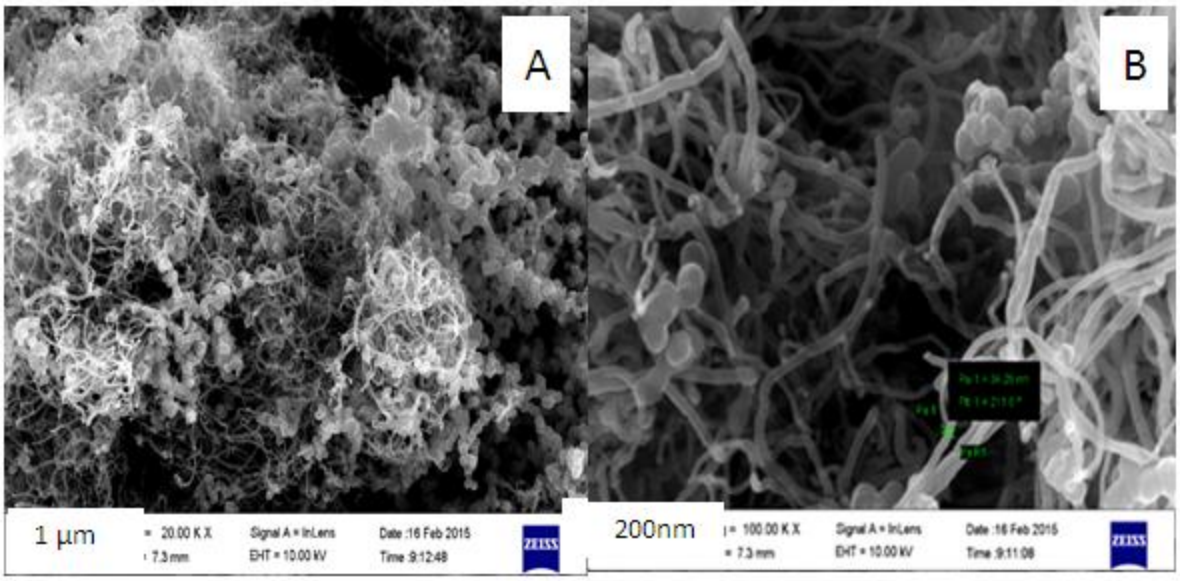

Figure 4.4: SEM images CNTs (A) entangled agglomerates (B) diameter of as-synthesized

Comparing Figure 4.4 and 4.5, it could be observed that SEM images of as- synthesized CNTs in Figure 4.4 show the bundles of CNTs clustering together in bundles (Figure 4.4 A and B). However when the as-synthesized CNTs were purified by mechanical stirring, the FCNTs spread out with much gaps in between them (Figure 4.5 and 4.6). This indicates that FCNTs will be more dispersed in the SPI matrix than as- synthesized CNTs. Figure 4.5 and 4.6 shows the method of purification by shear mixing and sonication respectively. Figure 4.6 shows the sonication method of purifying the CNTs. It could be observed from Figure 4.5 and 4.6 that even after purification, there were still some aggregates of CNTs that were not spread out evenly.

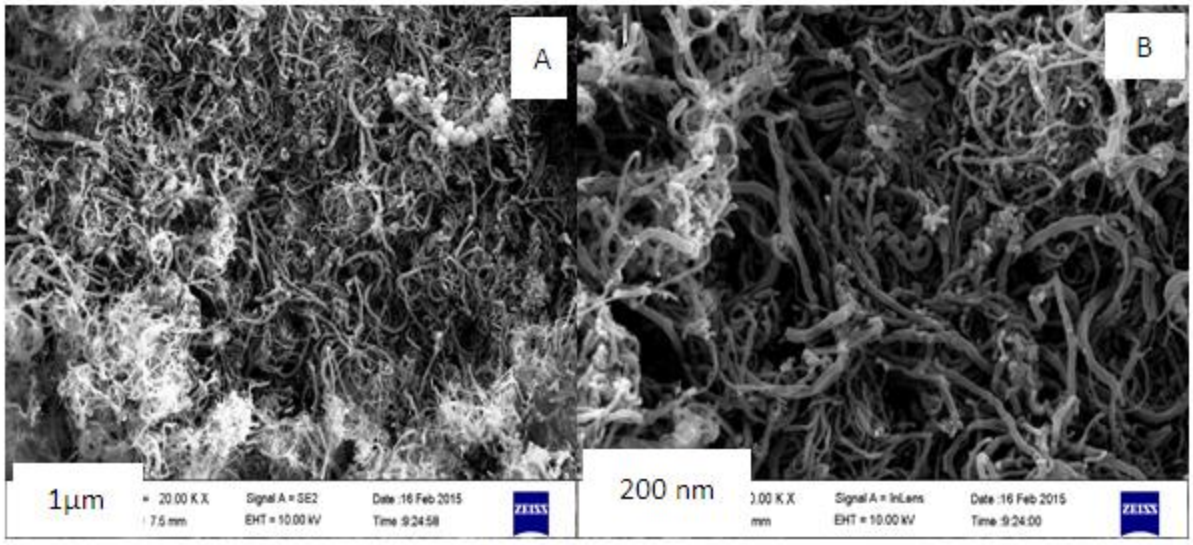

Figure 4.5: SEM images of FCNTs by shear mixing method of purification at 1 µm and 200 nm magnifications

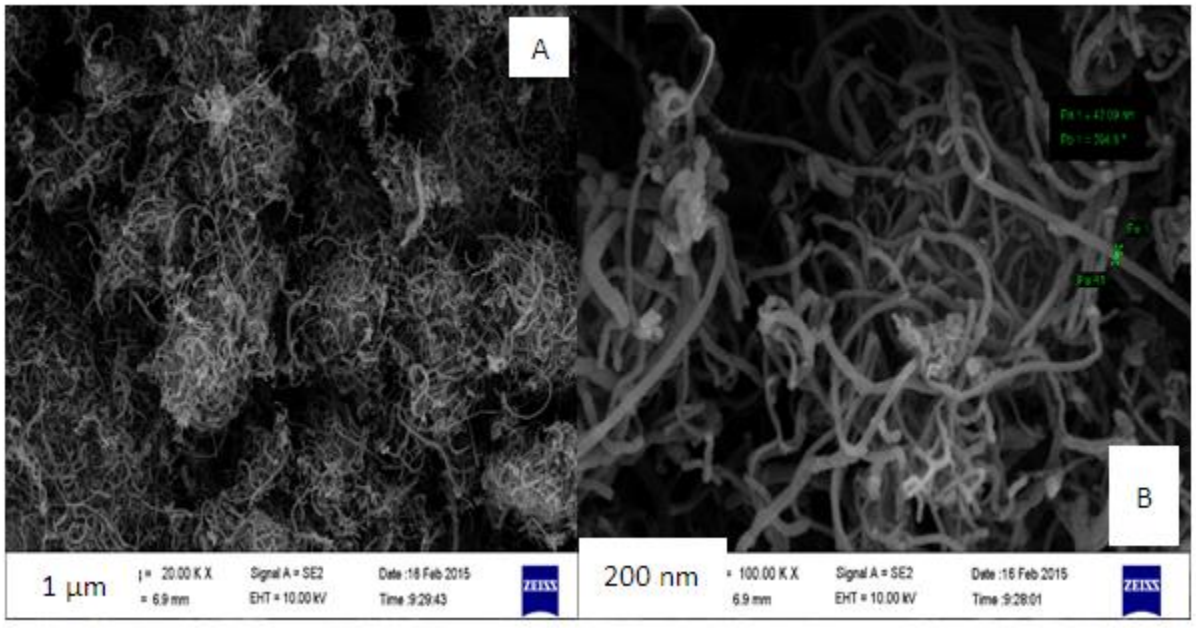

Figure 4.6: SEM images of FCNTs by sonication method of purification at 1 µm and 200 nm magnification

4.2.2 Morphology structures of adhesive nanocomposites

SEM images in Figure 4.7 and 4.8 show the morphological structure of SPI/CNTs and SPI/FCNTs dispersed by two different methods. In order to improve the distribution of CNTs in the polymer adhesive, 2 hours ordinary shear mixing and 90 minutes sonication with additional 30 minutes of shear stirring was employed. In shear mixing, it was noticed that bubbles were generated which was challenging to remove (Samal, 2009). However, sonication method reduced the amount of bubbles generated during mixing, although some agglomerates of CNTs could still be seen after 90 min of sonication until shear mixing was employed for 30min (Yu et al., 2010). In high shear mixing and sonication, the CNTs were homogenously dispersed in the SPI nanocomposite adhesive, only a few small aggregated bundles could be observed as shown in Figure 4.7(A and B) and 4.8 (A and B). Additionally, the CNTs were distributed randomly in the SPI matrix, providing the enhanced properties in all directions.

Figure 4.9 and 4.10 show dispersion of FCNTs in the nanocomposite adhesive. It could be observed that the nanotubes are homogenously dispersed in the soy protein matrix, giving room for transference of unique properties of CNTs into the adhesive. There were no much obvious aggregations and damage of the nanotubes in the SPI/FCNTs nanocomposite adhesive (Bulkholder, 2009). These suggest suitable processing procedures and parameters used to disperse the CNTs and FCNTs into the SPI by shear mixing and sonication with 30 minutes of shear mixing (Yu et al., 2010). Nevertheless, the two methods have proven to be suitable for dispersion of CNTs in SPI adhesive.

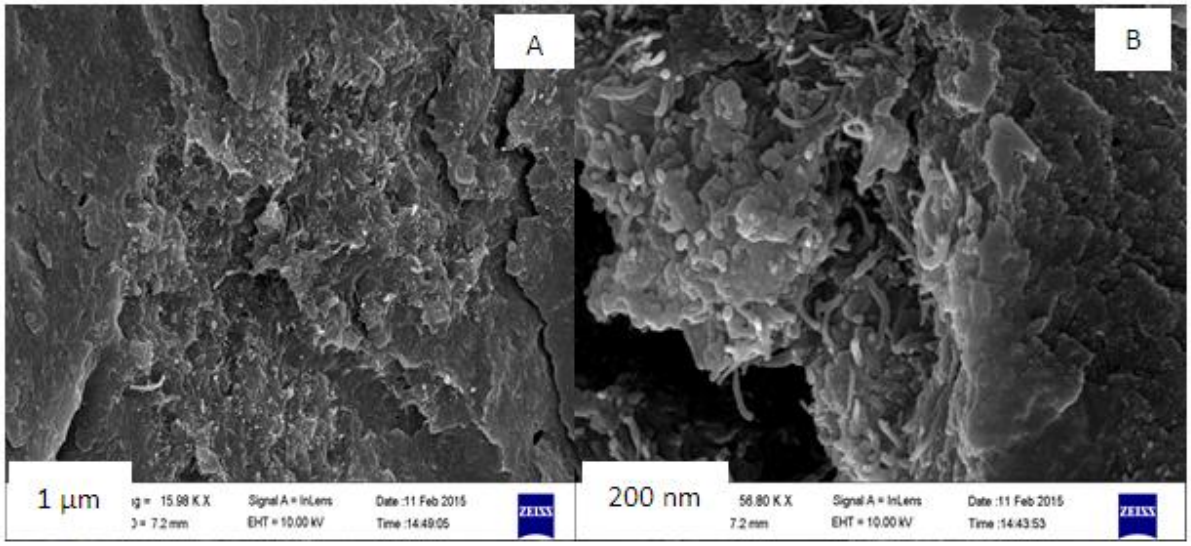

Figure 4.7: SEM images 0.1 wt% of SPI/CNTs nanocomposite adhesive dispersed by shear mixing method at (A) 1 µm and (B) 200 nm

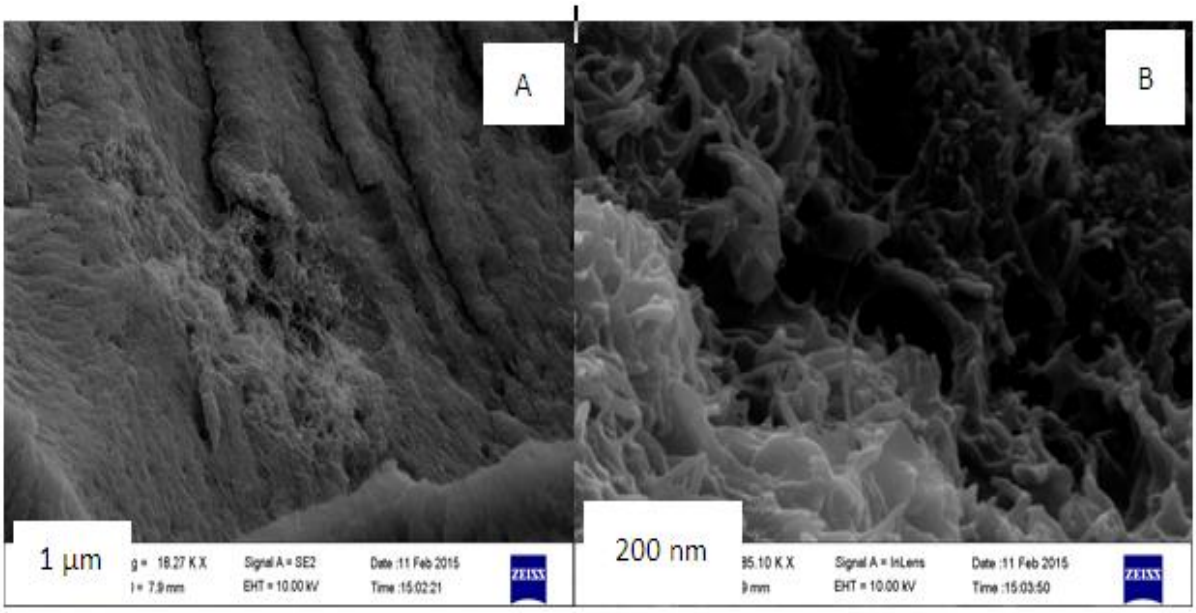

Figure 4.8: SEM images of 0.1 wt% SPI/CNTs nanocomposite adhesive dispersed by 90 minutes sonication/ 30 minutes mixing method at (A) 1 µm and (B) 200 nm.

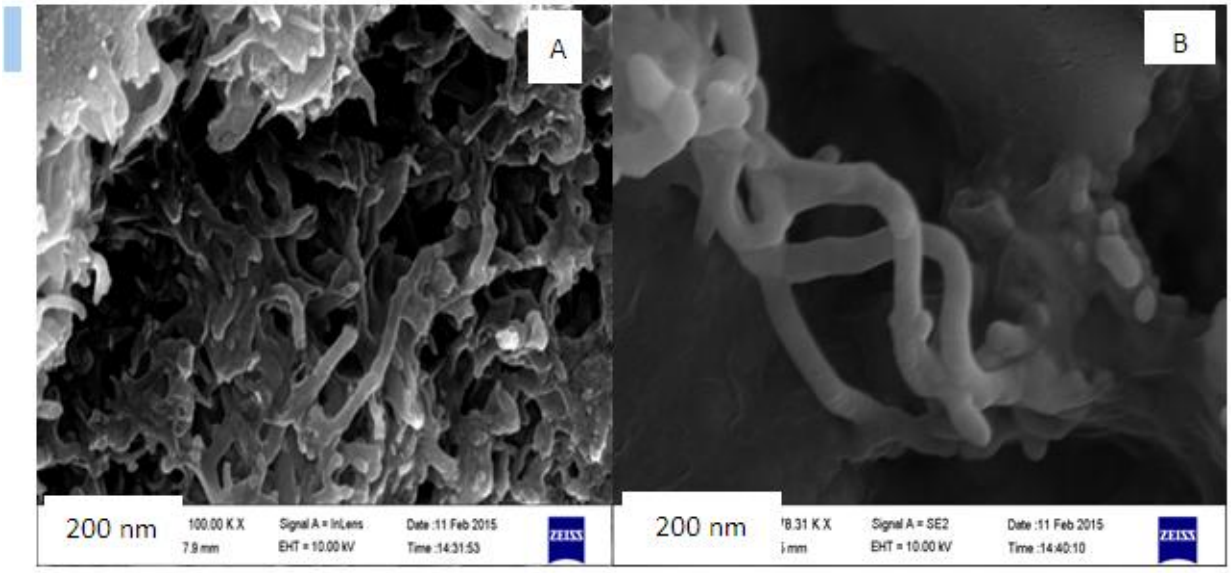

Figure 4.9: SEM images of dispersion of 0.1wt% FCNTs in SPI nano-composite adhesive by mechanical mixing.

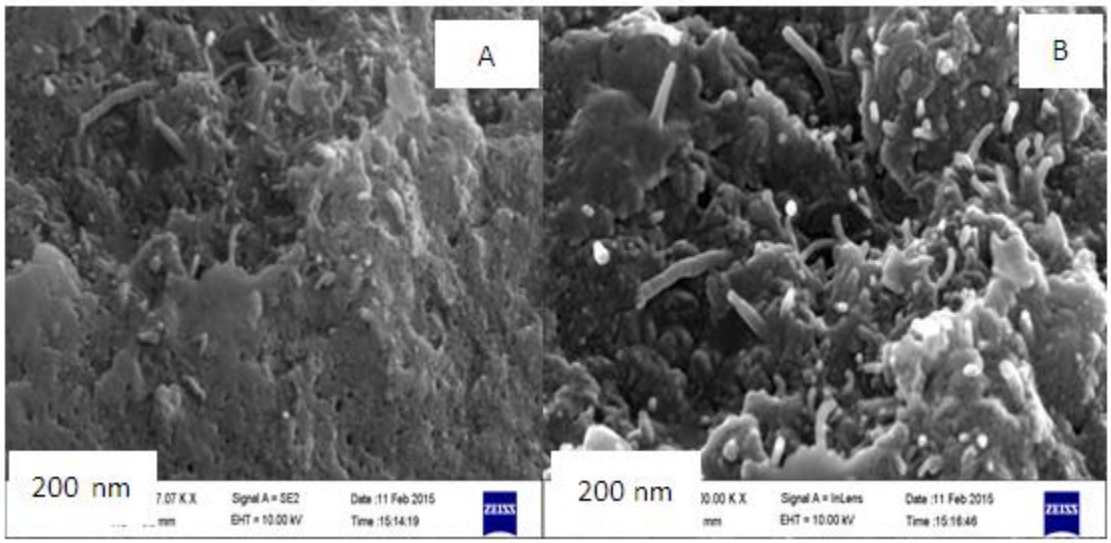

Figure 4.10: SEM images of dispersion of 0.1wt% FCNTs in SPI nanocomposite adhesive by 90 minutes sonication and 30min mechanical mixing.

4.2.3 Morphological structures of fractured surfaces

Figure 4.11 shows the morphological structure of the fractured surface of the wood after shear strength test. It was observed that the SPI adhesive with no CNTs underwent a cohesive failure at the adhesive layer, which indicates that the cohesive forces were weaker than the interfacial layers. Conversely, for the nanocomposite adhesive with 0.1 wt%, interfacial failure was the principal failure mode (Li et al., 2015).This indicates that the incorporation of the CNTs into SPI adhesive considerably strengthened the cohesive force, which resulted into effective bonding. The pressure mounted on the wood composites at 1.4Mpa shortened the distances between the active sites in soy protein molecules and hydroxyl groups from fiber walls on wood surface. Therefore, this enhanced the shear strength of the nanocomposite adhesive as a result of more chemical bonds, hydrogen bonds and the Vander Waal forces that were established at the interface (Chen and Sun, 2006).

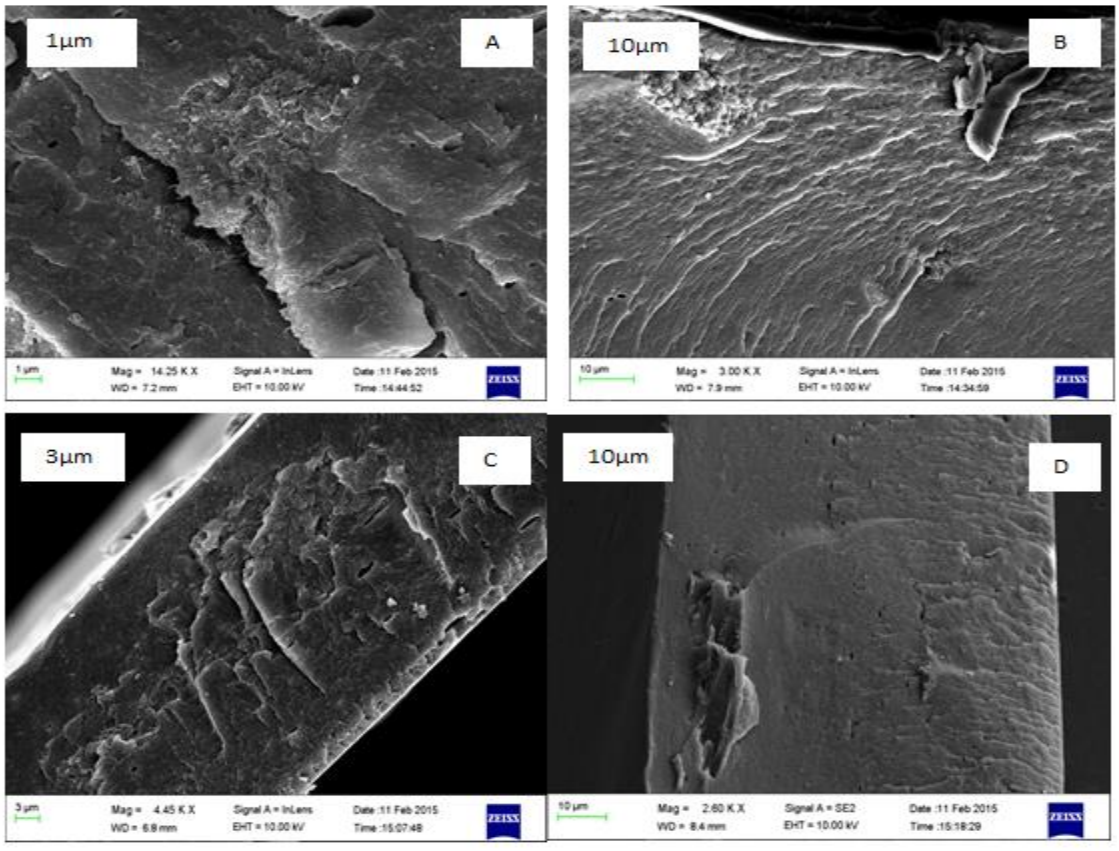

Figure 4.11: SEM images of fractured surface of (A) 0.1wt% SPI/CNTs (B) 0.1wt% SPI/FCNTs (C) SPINaOH (D) 0.1wt% SPI/SFCNTs adhesive samples

4.3 FTIR spectra of CNTs, FCNTs and SPI/CNTs nanocomposite adhesive samples

4.3.1 FTIR spectra of CNTs and FCNTs

Figure 4.12 describes the chemical functionalities of CNTs and FCNTs and the types of functional group attached to the surface of the nanotubes. The FTIR spectra describe the chemical functionalities of the samples (Lin et al., 2012). The FTIR spectra of CNTs and FCNTs are presented in Figure 4.12. It can be seen from this figure that the CNTs show a peak at 1527cm^{-1} which is assigned to the C-C bond. The weak peak at approximately 1720 cm^{-1} is attributed to the C =O bonds (Naseh, et al., 2010). The FTIR spectrum of CNTs treated by 55% HNO_3 shows two weak peaks at approximately 1780 and 3409 cm^{-1} which can be attributed to the acidic carbonyl and hydroxyl groups, respectively on the surface of the acid treated CNTs as shown in Figure 4.12 [Lin et al., 2012]. This indicates the attachments of the carboxyl groups on the surface of CNTs. The peak at 1294cm^{-1} is characterized as the acidic C–O bonds.

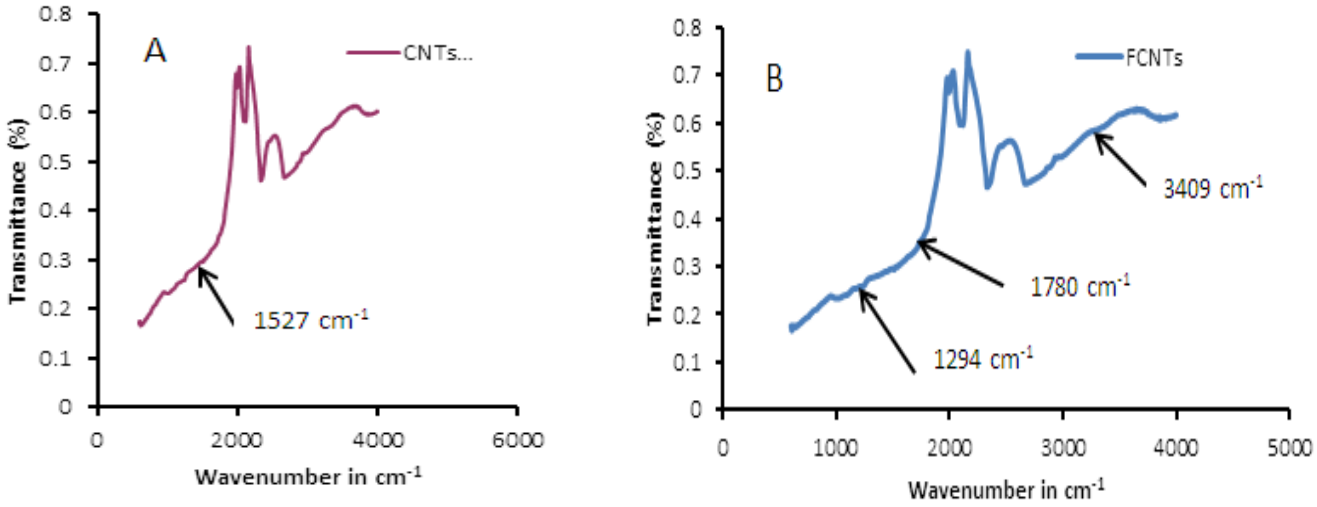

Figure 4.12: FTIR spectra of (A) CNTs and (B) FCNTs.

4.3.2 FTIR spectra of 0.7wt% SPI/FCNTs by mechanical shear mixing and sonication/mixing sonication/mixing

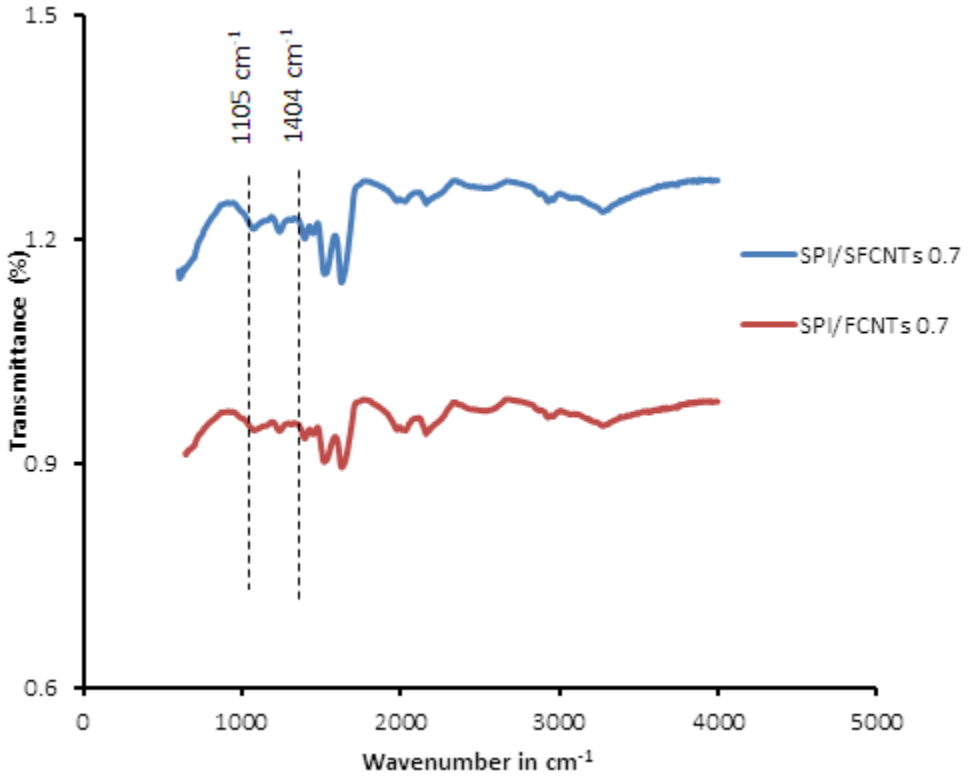

Figure 4.13: FTIR spectra of SPIFCNTs 0.7wt % adhesive dispersed by mechanical and sonication/mixing methods

Figure 4.13 shows the FTIR spectra of 0.7wt % of FCNTs dispersed into SPI adhesive by mechanical shear mixing and sonication/mixing. The spectra bands at 1404 cm^{-1} and 1105 cm^{-1} is corresponding to the COO- and C-NH_2 bending in SPI/SFCNTs 0.7.

4.3.3 FTIR spectra of pure SPI and SPI/CNTs nanocomposite adhesive samples

Figure 4.14 shows the FTIR spectra of pure SPI adhesive and SPI/CNTs nanocomposite adhesives. This figure shows that absorption peaks in the ranges of 1700-1750cm^{-1} were not observed in alkaline-modified SPI without CNTs. This is an indication that carboxylic acid (COO-) did not exist in pure soy protein adhesive (Lin et al., 2012). Hence the presence of

amine group ($–NH_2$) in the modified SPI adhesive is an indication of the existence of the stretching vibration of N–H at 3344 cm^{-1} and absorption peaks of amide spectral bands II [Silverstein et al., 2005 and Lin et al., 2012). However, this FTIR spectra show that all samples of the SPI/CNTs nanocomposite adhesive scanned have characteristic infrared spectra. Amide band I is the most susceptible to changes in the secondary structure of protein. This was found to be around spectra band range of $1637cm^{-1}$-$1664cm^{-1}$ in all the SPI/CNTs nanocomposite adhesive samples, which is related to C=O stretching. This can be attributed to the pH adjustment of adhesive samples to 10 (Bonwell and Wetzel, 2009 and Subirade et al., 1998). Amidic band II which is related to N-H bending is located around $1535cm^{-1}$-$1558cm^{-1}$ in all the samples (Lin et al., 2012). Amide band III which is C-N and N-H stretching is located around $1245cm^{-1}$.

The band in all the SPI/CNTs nanocomposite adhesive samples around $3249cm^{-1}$-$3328cm^{-1}$ is related to O-H functional group which is attributed to the availability of amidic band due to unfolding of protein by adjustment of adhesive pH (Subirade et al., 1998). This results show that carboxyl (COO-) functional group was successfully attached to the surface of the nanocomposite adhesive samples by the help of acid - treated CNTs (Subirade et el., 1998 and Lin et al., 2012).

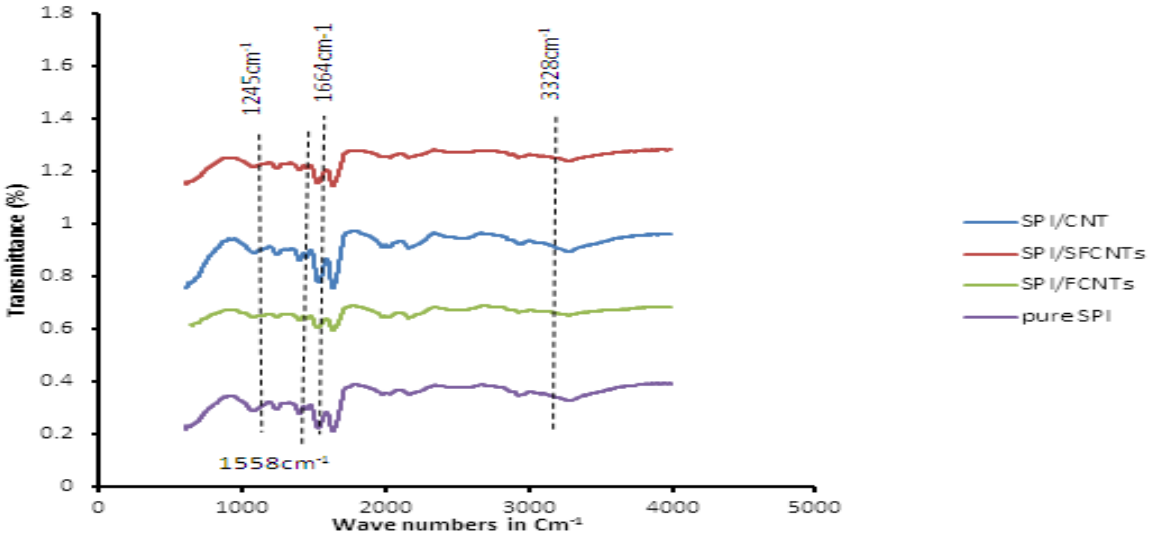

Figure 4.14: FTIR spectra of pure SPI/CNTs, SPI/FCNTs and SPI/SFCNTs at 0.7wt % concentration

4.4 Thermal stability and thermal degradation of CNTs, FCNTs and SPI/CNTs nanocomposite adhesives

4.4.1 TGA profile of CNTs and FCNTs

Figure 4.15 describes the thermal stability and weight degradation of the CNTs and FCNTs. The TGA determines the derivative weight change and percentage weight as a function of temperature (Schmitt et al., 2006)). This analysis was carried out to determine the thermal stability of the adhesive samples. According to existing literature, amorphous carbon typically oxidizes in air at temperatures below 400 °C, (Landi et al., 2005), whereas CNTs oxidize at higher temperatures up to 800 °C (Liu et al., 2007). The TGA profile indicated that there was no weight loss below 400 °C, this confirmed that there was no amorphous carbon present in the as-synthesized CNTs (Tetana et al., 2012). The TGA of the CNTs shows that Fe-Co/$CaCO_3$ catalysts are thermally stable up to 450^{o}C and 550 °C in CNTs and FCNTs respectively where oxidation of carbon begins to occur. The catalyst support $CaCO_3$ started decomposing at this temperature into CaO and CO_2 (Schmitt et al., 2006). At temperatures around 600°C, only the support and Fe-Co catalyst remain (Mhlanga and Coville, 2008). It was also observed that the amount of residual catalyst decreased as the synthesis temperature increased, after acid-treatment of CNTs. This suggests that the residual Fe-Co catalyst particles were mostly removed (Tetana et al., 2012). The TGA profile for the as- synthesized carbon nanotubes at temperature below 450^{o}C shows a weight loss of about 78 %. This may be due to the presence of metallic particles and catalyst support in this sample (Afolabi et al., 2011). Functionalized CNTs shows a weight loss of over 81%, at temperature lower than 550^{o}C, this is an indication that the FCNT is 81% pure. The ~19% impurities are probably as a result of metallic particles that were not removed during purification with HNO_3. It was clearly observed that some CaO and Fe-Co were not removed despite the acid treatment (Mhlanga et al., 2009).

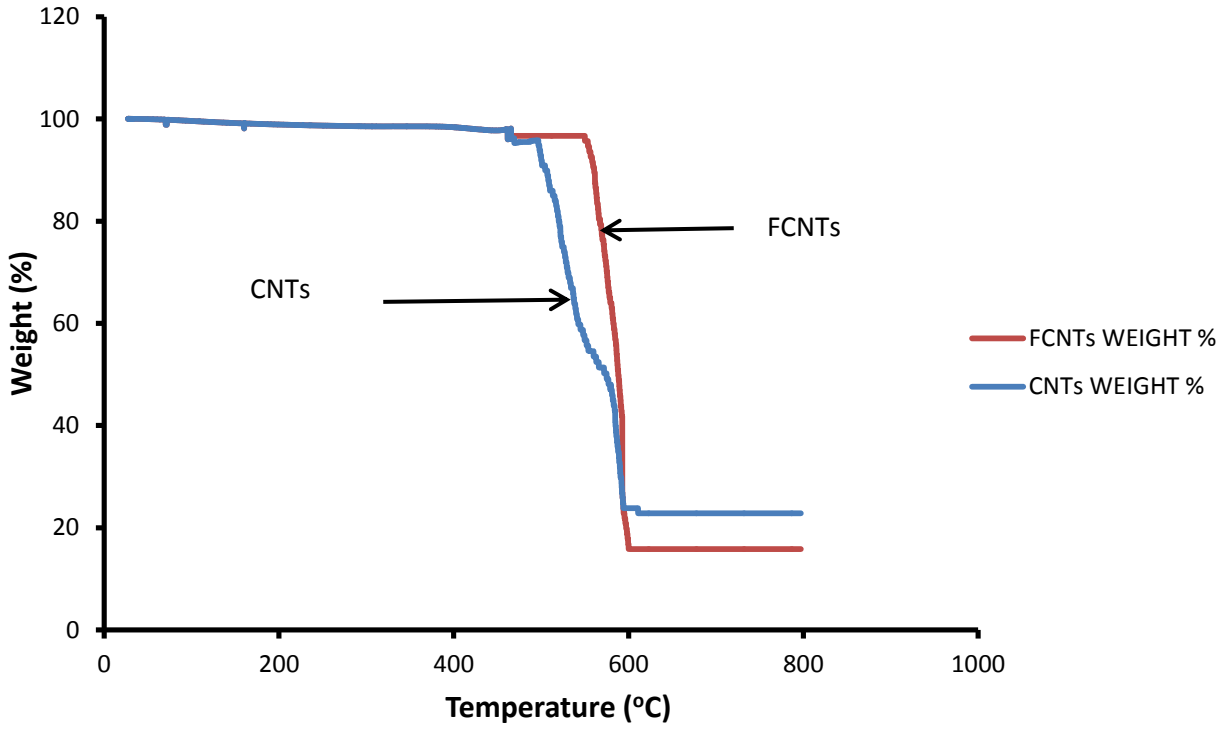

Figure 4.15: TGA profiles of synthesized CNTs and FCNTs.

4.4.2 TGA profile of pure SPI and SPI/CNTs nanocomposite adhesive samples

Figure 4.16 explains the thermal stability and weight degradation of pure SPI and 0.1-0.5wt% SPI/CNTs nanocomposite adhesive samples

The result depicted in Figure 4.16 indicates that all adhesive nanocomposites with different percentage of FCNTs underwent two stages of weight loss from 23^{o}C to 800^{O}C. The first weight loss occurred before 200^{o}C, which may be attributed to the lower molecular weight of material. The weight loss for the second stage occurred between temperature of 319^{o}C and 387^{o}C, which is attributed to the thermal degradation of soy protein isolate at higher molecular weight formed after oven-curing of the adhesive (Yu et al., 2010). It was observed that, there was a slight improvement in the thermal stability of the nanocomposite adhesive samples containing CNTs, as compared to the pure SPI adhesive. The TGA profile also shows that SPI/FCNTs0.5 had weight loss of 80% at 800^{o}C while others with lower loading of FCNTs had over 80% weight

losses. This may be as a result of metallic particles remaining in the CNTs. At temperature around 800^{O}C, 11.77% was remaining for nanocomposite adhesive with 0wt% and 0.1% FCNTs, 15.20% for SPI/FCNTs with 0.3% and 19.96% for SPI/FCNTs with 0.5%. These results show that SPI adhesives with CNTs are more thermally stable than SPI adhesive with no CNTs.

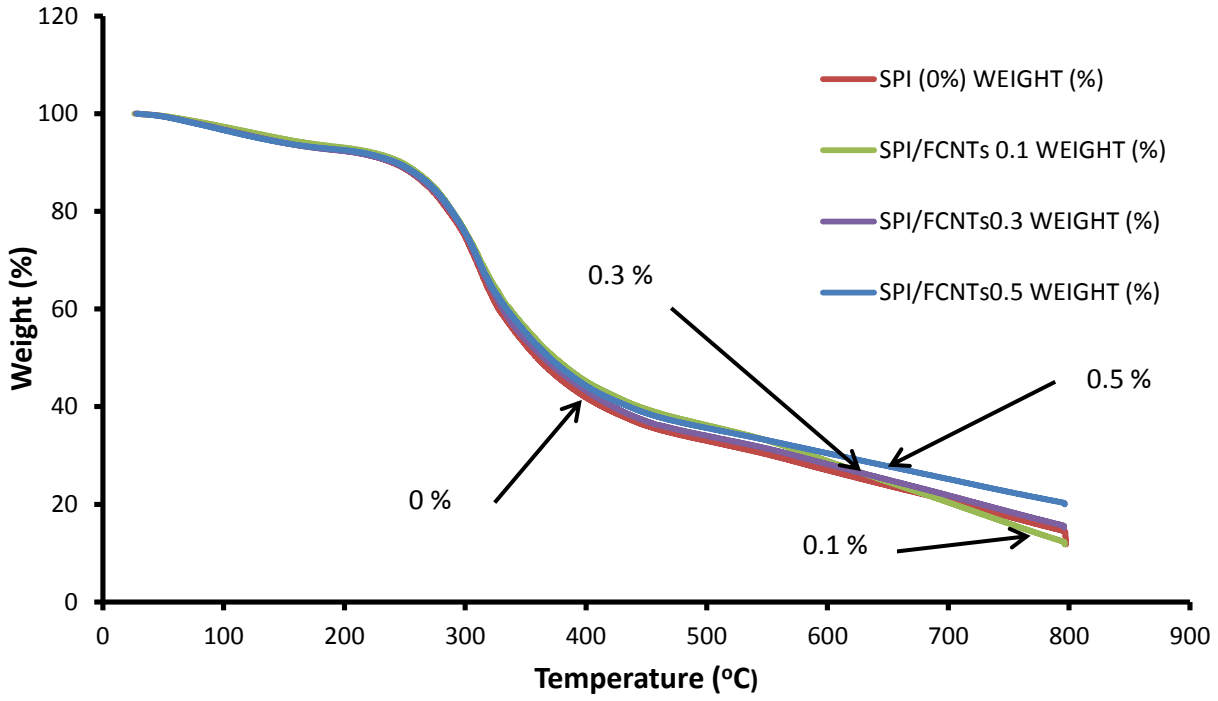

Figure 4.16: TGA profiles of adhesive nanocomposite with varying concentrations of FCNTs ranged from 0 wt% to 0.5 wt%.

4.5 Performance evaluation of SPI/CNTs nanocomposite adhesive for wood application

4.5.1 Effect of concentration on the shear strength and water resistance of adhesive nanocomposite

Table 4.4 shows the effect of CNTs loading fraction on the maximum force at breakage for each sample of adhesive nanocomposite and the equivalent shear strength measured in MPa. This

table shows that as the concentration of the CNTs and FCNTs increase from 0.1 wt% to 0.3 wt% the shear strength also increased. It could be observed that the shear strength started decreasing at percentage loading fraction of 0.5.

Table 4.4: Effect of concentration and method of dispersion on the shear strength and water resistance of adhesive nanocomposite

Maximum force at breakage (KN)	**Area bonded with adhesive ($mm^2 \times 10^{-6}$)m^2**	**Shear strength(MPa)**	**Nanocomposite adhesive samples on maple wood**
1.04	300	3.48	SPINaOH
0.34	300	1.12	WSPINaOH
1.37	300	4.57	SPI/CNTs0.1
0.92	300	3.05	WSPI/CNTs0.1
1.58	300	5.25	SPI/FCNTs0.1
1.51	300	5.02	WSPI/FCNTs0.1
2.07	300	6.91	SPI/CNTs0.3
1.64	300	5.48	WSPI/CNTs0.3
2.52	300	8.40	SPI/FCNTs0.3
2.48	300	8.25	WSPI/FCNTs0.3
1.29	300	4.29	SPI/CNTs0.5
1.21	300	4.04	WSPI/CNT0.5
1.52	300	5.06	SPI/FCNTs0.5
1.24	300	4.13	WSPI/FCNTs0.5
1.21	300	4.04	SPI/CNTs0.7
0.88	300	2.94	WSPI/CNTs0.7
1.23	300	4.12	SPI/FCNTs0.7
1.05	300	3.59	WSPI/FCNTs0.7
1.33	300	4.44	SPI/SFCNTs0.7
1.25	300	4.05	WSPI/SFCNTs0.7
0.60	300	2.01	SPICNT1.0
0.38	300	1.27	WSPI/CNTs1.0

0.76	300	3.54	SPI/FCNTs1.0
0.52	300	1.72	WSPI/CNTs1.0

WSPI/CNTs and WSPI/FCNTs (0.1-1.0) – samples of varied concentrations of adhesive nanocomposites on bonded wood composites that underwent WSAD test (mixing), WSPI/SFCNTs0.7- sample of 0.7 wt% FCNTs by sonication /mixing method of dispersion in SPI adhesive that underwent WSAD test. Other samples are as stated in Table 4.3

Table 4.5 shows the effect of concentration of CNTs on the shear strength of adhesive nanocomposite. It can be seen that the shear strength of the pure adhesive increased from 3.48 MPa at dry state to 6.91 MPa when 0.3 wt% of CNTs was incorporated.

Table 4.5: Effect of concentration of CNTs on the tensile strength of SPI nanocomposite adhesive at dry and wet state

Concentration (wt%) of CNTs in SPI	**Shear strength at dry state (MPa)**	**Shear strength at wet state(MPa)**
0	3.48	1.12
0.1	4.57	3.05
0.3	6.91	5.48
0.5	4.29	4.05
0.7	4.04	2.94
1.0	2.01	1.27

Figure 4.17 and 4.18 describe the shear strength of the adhesive nanocomposite. The SPI/CNTs nanocomposite adhesives with different loading fractions were used to bond wood pieces together. The shear bond strength of the adhesive nanocomposite was investigated by tensile machine. From the data in Figure 4.17 and 4.18 pure adhesive with 0 wt% loading of CNTs had higher shear strength (3.38 MPa) against ≥1.0 MPa which was the minimum for soy protein adhesive for interior wood application according to the JISK6806-2003 Standard (Zhang et al., 2014). This could be attributed to the unfolding of protein structure by NaOH. This enabled the

amino acid buried inside to be made available during curing, thus, enhancing the penetration and adhesion of SPI without CNTs as well as SPI/CNTs nanocomposite adhesive (Huang and Li, 2008).

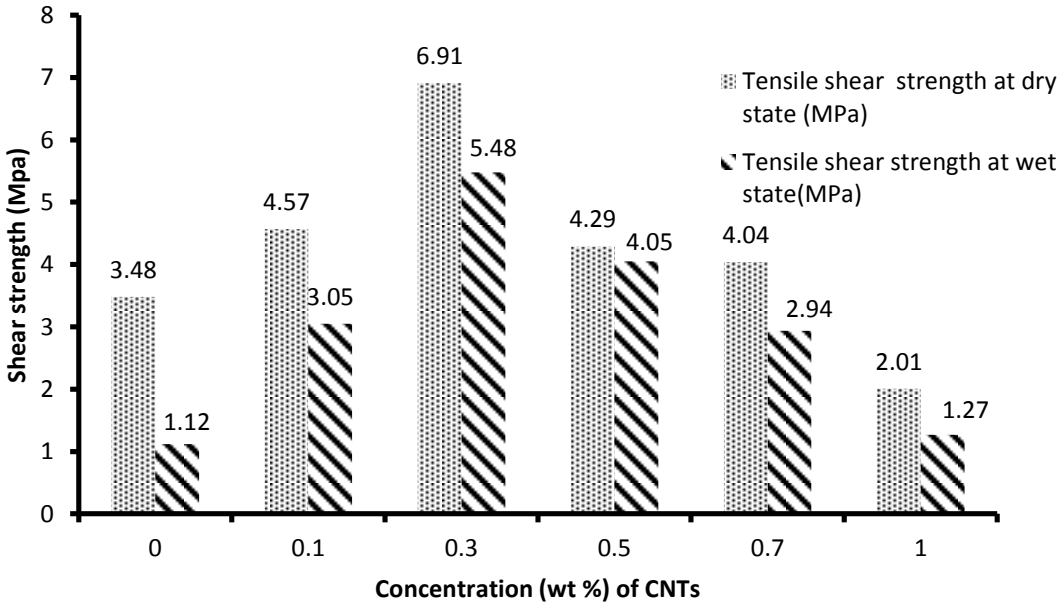

Figure 4.17: Effect of concentration of CNTs on the shear strength and water resistance of SPI adhesive nanocomposite at dry and wet state.

Table 4.6 shows the effect of concentration of FCNTs on pure SPI and SPI/CNTs nanocomposite adhesive. It can be seen from the table that the maximum shear strength was observed at 0.3 percentage loading fraction of FCNTs. The tensile strength increases from 3.48 MPa to 8.4 MPa and started decreasing at percentage loading above 0.3. This is an indication that FCNTs improves the shear strength of an adhesive at reduced concentration.

Table 4.6: Effect of concentration of FCNTs on the SPI adhesive nanocomposite at dry and wet state.

Concentration of SPIFCNTs (wt%)	Shear strength at Dry state (MPa)	Shear strength at wet state (MPa)
0	3.48	1.12
0.1	5.25	5.02
0.3	8.4	7.25
0.5	5.06	4.13
0.7	4.12	3.59
1.0	3.40	1.72

From Figure 4.17 and 4.18, there are obvious differences in the shear bond strength of the adhesive samples with and without the incorporation of carbon nanotubes. It was observed that the shear strength of adhesive with 0wt% loading fraction of CNTs (3.48 MPa) was lower than that of the one with 0.1 wt % for both CNTs (4.57 MPa) and FCNTs (5.25 MPa), which is over 50% lower. The shear bond strength increases through 0.3 wt % (8.4 MPa and 7.25 MPa) and started decreasing at 0.5 wt % for both carbon nanotubes (4.29Mpa and 4.05MPa) and FCNTs (5.06 MPa and 4.13 MPa) at dry and wet states respectively (Li et al., 2015). Initially, it was observed that the shear strength was increasing with increasing CNTs fraction. However, it started decreasing when the CNTs fraction became higher than 0.3 wt %. From Figure 4.17, it was noticed that the shear bond strengths of adhesive with CNTs were lower than the bond strength of adhesive with FCNTs in Figure 4.18 at all percentage loading fraction both at dry and wet state. This may be attributed to the agglomeration of CNT in the SPI nanocomposite adhesive (Figure 4.8a). Higher shear strength observed in nanocomposite adhesive with FCNTs could be attributed to the attachment of carboxyl functional group as shown by the FTIR result discussed above. These results show that concentration loading of CNTs affects the shear strength of nanocomposite adhesive. This may be attributed to the believed that at too high concentration of carbon nanotubes, the nanotubes will begin to slip past one another and reduce the shear strength of the adhesive. However, the shear strength of the adhesive will also reduce if

the loading fraction of carbon nanotubes is too low, due to insufficient mass transfer of strength to the adhesive and the bonding surface of the wood samples (Bulkholder, 2009). The result show that the shear strength of nanocomposite adhesive with 0.3 wt% loading fraction of FCNTs was over 100% higher than the shear strength of pure alkaline modified SPI adhesive without reinforcement at both dry and wet state. Therefore, considering the improvement of the shear strength in both dry and wet state, SPI nanocomposite adhesive with 0.3% FCNTs displayed the best performance in bonding wood. This is an indication that incorporation of CNTs into SPI adhesive improves the performance of both shear strength and the water resistance of the nanocomposite adhesive.

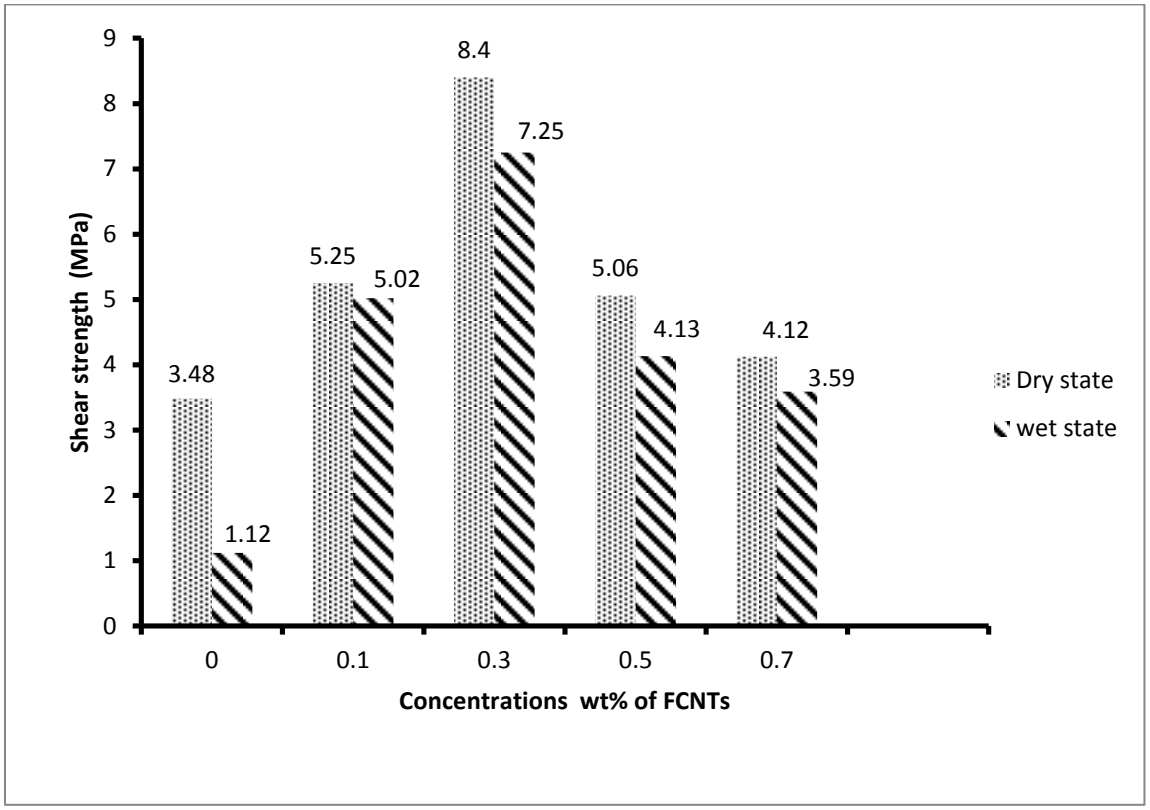

Figure 4.18: Effect of concentration of FCNTs on the shear strength of SPI adhesive nanocomposite at dry and wet state.

4.5.2 Effect of dispersion method on the shear strength of adhesive nanocomposite

Table 4.7 shows the effect of dispersion methods on the maximum force at breakage and the shear strength of 0.7 wt % SPI adhesive nanocomposite. Effect of method of dispersion of CNTs on the shear strength of the SPI can be seen in table 4.8. This table shows that shear strength of SPI nanocomposite adhesive dispersed by sonication/mixing is slightly higher than that of SPI nanocomposite dispersed by shear mixing.

Table 4.7: Effect of method of dispersion on the maximum force at breakage and shear strength of SPI nanocomposite adhesive

Maximum force at breakage (KN)	**Area bonded with adhesive($mm^2 \times 10^6$)m^2**	**Shear strength (MPa)**	**Nanocomposite adhesive samples**
1.21 0.88	300 300	4.04 2.94	SPI/CNTs0.7 WSPI/CNTs0.7
1.23	300	4.12	SPI/FCNTs0.7
1.05	300	4.01	WSPI/FCNTs0.7
1.33	300	4.44	SPI/SFCNTs0.7
1.25	300	4.05	WSPI/SFCNTs0.7

Table 4.8: Effect of dispersion method on the shear strength of SPI nanocomposite adhesive

High speed and sonicator dispersion	**Shear strength at dry state (MPa)**	**Shear strength at wet state (MPa)**
SPI/CNTs0.7	4.04	2.94
SPI/FCNTs0.7	4.12	3.59
SPI/SFCNTs0.7	4.44	4.05

SPICNTs= 1 hour high speed method of dispersion, SPI/FCNTs- 1 hour high speed method of dispersion of FCNTs in SPI, SPI/SFCNTs- 1 hour 30 minutes of sonication + 30 minutes high speed dispersion.

Figure 4.19 shows the effect of methods of dispersion on the shear strength of the SPI nanocomposite adhesive. Two different methods of dispersion of 0.7 wt % loading of CNTs and FCNTs were investigated on their effect on the shear strength of the adhesive. It could be observed that the shear bond strength of adhesive (SPI/SFCNTs0.7) dispersed by method of sonication had shear strength of 4.44 MPa, which is around 10% higher than the shear bond strength of adhesive (SPI/FCNTs0.7) dispersed by shear mixing with shear strength of 4.12 MPa. This indicates that the ultrasound energy in the adhesive mixed by sonication generated vibration which and frequency generated resulted into better dispersion of the CNTs in the SPI adhesive.. In addition the wave nature which resulted into energy transfer in the nanocomposite SPI adhesive during sonication enhanced the tensile strength of the adhesive compared with the shear mixing method (Cheng et al., 2010) Adhesives with 0.7 wt% loading fraction of FCNTs for both sonication and shear mixing methods had higher shear strengths than that of as-synthesized CNTs. In addition, attachment of carboxyl group during purification of CNTs improved the dispersion of FCNTs in the adhesive matrix, hence the shear strength.

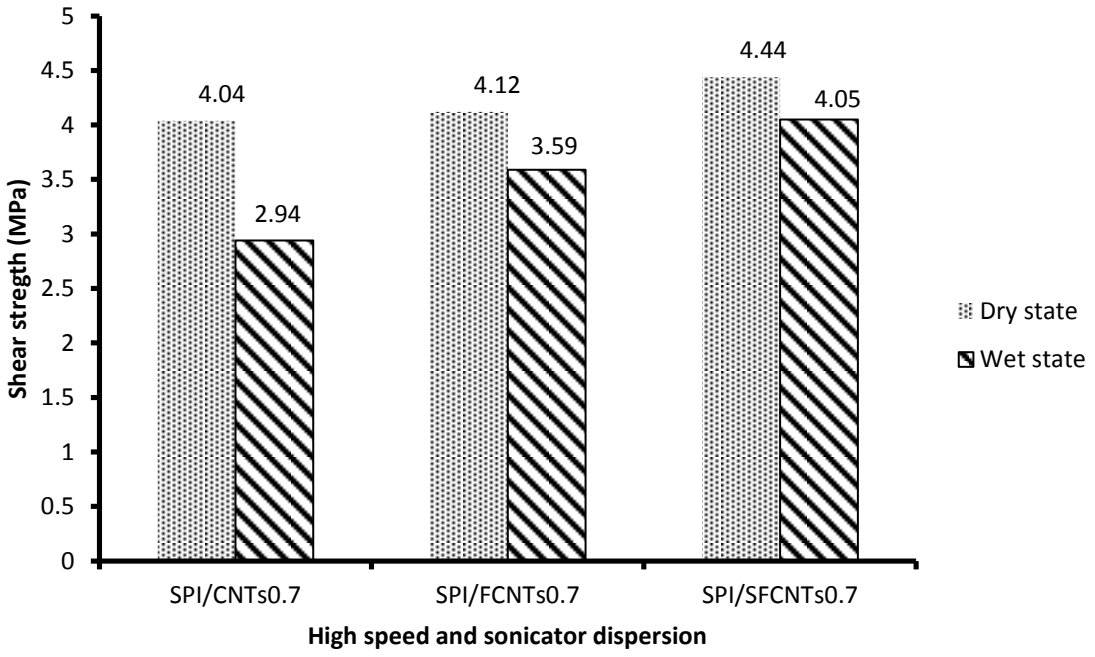

Figure 4.19: Effect of dispersion method on the shear strength of SPI adhesive nanocomposite.

The wood specimen also showed different behaviors when immersed in water. The addition of CNTs produced a greater percent increase in shear strength in the dry state than it did in the wet

state, indicating that incorporation of CNTs prevents the damage of the joint during water exposure. However the shear strength of the adhesive at all percentage loadings of carbon nanotubes was higher than that of the pure SPI adhesive. Wood specimen bonded with adhesive without CNTs showed the lowest shear bond strength both at dry and wet state, indicating that CNTs addition improved the barrier properties of the SPI/CNTs nanocomposite adhesive toward water (Esposito Corcione, et al., 2009). Observation from all samples that underwent shear strength test at dry and wet states indicated that wet test dropped with respect to their dry tests. This poor water resistance is attributed to the low molecular weights of soy proteins, which results in a good water solubility and poor cohesive strength [Esposito Corcione, et al., 2009). The better performance of dry strength of the nanocomposite soy protein adhesive was primarily attributed to the good adsorption of polar groups such as amino, hydroxyl and carboxyl groups to the surface of the wood substrate and the mechanical interlocking between the protein and the porous wood (Zhang et al., 2014). However, since water is a polar liquid and has a strong ability to bond to the polar wood. It competed with both soy protein and wood to form hydrogen bonds. Therefore, few interactions were left between the protein and the wood, which dropped the wet strength compared to the dry test (Xu et al., 2011).

4.5.3 Comparison of effect of fillers on the shear strength of soy-based adhesives from literatures

Table 4.9 shows the comparison of shear strength of soy protein adhesive from literatures with this study. This table shows that incorporation of other fillers into soy-based adhesives improved the shear strength, although at higher percentage loading. However, CNTs an example of a nanofiller used in this study, improve the shear strength of adhesive at a reduced percentage loading compared to other modifiers. This table also shows that incorporation of CNTs improved the shear strength and water resistance of soy protein based adhesive.

Table 4.9: Comparison of effect of fillers on the shear strength of soy-based adhesives with literatures

Modifier/Filler	**Polymer matrix**	**% concentration of modifier**	**Shear strength at dry state**	**Shear strength at wet state**	**References**
$CaCl_2$+ NaOH	DSF		0.85	0.64	Lin et al., 2012
PI	SBP	0.49	2.53	_	Zhang et al., 2014
MMT	SBP	3	3.06	0.64	Zhang et al., 2014
PEI +MA	SF	1.32	Improved	Improved	Huang and Li, 2008
$CaCO_3$	SP	10	5	5	Liu et al., 2010
FCNTs	SPI	0.3	8.4	7.25	This study
CNTs	SPI	0.3	6.91	5.48	This study

MMT- montmorrilonite, PEI +MA- polyethylenimine/maleic anhydride, SBP- soy-bean protein, SF- soy flour, SP- soy protein, PI- polyisocyanate

References

Afolabi, A.S., Abdulkareem, A.S., Mhalanga, S.D., Iyuke, S.E. (2011) Synthesis and purification of bimetallic catalyzed carbon nanotubes. Journal of Experimental Nanoscience. Vol. 6, No 3, pp 248-262.

Bonwell, E., Wetzel, D., (2009) Innovative FT-IR imaging protein film secondary structure before and after heat treatment. J. Agric. Food Chem. Vol. 57, pp 10067–10072.

Burkholder, G.L (2009) The effects of carbon nanotube reinforcement of adhesive joints for naval applications. A thesis submitted to the Naval school of postgraduate, Monterey, California.

Cheng, E. and Sun, X. (2006) Effects of wood-surface roughness, adhesive viscosity and processing pressure on adhesion strength of protein adhesive, J. Adhes. Sci. Technol., Vol. 20 No. 9, pp. 997-1017.

Cheng, Q., Debnath, S., Gregan, E and Byrne, H.J (2010) Ultrasound - Assisted SWNTs: Effect of sonication parameters and solvent properties. Journal of Phys. Chem.C. Vol. 114, pp. 8821-8827.

Esposito Corcione, C., Mensitieri, G., and Maffezzoli, A. (2009) Analysis of the structure and mass transport properties of nanocomposite polyurethane. Polymer Engineering & Science. Vol. 49, No. 9, pp 1708–1718.

Gao, Q., Shi, S., Li, J., Liang, K., Zhang, X., (2012) Soybean meal-based wood adhesives enhanced by modified polyacrylic acid solution. BioResources. Vol. 7, pp 946–956.

Huang, J and Li, K. (2008) A New Soy Flour-Based Adhesive for Making Interior .Type II Plywood .J Am Oil Chem Soc. Vol. 85, pp 63–70.

Landi, B.J., Cress, C.D., Evans, C.M., and Raffaelle, R.P. (2005) Thermal oxidation profiling of single-walled carbon nanotubes. Chem. Matter. Vol. 17, pp 6819–6834.

Li, Z., Wang, J., Li, C., Gu, Z., Cheng, L. and Hong, Y. (2015) Effects of montmorillonite addition on the performance of starch-based wood adhesive. Carbohydrate Polymers. Vol. 115, pp 394–400.

Lin, Q., Chen, N., Bian, L. and Fan, M. (2011) Development and mechanism characterization of high performancesoy-based bio-adhesives. International Journal of Adhesion & Adhesives. Vol. 34, pp 11–16.

Lin, Q., Chen, N., Bian, L. and, Mizi Fan, M. (2012) Development and mechanism characterization of high performance soy-based bio-adhesives. International Journal of Adhesion & Adhesives. Vol. 34, pp 11–16.

Liu, Q., Ren, W., Li, F., Cong, H. and Cheng, M. (2007) Synthesis and high thermal stability of double-walled carbon nanotubes using nickel formate dihydrate as catalyst precursor J. Phys. Chem. C. Vol. 111, pp 5006–5013.

Liu, D., Chen, H., Chang, P.R., Wu, Q.,Li, K. and Guan, L. (2010)Biomimetic soy protein nanocomposites with calcium carbonate crystalline arrays for use as wood adhesive. Bioresource Technology. Vol. 101, pp 6235–6241.

Mhlanga, S.D. and Coville, N.J. (2008) Iron–cobalt catalysts synthesized by a reverse micelle impregnation method for controlled growth of carbon nanotubes. Diamond & Related Materials. Vol. 17, pp 1489–1493.

Mhlanga, S.D.,MondalK.C., Carter, R., Witcomb, M.J and Coville, N.J. (2009) The Effect of Synthesis Parameters on the Catalytic Synthesis of Multiwalled Carbon Nanotubes using Fe-Co/$CaCO_3$ Catalysts. S. Afr. J. Chem. Vol. 62, pp 67–76.

Naseh, M.V., Khodadadi, A.A., Mortazavi, Y., Pourfayaz, F., Alizadeh, O. and Maghrebi, M. (2010) Fast and clean functionalization of carbon nanotubes by dielectric barrier discharge plasma in air compared to acid treatment, Carbon. Vol. 48, pp 1369–1379.

Samal, S.S. (2009) Role of Temperature and Carbon Nanotube Reinforcement on Epoxy based Nanocomposites. Journal of Minerals & Materials Characterization & Engineering, Vol. 8, No.1, pp 25-36.

Schmitt, T.C.,Biris, A.S.,Miller, D.W., Biris, A.R., Lupu, D., Trigwell, S.and Rahman, Z.U. (2006) Analysis of effluent gases during the CCVD growth of multi-wall carbon nanotubes from acetylene. Carbon. Vol. 44, pp 2032–2038.

Silverstein, R.M., Webster, F.X. and Kiemle D. (2005) Spectrometric identification of organic compounds. USA: John Wiley & Sons, Inc. (p. 90–100)

Stobinski, L., Lesiak, B., Kövér, L., Tóth, j., Biniak, S., Trykowski, G.and Judek, J. (2010)Multiwall carbon nanotubes purification and oxidation by nitric acid studied by the FTIR and electron spectroscopy methods. Journal of Alloys and Compounds. Vol. 501, pp 77–84.

Subirade, M. Kelly, I., Guéguen, J., Pézolet, M. (1998) Molecular basis of film formation from a soybean protein: Comparison between the conformation of glycinin in aqueous solution and in films. Int. J. Biol. Macromol. Vol. 23, pp 241–249.

Tetana, Z.N., Mhlanga, S.D., Bepete, G., Krause, R.W.M.,and Coville, N.J. (2012) The Synthesis of Nitrogen-Doped Multiwalled Carbon Nanotubes Using an Fe-Co/CaCO3 catalyst. S. Afr. J. Chem. Vol. 65, pp 39–49.

Xu, H., Shufeng Ma, S., Lv, W. and Wang, Z. (2011) Soy protein adhesives improved by SiO_2 nanoparticles. Pigment & Resin Technology.Vol. 40, Number 3, pp 191 –195.

Yu, S., Tong, M.N. and Critchlow, G. (2010) Use of carbon nanotubes reinforced epoxy as adhesives to join aluminum plates. Materials and Design. Vol. 31, S126–S129.

Zhang, Y., Zhu, W., Lu, Y., Gao, Z. and Gu, J. (2014) Nano-scale blocking mechanism of MMT and its effects on the properties of polyisocyanate-modified soybean protein adhesive. Industrial Crops and Products. Vol. 57, pp 35–42.

Chapter Five

5.0 Conclusion and recommendation

5.1 Conclusion

- A novel adhesive for wood application was successfully prepared with enhanced tensile strength and water resistance. The FTIR spectra showed the surface functionalities of the FCNTs and SPI adhesive nanocomposite. The attachment of COO- functional group on the surface of the CNTs after purification contributed to the effective dispersion of the FCNTs in the nanocomposite adhesive. Hence, enhanced properties of FCNTs were successfully transferred into the SPI/CNTs nanocomposite adhesive. These unique functionalities on FCNTs however, improved the mechanical properties of the adhesive. The tensile shear strength and water resistance of SPI/FCNTs is higher than that of the SPI/CNTs.
- SEM images showed the homogenous dispersion of functionalized carbon nanotubes (FCNTs) in the SPI nanocomposite adhesive. The carbon nanotubes were distributed uniformly in the soy protein adhesive with no noticeable clusters at relatively reduced fractions of CNTs as shown in the SEM images, which resulted into better adhesion on wood surface. Mechanical (shear) mixing and ultrasonication with 30 minutes of shear mixing both showed an improved dispersion of CNTs in the soy protein matrix. However, ultrasonication method of dispersion showed higher tensile shear strength and water resistance than in mechanical (shear) mixing method. Thermogravimetric analysis of the samples also showed that the CNTs incorporated increases the thermal stability of the adhesive nanocomposite at higher loading fraction.
- Incorporation of CNTs and FCNTs into soy protein isolate adhesive improved both the shear strength and water resistance of the prepared adhesive prepared. There was over 100% increase in shear strength both at dry and wet state compared to the pure SPI adhesive. The 19% lower value of the new adhesive compared to the minimum value of ≥10MPa of European standard for interior wood application may be attributed to the presence of metallic particles remaining after purification of CNTs. The presence of

metallic particles will prevent the proper penetration of the adhesive into the wood substrate.

However, the preparation of new nanocomposite adhesive from soy protein isolate with improved tensile strength and water resistance will replace the formaldehyde and petrochemical adhesive in the market and be of useful application in the wood industry.

5.1 Recommendation

Due to unavailability of Brookfield viscometer, viscosity of the adhesive samples was not determined. There are already existing literatures on viscosity using the appropriate ratio of SPI to H_2O (1:9). Therefore, failure to determine the viscosity of the adhesive samples did not affect the result in anyway.

In this study, it was observed that the value of shear strength obtained was lower than the minimum value prescribed by EN-204 standard for interior wood application. This may be due to weak attachment of COO- functional group on the surface of the FCNTs, the type of wood used and the processing parameters. Therefore, the following investigations are recommended;

- The carboxylic acid groups on the surface of the CNTs after purification are usually needed to be converted into acyl chloride group by reaction with thionyl chloride at room temperature, in order to increase the reactivity of CNTs (Liu et al., 1998). Hydroxyl groups on the surface of CNTs will converted into hydroxymethyl groups ($–CH_2OH$) by the formalization reaction with formaldehyde (Wu et al., 1995).
- The molecular weight and distribution of the adhesive contribute significantly to the bonding strength. For example, the gluing strength with pine is much lower than that for walnut, cherry, maple, and poplar samples (Sun and Bian, 1999). This SPI/CNTs nanocomposite adhesive prepared may therefore be suitable for pine, walnut and cherry wood samples because they are softer than maple wood samples and will allow penetration of adhesive which will result into higher tensile shear strength than what was obtained in this study.

- Optimization of the processing parameters might also be a useful suggestion to achieve an optimum result of this newly developed nanocomposite adhesive.

References

Liu, J., Rinzler, A.G., Dai, H., Hafner, J.H., Bradley, R.K., Boul, P.J. and et al. (1998) Fullerene pipes. Science. Vol. 280, pp 1253–1256.

Sun, X. and Bian, K (1999). Shear Strength and Water Resistance of Modified Soy Protein Adhesives. Journal of American Oil Chemist Society Vol. 76, pp 977–980.

Wu, B.Y., Liu, A.H., Zhou, X.P., Jiang, Z.D. (1995) Chem. J. Chinese Univ. Vol. 16, pp 1641.

Appendix A

Calculation on Fe-Co catalyst Supported on Calcium Carbonate

Relative atomic masses

Fe =55.85, Co = 58.93, N = 14, O =16, H = 1

Molar mass of Fe $(NO_3)_3.9H_2O$ = 55.85 + 3 (14 +48) + 9 (18) = 403.85 g/mol.

Molar mass of Co $(NO_2)_2.6H_2O$ = 58.93 + 2 (14+48) + 9 (18) = 290.93 g/mol.

5 % mass of Fe in the metal salt

5 % Fe of 10 g $CaCO_3$ =0.5 g of Fe

55.85 g of Fe is contained in 403.85 g/mol. of Fe $(NO_3)_3.9H_2O$

$$0.5\ g\ of\ Fe = \frac{(0.5 \times 403.85)}{55.85}$$

Therefore, 0.5 g of Fe will be contained in 3.61 g/mol. of Fe $(NO_3)_3.9H_2O$

5 % mass of Co in the metal salt

5 % Co of 10 g $CaCO_3$ = 0.5 g of Co

58.93 g of Co is contained in 290.93 g/mol. of Co $(NO_3)_2.6H_2O$

$$0.5\ g\ of\ Co\ = \frac{(0.5 \times 290.83)}{58.93}$$

Therefore, 0.5 g of Co will be contained in 2.47 g/mol. of Co $(NO_3)_2.6H_2O$

<u>Determination of mass for hydraulic machine</u>

$Pressure = 1.4Mpa$

$Total\ area = (15 \times 20)mm^2 \times 12$

= $3600mm^2$

$$Pressure = \frac{Force}{\text{Area}}$$

$$1.4 = \frac{\text{Force}}{3600}$$

$$Force(F) = 5{,}040N$$

$$F = Mg$$

Where M is the mass and g ($9.81 m/s^2$) is acceleration due to gravity

Therefore,

$$M = \frac{5{,}040}{9.81}$$

$$Mass\ (M) = 513.76kg$$